

172-30774



HIGH-LOADING, 1800 FT/SEC TIP SPEED
TRANSONIC COMPRESSOR FAN STAGE
I. AERODYNAMIC AND MECHANICAL DESIGN

by

A.L. Morris, J.E. Halle, and E. Kennedy

PRATT & WHITNEY AIRCRAFT DIVISION
UNITED AIRCRAFT CORPORATION

prepared for

NATIONAL AERONAUTICS AND SPACE ADMINISTRATION

NASA Lewis Research Center
Contract NAS 3-13493
W.L. Beede, Project Manager
Fluid System Components Division

1. Report No. NASA CR-120907		2. Government Accession No.		3. Recipient's Catalog No.	
4. Title and Subtitle HIGH-LOADING, 1800 FT/SEC TIP SPEED, TRANSONIC COMPRESSOR FAN STAGE, I. AERODYNAMIC AND MECHAN- ICAL DESIGN				5. Report Date September 1972	
				6. Performing Organization Code	
7. Author(s) A. L. Morris, J. E. Halle, and E. Kennedy				8. Performing Organization Report No. PWA-4534	
				10. Work Unit No.	
9. Performing Organization Name and Address Pratt & Whitney Aircraft Division United Aircraft Corporation East Hartford, Connecticut 06108				11. Contract or Grant No. NAS3-13493	
				13. Type of Report and Period Covered Contractor Report	
12. Sponsoring Agency Name and Address National Aeronautics and Space Administration Washington, D.C. 20546				14. Sponsoring Agency Code	
15. Supplementary Notes Project Manager, W. L. Beede, Fluid System Components Division, NASA Lewis Research Center, Cleveland, Ohio					
16. Abstract A single stage fan with a tip speed of 1800 ft/sec (548.6 m/sec) and hub/tip ratio of 0.5 was designed to produce a pressure ratio of 2.285:1 with an adiabatic efficiency of 84.0%. The design flow per inlet annulus area is 38.7 lbm/ft ² -sec (188.9 kg/m ² -sec). Rotor blades have modified multiple-circular-arc and pre-compression airfoil sections. The stator vanes have multiple-circular-arc airfoil sections.					
17. Key Words (Suggested by Author(s)) Transonic Compressor Stage Precompression Blading			18. Distribution Statement Unclassified - Unlimited		
19. Security Classif. (of this report) Unclassified		20. Security Classif. (of this page) Unclassified		21. No. of Pages 114	
				22. Price* \$3.00	

**HIGH-LOADING, 1800 FT/SEC TIP SPEED
TRANSONIC COMPRESSOR FAN STAGE
I - AERODYNAMIC AND MECHANICAL DESIGN**

A. L. Morris, J. E. Halle, and E. Kennedy
Pratt & Whitney Aircraft Division
United Aircraft Corporation

I. SUMMARY

A highly loaded, high tip speed, single stage compressor has been designed under Contract NAS3-13493. This report presents the details of the aerodynamic and mechanical design. The purpose of the program is to determine the feasibility of using high tip speeds and high aerodynamic loadings to obtain high pressure ratios at acceptable levels of efficiency. The rotor has been designed for precompression (external compression) where inlet Mach numbers are high. No inlet guide vane or preswirl was used. The stator vanes were designed for zero exit swirl.

The aerodynamic design was based on the approximate parameters specified in the contract except that the specific flow had to be lowered from $42 \text{ lbm/ft}^2\text{-sec}$ ($205 \text{ kg/m}^2\text{-sec}$) to $38.7 \text{ lbm/ft}^2\text{-sec}$ ($188.9 \text{ kg/m}^2\text{-sec}$) in order to prevent meridional Mach number choking. The rotor blade was designed for a constant spanwise pressure ratio of 2.34:1. Blade losses for the rotor were estimated using a loss model in which shock and profile losses were considered separately. Shock loss estimates were based on relative inlet Mach number and airfoil shape; profile losses were estimated using a correlation of loss parameter versus diffusion factor and precent span. Stator losses were estimated using only a loss parameter correlation.

The rotor was designed using modified multiple-circular-arc blade sections from the hub to 32% span and precompression blade sections from 37% span to the blade tip, with a transition region in between. The purpose of the precompression sections is to reduce the strength of the main passage shock. The rotor was designed using a part-span shroud at 65% span to avoid flutter. The stator was designed with multiple-circular-arc airfoils which approached double-circular-arc geometry toward the outer portion of the span. The design parameters are summarized in Table I.

The stator leading edge was located close behind the rotor trailing edge. The calculated absolute stator inlet Mach number at the hub was 0.892.

Calculated centrifugal stress, gas bending stress, and untwist stress are within the capabilities of the AMS 4972A titanium alloy to be used for the rotor blades. Vibratory blade stresses should be low since the 1E, 2E, and 3E excitations for the first mode are outside of the rig operating range, and the higher order excitations are not expected to occur at low speeds. Although three rotor critical speeds were calculated within the rig operating range, no vibrational problems are anticipated since calculated deflections are within acceptable limits.

TABLE I
DESIGN PARAMETERS

Corrected Speed, rpm	12,464
Rotor Tip Speed, ft/sec (m/sec)	1800 (548.6)
Corrected Flow, lbm/sec (kg/sec)	173.8 (78.8)
Corrected Weight Flow Per Annulus Area, lbm/ft ² -sec (kg/m ² -sec)	38.7 (188.9)
Rotor Pressure Ratio	2.34:1
Stage Pressure Ratio	2.285:1
Rotor Adiabatic Efficiency, Percent	86.8
Stage Adiabatic Efficiency, Percent	84.0
Tip Diameter, Inches (meters)	33.1 (0.84)
Hub/Tip Ratio at Rotor Inlet	0.5
Rotor Tip Solidity	1.635
Rotor Aspect Ratio	2.87
Stator Hub Solidity	2.20
Stator Aspect Ratio	2.22
Stator Exit Flow Angle at all Radii, Degrees	0

II. INTRODUCTION

Future aircraft powerplants will require lightweight highly loaded compressors which are efficient over a wide range of operation. Pressure ratio per stage can be increased considerably above current levels by increasing rotor wheel speed and blade loadings. However, careful consideration must be given to blade element design in order to avoid severe aerodynamic losses. These losses result from in-passage shocks at high Mach numbers, boundary layer growth due to shock impingement, and high blade loadings. Recent tests, Reference 1*, of a highly

*See page 100 for list of References

loaded, 1600 ft/sec (487.7 m/sec), transonic compressor have been very successful; this rotor produces a pressure ratio of 2:1 at an adiabatic efficiency of 89%. Because of this, the design of a higher tip speed, higher pressure ratio rotor was undertaken. Precompression has been incorporated into the blade design in order to maintain a high level of efficiency. The precompression blade design is based on the external compression principle, described in Reference 2.

This report presents the aerodynamic and mechanical design of a single stage fan with a tip speed of 1800 ft/sec (548.6 m/sec) and an inlet hub/tip ratio of 0.5. The design flow per inlet annulus area is 38.7 lbm/ft²-sec (188.9 kg/m²-sec). No inlet swirl is used and the design stator exit swirl is zero. The design stage pressure ratio is 2.285:1, and the predicted stage adiabatic efficiency is 84.0%.

III. FLOWPATH AND VECTOR DIAGRAM DESIGN

A basic stage configuration consisting of no inlet guide vanes, hub/tip ratio of 0.5 at the rotor leading edge, and aspect ratios of 2.87 and 2.22 for the rotor and stator was specified by contract.

The flowpath design evolved from a series of iterations. All values presented are from the final iteration except where otherwise noted. The iteration was started using a reasonable flowpath shape, estimated flow blockages, and estimated efficiency profiles. The axisymmetric streamline analysis calculation outlined in Appendix 1 was used to obtain velocity vectors and flow conditions in the flowpath. This information, together with assumed rotor and stator solidities, was used to design rotor and stator blade elements. Adjustments were made to the flowpath shape and blade solidities to control velocities and loadings, and efficiencies were reestimated using these new loadings and aerodynamic conditions. Blade sections were defined after each iteration to determine the location of blade leading and trailing edges for use in the streamline calculation. The final flowpath design was compatible with blade element designs and the mechanical design.

Rotor losses were calculated as the sum of profile losses and shock losses. The profile losses were calculated using a correlation of loss parameter, $\frac{\overline{\omega}_p \cos \beta'_2}{2\sigma}$, versus diffusion factor and

percent span. Shock losses were calculated for each particular blade element as described in the Rotor Blade Design section. Different shock loss models were used for the multiple-circular-arc sections (hub to 32 percent span) and the precompression blade sections (37 to 100 percent span). The difference in calculated shock losses for the two airfoil types made it necessary to fair the estimated shock losses in the region from 17 to 54 percent span from the hub. Figure 1 shows the radial distributions of calculated shock total pressure recovery for the MCA and precompression shock models and the faired region between the two models. Figure 2 shows the final radial profile of estimated shock loss coefficients calculated from this pressure recovery curve and the total loss coefficient for the rotor blades.

Stator losses were calculated using a correlation of loss parameter versus diffusion factor and percent span. Figure 3 shows the final radial distribution of stator loss coefficient.

Blockages were included in the aerodynamic design to account for boundary layer growth on the casing walls and for the presence of the rotor part-span shroud at 65 percent span from the hub. Flow blockage due to casing boundary layers was estimated based on data from Pratt & Whitney Aircraft's research programs. To account for the presence of the part-span shroud, a blockage equal to the percent of total annulus area occupied by the shroud was applied locally at the exit of the rotor and to the inlet of the stator; one-half this shroud blockage was applied locally to the rotor inlet and stator exit stations. A constant radial value of blockage due to casing boundary layers was applied at these stations in addition to the part-span shroud blockages. The spanwise blockage factor distributions, in the vicinity of the part-span shroud, are shown in Figure 4. These distributions of flow blockage were used in the streamline analysis program. Table II lists these blockages in terms of radial averages.

TABLE II
FLOW BLOCKAGES (PERCENT OF TOTAL FLOW AREA)

<u>Blade Row and Station Number (Figure 6)</u>	<u>Casing Boundary Layer Blockage</u>	<u>Part-Span Shroud Blockage</u>	<u>Total Blockage</u>
Rotor Leading Edge (1)	2.0	0.6	2.6
Rotor Trailing Edge (2)	3.0	1.2	4.2
Stator Leading Edge (3)	3.0	1.2	4.2
Stator Trailing Edge (4)	4.0	0.6	4.6

The flowpath, including stage inlet and exit ducting, is shown in Figure 5. Figure 6 shows the rotor and stator portion of the flowpath in more detail. A highly convergent flowpath was necessary to keep end wall loadings of both rotor and stator within acceptable limits. High blade solidities were selected to control loadings. Figure 7 shows the spanwise distribution of rotor and stator solidities.

The large convergence together with relatively high aspect ratios gave wall slopes which caused the meridional velocity at the rotor leading edge to accelerate in the mid-span region and decelerate near the walls. Bow wave losses and blockages at the rotor leading edges further increased the meridional velocity. For the desired specific flow of 42 lbm/sec-ft² (205 kg/m²-sec) the meridional Mach number at the center of the span became so high that leading edge blockages caused the flow to choke before it could enter the blade channel. Mid-span choke problems caused by abrupt flowpath convergence are discussed in Reference 3. In order to avoid choking, the flowpath at the rotor leading edge plane was designed with large radii of curvature, and the specific flow was lowered to 38.7 lbm/ft²-sec (188.9 kg/m²-sec). A comparison of the inlet meridional Mach number profiles for 42 and 38.7 lbm/ft²-sec (205 and 188.9 kg/m²-sec) is shown in Figure 8. Calculation of boundary layer shape factors along the inlet walls using the method of Reference 4 indicated that the decelerating meridional velocity would not cause the end wall boundary layer to separate.

Figure 9 shows the rotor and stator inlet and exit meridional velocity profiles. The average velocity at the stator exit was 680 ft/sec (207 m/sec). Inlet Mach numbers for the rotor and stator are shown in Figure 10. The rotor inlet relative Mach number is supersonic from 9.5 percent span to the tip. The rotor exit relative Mach number is subsonic throughout the span. The stator inlet Mach numbers vary from approximately 0.9 at the hub to approximately 0.7 at the tip. By minimizing the gap between the stator leading edge and the rotor trailing edge, the absolute stator inlet Mach numbers and loadings were minimized.

Figure 11 shows the rotor inlet and exit relative air angles along with the spanwise stator inlet angles. The stator discharges axially, $\beta'_3 = 0^\circ$. An upturn in the rotor exit relative air angle, β'_2 , occurs between 90 and 100 percent span in the boundary layer region due to the high tip losses estimated for the rotor. Difficulties were encountered in selecting blade sections near the tip because of this abrupt rise in β'_2 , and made it necessary to fair a continuous curve of β'_2 versus span through the rotor tip region. The faired β'_2 curve is shown in Figure 11.

Rotor and stator diffusion factors are shown in Figure 12. Hub D-factors for the rotor and stator are quite high even though the design has high solidity rotors and stators. Stall characteristics of this stage are expected to be strongly influenced by these high hub loadings.

Figure 13 shows the spanwise distribution of rotor and stage adiabatic efficiencies. The mass-averaged efficiencies are 86.8 percent for the rotor and 84.0 percent for the stage.

Spanwise distributions of local specific flow, $(W/A)_{\text{local}} = \rho V_z$, at the rotor and stator leading and trailing edges are shown in Figure 14. The decrease in specific flow at the rotor tip from leading to trailing edges and the large increase across the stator tip in relationship to the average increase across the stator, are caused by the expected rotor tip losses. High rotor work in this high loss area gives a large swirl velocity and a low axial velocity so that tip stream tubes expand through the rotor. When the swirl is removed by the stator, the outer stream tubes contract. The stream tube expansions and contractions at the tip are beyond the experience on which the blade design system is based and some discretion in selecting airfoils in the outer span was required; this will be discussed further in Sections IV and V.

The design velocity vector data calculated along streamlines at the rotor and stator leading and trailing edges are tabulated in Appendix 2, Aerodynamic Summary.

IV. ROTOR BLADE DESIGN

The rotor blade was designed to produce a total pressure ratio of 2.34:1 at a tip speed of 1800 feet per second (548.6 m/sec). There are 38 rotor blades with an aspect ratio of 2.87 (based on average blade length and axial projected chord at the hub) and a tip solidity of 1.635.

The rotor blade consists of multiple-circular-arc (MCA) airfoil sections from hub to 32% span and precompression (PC) sections from 37% span to the tip, with a transition region in between. Transition blade sections were necessary to provide reasonably smooth airfoil shapes

between the MCA and precompression airfoil sections. Precompression airfoils were chosen to reduce shock losses wherever possible, i.e., wherever the relative inlet Mach number and blade leading edge wedge angle allowed an attached oblique shock. Airfoil sections were designed on conical surfaces approximating stream surfaces of revolution.

A preliminary parametric study of blade mechanical properties was made assuming MCA airfoils at all spanwise locations since the MCA sections are more easily specified than PC sections. The more complicated PC airfoil design was begun after general mechanical design criteria were established. Essentially the same mechanical properties were maintained in the blade with PC as MCA airfoils by adjusting the PC section at each spanwise position to obtain the same cross section area.

Multiple-Circular-Arc Design

MCA sections extend from the root to 32% span. True multiple-circular-arc airfoils were used in the design procedure. These airfoils were subsequently thinned to provide more flow area, and these thinned MCA airfoils will be referred to as "modified" MCA airfoil sections in this report.

Airfoil sections were defined by specifying total and front chord, total and front camber angle, maximum thickness and its location, and leading and trailing edge radii, as shown by Figure 15a. The front chord was selected to provide a transition point just forward of an assumed normal shock impingement point on the suction surfaces.

For the MCA blade sections, a normal shock is assumed at the first covered section of the blade passage as shown in Figure 15b. A Mach number upstream of the assumed normal shock is calculated by using the equations of continuity and conservation of angular momentum. This calculation accounts for stream tube contraction and radius change. Next, the critical area ratio (A/A^*) resulting from the Mach number calculation is adjusted to account for blade blockage by multiplying the A/A^* by the ratio of blade entrance channel width to ($s \cos \beta'_1$). The resulting A/A^* determines the upstream shock Mach number. The shock total pressure recovery (shown in Figure 1) was then computed based upon the assumption of a normal shock at this upstream Mach number.

Maximum thickness-to-chord ratio at the root is 0.077 which gives calculated combined steady state stresses, including untwist stresses, within the allowable limits of AMS 4972A titanium alloy selected for blade material. The spanwise distribution of maximum thickness-to-chord ratio is shown in Figure 16. Total and front chords for the modified MCA rotor blade are shown in Figure 17.

Incidence angle to the suction surface at the leading edge versus span is shown in Figure 18. Two incidence criteria were used: 1) subsonic and transonic MCA, and 2) supersonic MCA.

Rotor incidences for the subsonic and transonic blade sections were set based on measured minimum loss incidence angles in Reference 1. Rotor incidence for the supersonic MCA

portion of the blade was selected as +1.5 degrees to the suction surface at a location half-way between the leading edge and the emanation point of the first captured Mach wave. This incidence selection is based on experience and accounts for bow wave shock loss, blade leading edge blockage, and development of the suction surface boundary layer.

The ratio of minimum blade channel flow area to critical area, A/A^* , was chosen as 1.02 to prevent choking. Distributions of A/A^* through five blade channels between 0 and 30.3 percent span are shown in Figure 19. Area distributions are along conical surfaces. The critical A/A^* ratio was calculated knowing the channel width, shock loss, and the assumptions of a linear specific flow variation from the leading edge to the trailing edge and a linear profile loss distribution from the blade channel entrance to the trailing edge. Front camber was the main parameter used to control blade channel width. An improved A/A^* calculation technique accounting for streamline radius ratio was developed after completing the rotor design. This calculation showed that the channel areas for sections from 9 to 32 percent of the rotor span were too small. Additional flow area was obtained by locally thinning the standard MCA airfoils as shown in Figure 20. The A/A^* distributions for this modification are included in Figure 19. Blade total and front camber angle distributions are shown in Figure 21.

Deviation was estimated using Carter's rule plus a correction based on a correlation of test data from Reference 1. The design deviation and Carter's rule deviations for the MCA blade sections are shown versus span on Figure 22.

Precompression Blade Design

For the outer radii, a low shock-loss precompression blade section was used because of the high rotor tip speed and high inlet relative Mach number associated with this rotor. Figure 23 is a schematic of the precompression airfoil. A general description of the precompression blade design is presented in the following paragraphs.

The precompression design model assumes that the shock across the channel entrance must be oblique and attached to the leading edge of the airfoil. Flow conditions upstream of the first captured Mach line are adjusted to account for the bow shock system which propagates upstream of the rotor inlet plane. The concave surface (BC in Figure 23) is the precompression ramp. The curvature of this ramp generates a series of compression waves which diffuse the supersonic flow. The wave system is designed to coalesce near A' , slightly downstream of the rotor inlet plane. The precompression wave system lowers the Mach number of the flow across the passage entrance, reducing the total pressure loss associated with the oblique shock ($A'-D$ on Figure 23). The flow deflection across this oblique shock is equal to the effective leading edge wedge angle (blade wedge angle plus boundary layer displacement) plus the precompression angle.

The shock $A'-D$ is constructed in increments across the gap to account for gapwise changes in flow conditions upstream of the shock. Shock losses are calculated for each increment and are mass averaged across the gap to obtain the oblique shock loss of the blade element. Channel flow downstream of the oblique shock is subsonic, and turning and stream tube area are made compatible with exit aerodynamic conditions.

Development of the blade suction surface AB beings by aligning the aerodynamic surface (blade surface plus boundary layer displacement) to a constant angular momentum stream-line from the leading edge to the first captured Mach wave. Suction surface curvature in segment CD is designed to adjust the supersonic flow upstream of the shock to be compatible with the shock deflection and subsonic flow condition downstream of the shock. Iterations were made on surface shape until compatibility was achieved, accounting for effect of radius change and stream tube convergence (or divergence).

The suction surface immediately behind the shock impingement, D, is aligned with the flow direction downstream of the shock. The surface is rounded at D to allow for boundary layer thickness changes in the region of the shock impingement. Channel area is blended from the value at D to the area determined by the core flow at the channel exit. A cosine variation of stream tube area determines the locus of points which define the suction surface (DG). The cosine variation equations are given in Appendix 3.

The pressure surface segment AE follows a free streamline downstream of the oblique shock. Segment FG of the pressure surfaces is designed to guide the flow to the desired exit angle. Segment EF blends smoothly between AE and FG. The chordwise locations of the pressure surface points, E and F, are tabulated in Appendix 4.

The resulting mean-line incidence and deviation angles for the entire blade are shown in Figures 24 and 25, respectively. The mean-line metal angles used in the calculation of these figures are average pressure and suction surface metal angles at the leading and trailing edges of the developed blade sections.

Precompression blade sections were designed for a radial distribution of cross-sectional area determined from the preliminary MCA design. The main purpose of this requirement was to provide good mechanical properties and blending of the MCA and PC blades. The blade span-wise cross-sectional areas are shown in Figure 26; this curve shows the areas for the modified MCA blade (dashed line) as well as the true MCA areas (solid line). The PC airfoil cross-sectional areas, which are shown in Figure 26, were obtained primarily by controlling the blade leading edge wedge angle and leading edge radius (Figure 27). The leading edge wedge angle and the location of the pressure surface point, E, (Figure 23) were chosen to avoid local chordwise narrowing of blade elements which could result in concentrations of vibrational stress.

Channel area between the blades was calculated from the aerodynamic blade surface contours and estimated stream tube height from the streamline analysis. This area was then increased to account for boundary layer displacement thicknesses which were determined using the boundary layer calculation of Reference 4. In this calculation, the abrupt pressure rise, caused by the passage shock wave, is spread linearly across the shock impingement- - from five boundary layer thicknesses upstream of the shock impingement point to the trailing edge.

A minimum critical area ratio (A/A^*) was calculated for the precompression sections based upon channel width between blades, bow wave losses, shock losses, streamline radius changes, and specific flow. This minimum A/A^* ratio occurs just downstream of the oblique shock

(A'D). The minimum A/A^* ratios for the precompression blade sections are plotted spanwise in Figure 28 for three types of assumed shock losses. Curve A of Figure 28 is computed on the basis of the design shock loss, i.e., the oblique shock of Figure 23; for this design case, the $(A/A^*)_{\min}$ ranged from 1.02 to 1.065, with a drop-off at the tip region due to high end wall losses. Curve B in Figure 28 is the minimum A/A^* distributions based on a normal shock at the channel entrance Mach number (e.g., depicted in Figure 15b), and curve C is based on a normal shock at the inlet relative Mach number, M_1' . Figure 28 shows that the flow will start if the blades are subjected to normal shock losses based on a channel entrance Mach number, but most of the flow in the outer 40 percent span will not start if these losses are based on M_1' ; i.e., the Kantrowitz-Donaldson criterion (Reference 5). It is thought, however, that the normal shock at M_1' is an extreme condition which will not occur due to the presence of the diffusing wave system associated with the precompression ramp. It is more reasonable to expect that in starting, the rotor passage will encounter a normal shock at a precompressed Mach number, so that the starting $(A/A^*)_{\min}$ distribution may be similar to curve B. It is believed that adequate flow area is provided for design entrance flow conditions to be established in the precompression blade sections under these conditions.

Blade chord, leading and trailing edge metal angles, and precompression ramp angles are shown in Figures 29, 30, and 31 for conical surfaces on streamlines. Rotor blade geometry is tabulated in Appendix 4, Table VII. Also included in Appendix 4 is a graphical description of an airfoil on the unwrapped conical surface (Figure 50). This figure is used in conjunction with Table VII. Rotor tip geometry was selected using the previously discussed faired β'_2 curve of Figure 11. For manufacturing purposes, the airfoil sections were defined on planes normal to a radial (stacking) line. The resultant blade coordinates are presented in Appendix 5, Table IX. Airfoil coordinate labels used in Table IX are graphically defined in Figure 51 (included in Appendix 5).

Transition

The region of the blade from 32 to 37% span provides transition from the modified MCA to PC sections. The last MCA conical section is at 32% span and the first PC section is at 37% span. The blade section stacking program which defines blade surfaces by a parabolic curve fit between conical input sections was used to determine transition blade sections. For manufacturing purposes, the airfoils in the 32-37 percent span region were defined on planes normal to a radial line.

V. STATOR VANE DESIGN

The stator has multiple-circular-arc airfoil sections (Figure 15a) with sections at the outer span approaching double-circular-arc (DCA). Airfoil sections were designed on conical surfaces approximating streamsurfaces of revolution.

The aerodynamic chord length tapers linearly from 2.48 inches (0.063 m) at the hub to 2.6 inches (0.066m) at the tip. The stator has 60 vanes resulting in a hub solidity of 2.2. Aspect ratio is 2.22 based on average blade length and axially projected chord at the hub. Maximum thickness-to-chord ratio is 0.07 at the tip tapering linearly to 0.05 at the hub. This stator vane thickness distribution was selected to provide mechanical integrity and low blade element loss.

Front chord length (c_f in Figure 15) for hub sections was selected to set the transition point just forward of the intersection on the suction surface of a line drawn from the leading edge of an adjacent blade and normal to the flow. Airfoil sections near the outer case have front chords approximately one-half the total chord and front cambers approximately one-half the total camber. Therefore, these sections are essentially DCA airfoils. Figure 32 shows the spanwise distributions of $\frac{c \sin \phi_f/2}{c_f \sin \phi/2}$ which is the average airfoil mean-line radius of curvature divided by the front section-mean-line radius of curvature. This parameter equals 1.0 for DCA airfoils and becomes smaller as the front section is uncambered relative to a DCA airfoil. Figure 33 shows the chordwise location of airfoil maximum thickness versus span.

Incidence angle was set at zero degrees to the suction surface in the near-sonic flow region at the hub, blending into minimum loss incidence angles for double-circular-arc sections near the tip (Figure 34). Camber distribution was used to control throat area in the channel between adjacent vanes. The optimum ratio of capture area to throat area, which provides minimum loss (Reference 6) varied from 0.97 at the hub to 0.985 at the stator tip. This capture-to-throat area parameter was used to set throat areas. Figure 35 shows the axial distributions of A/A^* in channels between stator airfoil sections.

Incidence angle and front camber did not control throat areas in the outer 15 percent span where the extremely low ratio of inlet to exit specific flow, $(\rho V_z)_3/(\rho V_z)_4$, caused the minimum throat area to occur at the channel exit (Figure 35, 100 percent span). Minimum channel flow area is lower than the optimum indicated by Reference 6, although A/A^* is adequate to prevent choking. Incidence angle selection was complicated by the unusually low specific flow ratio, $(\rho V_z)_3/(\rho V_z)_4$, and high inlet air angle which fell outside the range of available stator blade-element data. Pratt & Whitney Aircraft cascade data for geometrically similar DCA cascades but with specific flow ratios closer to 1.0 were considered most applicable and were used to select stator tip incidence angles.

Stator deviation angles were determined using Carter's rule plus an adjustment based on data from References 1 and 7. The spanwise distribution of Carter's rule and design deviation angles are given in Figure 36.

Figure 37 presents mean-camber-line metal angles versus span, and Figure 38 presents front and total camber angles. All angles in these figures are measured on conical surfaces on which the airfoils were designed. Stator vane geometry on conical surfaces is summarized in Appendix 4, Table VIII. Also included in Appendix 4 is a graphical description of an airfoil on the unwrapped conical surface (Figure 50). This figure is used in conjunction with Table VIII.

For manufacturing purposes, airfoil sections were defined on planes normal to a radial line which passes through the center of gravity of the hub section. Coordinates of these sections are tabulated in Appendix 5, Table X. Airfoil coordinate labels used in Table X are graphically defined in Figure 51 (included in Appendix 5).

VI. STRUCTURAL AND VIBRATION ANALYSIS

The mechanical design included an investigation of the rotor and stator airfoil steady and vibrational stresses and flutter parameters. The natural modes of the rotor and stator systems were calculated and a rotor-frame critical speed analysis was performed to investigate the vibrational characteristics of the fan stage.

The final design is stress limited in the blade attachment to a mechanical speed of 13,650 rpm which is 109.5 percent of the standard day design speed of 12,464 rpm and 106.5 percent of design speed based on a 90°F (305.2°K) rig plenum temperature. All mechanical analyses are based on this 90°F plenum temperature.

A. Rotor Blade and Stator Vane Stresses

Combined centrifugal pull and untwist rotor blade stresses were calculated at 110 percent of design speed and results are shown in Table III along with the allowable stresses for the blade material, AMS 4972A titanium alloy bar stock, based on 200°F (366.3°K) metal temperature. The maximum combined centrifugal pull and untwist stress of 77,700 psi ($536 \times 10^6 \text{ N/m}^2$) occurs at 13 percent span, near maximum thickness on the concave side of the airfoil. This stress is comparable to stress levels present in experimental and production blades and is well below the allowable stress of 94,000 psi ($648 \times 10^6 \text{ N/m}^2$). The maximum vibratory stress occurs at 22 percent span near the trailing edge on the concave side of the airfoil. The static stress in this area is only 54,000 psi ($372 \times 10^6 \text{ N/m}^2$). Figure 39 shows these maximum stress locations. A modified Goodman diagram, Figure 40, indicates that, at the maximum steady state stress level of 77,700 psi ($536 \times 10^6 \text{ N/m}^2$), the maximum allowable vibratory stress is slightly above 10,000 psi ($69 \times 10^6 \text{ N/m}^2$). Since no low order resonances are expected in the blade's high speed operating range, the actual vibratory stress levels should be less than the allowable value of 10,000 psi ($69 \times 10^6 \text{ N/m}^2$) indicated by the Goodman diagram for this point on the blade. During testing, the vibratory stress will also be limited to 10,000 psi ($69 \times 10^6 \text{ N/m}^2$).

Gas bending stresses with centrifugal restorations were calculated at design speed for various tangential tilts of the blade, see Figure 41. Airfoil stresses were minimized for the combination of load and no-load conditions. The selected tangential tilt is 0.050 inch (0.00127 m) which results in a maximum tensile bending stress of 7000 psi ($48 \times 10^6 \text{ N/m}^2$) at 12,464 rpm.

The part-span shroud was designed to insure minimum aerodynamic interference while providing adequate strength under centrifugal loading and bearing forces. The part-span shroud is located at 65 percent of span. A sketch of the part-span shroud is shown in Figure 42. The Z^* ratio, defined as shroud section modulus/adjacent airfoil section modulus, has a value of 0.84 which is consistent with successful experience. Pertinent shroud stresses are shown in Table III.

Stator vane (AMS 5613 stainless steel material) gas bending stresses were calculated assuming both fixed and pinned ends. The maximum bending stress of 38,300 psi

($264 \times 10^6 \text{ N/m}^2$) was well below the allowable of 108,000 psi ($755 \times 10^6 \text{ N/m}^2$). Maximum allowable vibratory stress limits for stator vanes are established based upon test experience with similar stator vane and attachment designs. For this stator, the test limit was the same as for the rotor; i.e., 10,000 psi ($69 \times 10^6 \text{ N/m}^2$). This stress limit is conservative because the stator's steady state stresses are lower than the rotor's steady state stresses, and, like the rotor, there are no critical stator vane resonances in the operating range.

TABLE III
CALCULATED STRESSES FOR ROTOR BLADE,
BLADE DISK, AND STATOR VANE

	38 Rotor Blades	AMS 4972A (titanium alloy)
	60 Stator Vanes	AMS 5613 (stainless steel)
	Disk	AMS 6415 (low-alloy steel)
Assumed Operating Conditions		
N = 110% of design speed, 90°F (304.2°K) plenum temperature, except where noted		
T = 200°F (366.3°K) metal temperature		
<u>Stress</u>	<u>Calculated</u>	<u>Allowable</u>
Blade airfoil max. combined stress	77,700 psi ($536 \times 10^6 \text{ N/m}^2$)	94,000 psi ($648 \times 10^6 \text{ N/m}^2$)
Blade airfoil max. root combined stress corrected for platform angle (at leading edge)	77,600 psi ($536 \times 10^6 \text{ N/m}^2$)	94,000 psi ($648 \times 10^6 \text{ N/m}^2$)
Blade shroud bearing stress	4075 psi ($28 \times 10^6 \text{ N/m}^2$)	5000 psi ($34 \times 10^6 \text{ N/m}^2$)
Blade shroud bending stress	64,700 psi ($446 \times 10^6 \text{ N/m}^2$)	66,000 psi ($455 \times 10^6 \text{ N/m}^2$)
Blade attachment max. combined stress (106.5% speed)	71,022 psi ($490 \times 10^6 \text{ N/m}^2$)	71,077 psi ($490 \times 10^6 \text{ N/m}^2$)
Blade attachment max. bearing stress (106.5% speed)	87,532 psi ($604 \times 10^6 \text{ N/m}^2$)	84,600 psi ($583 \times 10^6 \text{ N/m}^2$)
Disk lug max. combined (106.5% speed)	63,633 psi ($439 \times 10^6 \text{ N/m}^2$)	103,367 psi ($713 \times 10^6 \text{ N/m}^2$)
Disk lug bearing stress (106.5% speed)	87,532 psi ($604 \times 10^6 \text{ N/m}^2$)	122,400 psi ($844 \times 10^6 \text{ N/m}^2$)
Disk average tangential stress	82,950 psi ($572 \times 10^6 \text{ N/m}^2$)	106,000 psi ($731 \times 10^6 \text{ N/m}^2$)
Disk max. radial stress	74,000 psi ($510 \times 10^6 \text{ N/m}^2$)	96,000 psi ($662 \times 10^6 \text{ N/m}^2$)
Vane airfoil max. bending stress	38,300 psi ($264 \times 10^6 \text{ N/m}^2$)	108,000 psi ($745 \times 10^6 \text{ N/m}^2$)

B. *Rotor Blade Attachment and Disk Stresses*

Critical speed considerations required that disk rim weight be minimized, necessitating the selection of a dovetail attachment rather than a firtree attachment. The final blade attachment design is stress limited to a mechanical speed of 13,650 rpm which is 109.5 percent of the standard day design speed of 12,464 rpm and 106.5 percent of design speed based on a 90°F (305.2°K) rig inlet temperature. The bearing stress in the blade attachment exceeds the nominal allowable by 3.5 percent. This is acceptable since the allowable limit is conservative and intended for production engines. All disk (AMS 6415 low-alloy steel material) stresses are well below allowable limits. See Table III for a summary of blade attachment and disk stresses.

The airfoil root stress/blade attachment stress is approximately 2.0, insuring that the attachment can withstand vibratory stresses higher than the airfoil can tolerate.

C. *Rotor Blade and Stator Vane Resonances*

Coupled blade-disk resonances which might be excited in the operating range were avoided by the proper choice of shroud location, shroud angle, blade material, and disk geometry and material. Low order excitation from circumferential distortion or other possible inlet pressure variations will not excite the system because the blade and disk were designed to insure that natural modes for the system would not occur at frequencies close to one, two or three excitations per revolution (1E, 2E, or 3E) during high speed operation. The bladed disk resonance diagram is shown in Figure 43. Performance testing will be avoided at those speeds where higher order resonances (6E, 8E, or 10E) might occur. However, there are no struts or instrumentation in the system to excite these resonances. The first bending mode 3E frequency margin is more than 8 percent at 105 percent of design speed, and more than 5 percent at 110 percent of design speed, which is considered adequate. Blade strain gages will indicate any resonant conditions that exist and test speeds can be adjusted accordingly to avoid operation at these resonant conditions.

The blade tip dynamic stress distribution in the first chordwise bending mode is shown in Figure 44. The maximum stress is six times the stress at maximum blade thickness and occurs at 25 percent chord. However, no tip fatigue problems are expected since the first tip chordwise bending mode occurs in the region of low static stress and is not excited by vane passing order or any 8E or lower frequency excitations as shown in Figure 45. A 10E resonance occurs in the high speed operating range but no evidence of this excitation was found in the stress records of a fan stage using the same inlet case and almost identical instrumentation. Higher order resonances are not expected to cause problems since they occur at lower speeds. The maximum stress location caused by the chordwise bending modes will be determined so that the blade tips can be adequately strain gaged.

The stator vane resonant frequencies were calculated assuming that the vanes were fixed at both ends of the airfoil and then adjusted based on past testing of similarly mounted vanes. The stator resonance diagram is shown in Figure 46. At design speed, the only resonance that exists is 5E for which there is no anticipated source of excitation. Below design speed the 38E vane resonance or other resonances can be avoided by proper selection of test speeds to avoid resonant conditions indicated by vane strain gages. As an additional safeguard against encountering high stresses throughout the operating range, the stator vane inner diameter shank will be supported with a flexible bushing as shown in Figure 47. Damping of stator vane vibration by supporting vanes in a flexible (polyurethane) compound has been successfully demonstrated in an engine program.

D. Rotor Blade and Stator Vane Flutter

To avoid rotor blade flutter a part-span shroud was located at 65 percent span from the hub with a shroud contact angle of 25 degrees. The supersonic torsional flutter parameter ($V/b\omega_t$) was calculated for the portion of the blade above the part-span shroud. The V and b terms are the relative velocity and semi-chord at 75 percent span for this portion of the blade, and the ω_t term is the torsional frequency of the blade portion above the shroud assuming the blade is fixed at the part-span shroud location. The flutter parameter was 1.02 at design speed and 1.04 at 110 percent of design speed; these values are below typical values where flutter problems occur; therefore, no supersonic torsional tip flutter is expected throughout the high speed running range.

The stator vane bending flutter parameter and torsional flutter parameter were calculated for these vanes; the calculated points fall well into the successful experience (no flutter) area.

E. Critical Speed

A rotor-frame critical speed analysis was performed to determine the vibrational characteristics of this rig. The analysis includes all of the significant structural members and uses the spring rates, masses, and gyroscopic stiffening of the system. The compressor rig spring location and spring rates are shown in Figure 48.

Three critical speeds occur within the rig operating range at 5500, 11,800 and 12,500 rpm. A fourth one occurs at 14,800 rpm which is above the maximum operating speed. The mode shapes at these four speeds are shown in Figure 49. To determine if the vibratory amplitudes of these modes are acceptable, a forced response analysis was performed. This analysis is similar to the critical speed analysis except that an unbalance is simulated and the resultant vibratory deflections calculated. Deflections were calculated at all significant rotor and case locations for an unbalance of one (1) ounce-inch (72×10^5 kg-m) located at each of five (5) locations: disk, No. 2 bearing, diaphragm coupling, forward spline, and rear spline. Table IV gives a listing of estimated deflections for the four (4) critical speeds, or modes.

TABLE IV
CALCULATED DEFLECTION FOR RIG CASINGS
AND SUPPORT MEMBERS

1.0 Ounce-Inch (72×10^{-5} kg-m) Unbalance*
NOTE: 1 Mil = 2.54×10^{-5} Meters

Unbalance Location	Disk				Diphragm Coupling				No. 2 Bearing				Forward Spline				Rear Spline				
Mode	1	2	3	4	1	2	3	4	1	2	3	4	1	2	3	4	1	2	3	4	
<u>Response Location</u>																					
Disk	-	12	1	-	-	3	-	-	-	2	-	-	-	2	-	-	-	3	-	-	
ID Stator Case	-	1	-	-	1	-	-	-	1	-	-	-	-	-	-	-	-	-	-	-	
OD Case	1	2	-	-	2	-	-	-	1	-	-	-	1	-	-	-	-	-	-	-	
Bellmouth	2	-	2	-	4	-	-	-	4	-	-	-	2	-	-	-	1	-	-	-	
ID Inlet Fairing	1	19	19	-	3	8	8	4	4	3	5	-	2	6	6	-	1	4	4	-	
No. 1 Bearing	-	6	1	-	-	2	-	1	-	1	-	-	-	2	-	1	-	1	-	-	
No. 1 Brg. Support	-	5	1	-	-	1	-	1	-	1	-	-	-	1	-	1	1	-	-	1	
No. 2 Bearing	-	2	-	-	1	1	1	3	1	-	-	2	-	1	1	4	-	-	-	3	
No. 2 Brg. Support	1	1	-	-	1	-	-	-	1	-	-	-	-	-	-	-	-	-	-	-	
No. 3 Bearing	-	2	-	-	-	-	-	6	-	-	-	3	-	1	1	6	-	-	-	5	
No. 3 Brg. Support	-	1	-	-	-	-	-	2	-	-	-	1	-	-	-	3	-	-	-	2	
No. 4 Bearing	-	-	-	-	-	-	-	-	-	-	-	-	-	-	-	-	-	-	-	-	
No. 4 Brg. Support	-	-	-	-	-	-	-	-	-	-	-	-	-	-	-	-	-	-	-	-	
Inlet Struts	-	-	-	-	-	-	-	-	-	-	-	-	-	-	-	-	-	-	-	-	
Exit Struts	-	1	-	-	1	-	-	-	1	-	-	-	-	-	-	-	-	-	-	-	
NOTE: Mode 1:	5500 RPM					Mode 2:	11800 RPM					Mode 3:	12500 RPM					Mode 4:	14800 RPM		

* The amplitudes in this table are approximate values and are estimated to be maximum values.

The 11,800 rpm mode was found to be the most sensitive to unbalance. The largest estimated deflections (for 1 ounce-inch unbalance) were 0.019 inches (0.0005 m) at the inlet fairing and 0.012 inches (0.0003 m) at the disk. Deflections at the inlet fairing are no threat to rig safety. The rotor assembly (consisting of disk, blades, forward and rear shaft assemblies, and diaphragm coupling) will be balanced to better than 0.05 oz-in (36×10^{-5} kg-m) unbalance resulting in a maximum disk deflection of 0.005 inches (0.00013 m). This is considered acceptable since the minimum blade tip clearance is 0.040 inches (0.0010 m) and the rig is adequately instrumented to detect and avoid critical speed regions. Also, actual sensitivity to unbalance may be considerably less since conservative values of damping coefficients were used in the analysis.

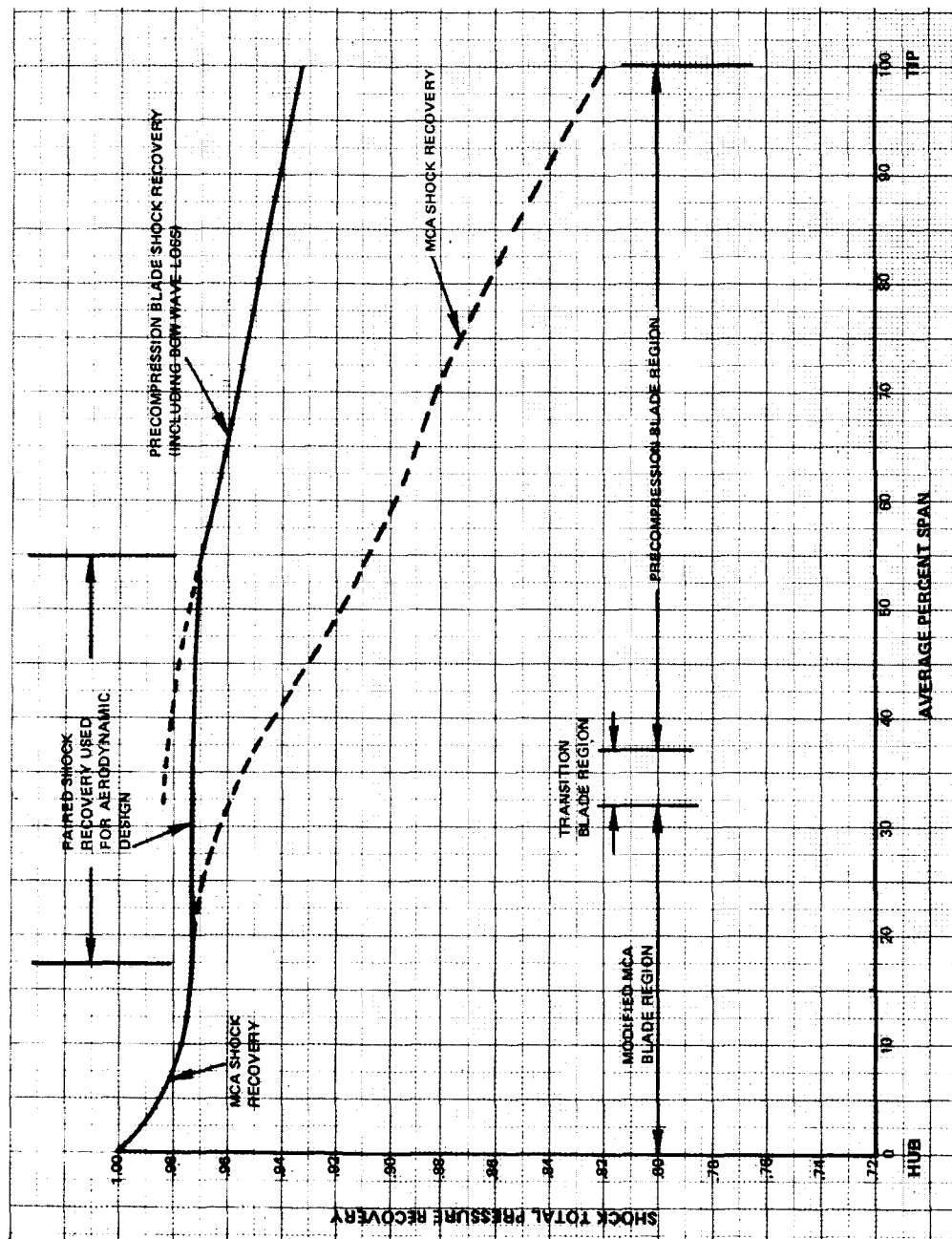


Figure 1 Spanwise Shock Recovery for Rotor Precompression and MCA Designs

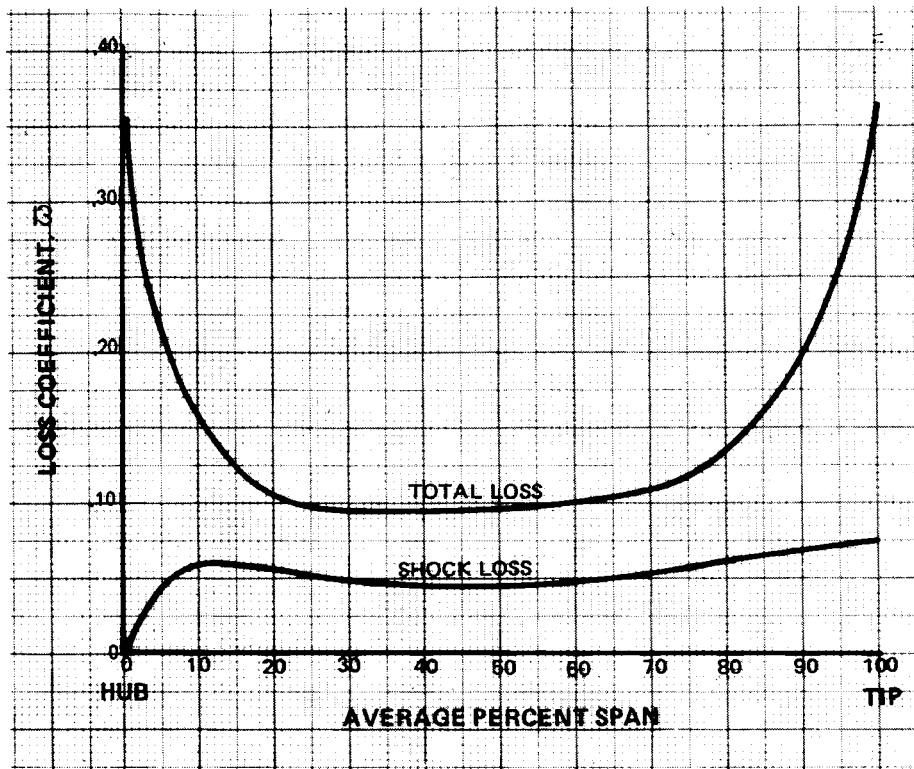


Figure 2 Rotor Blade Total and Shock Loss Coefficients (Design)

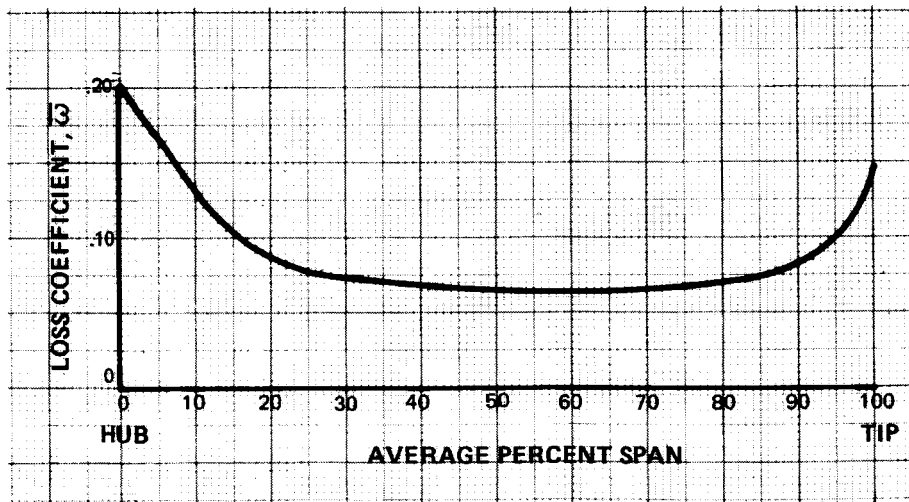


Figure 3 Stator Vane Loss Coefficient (Design)

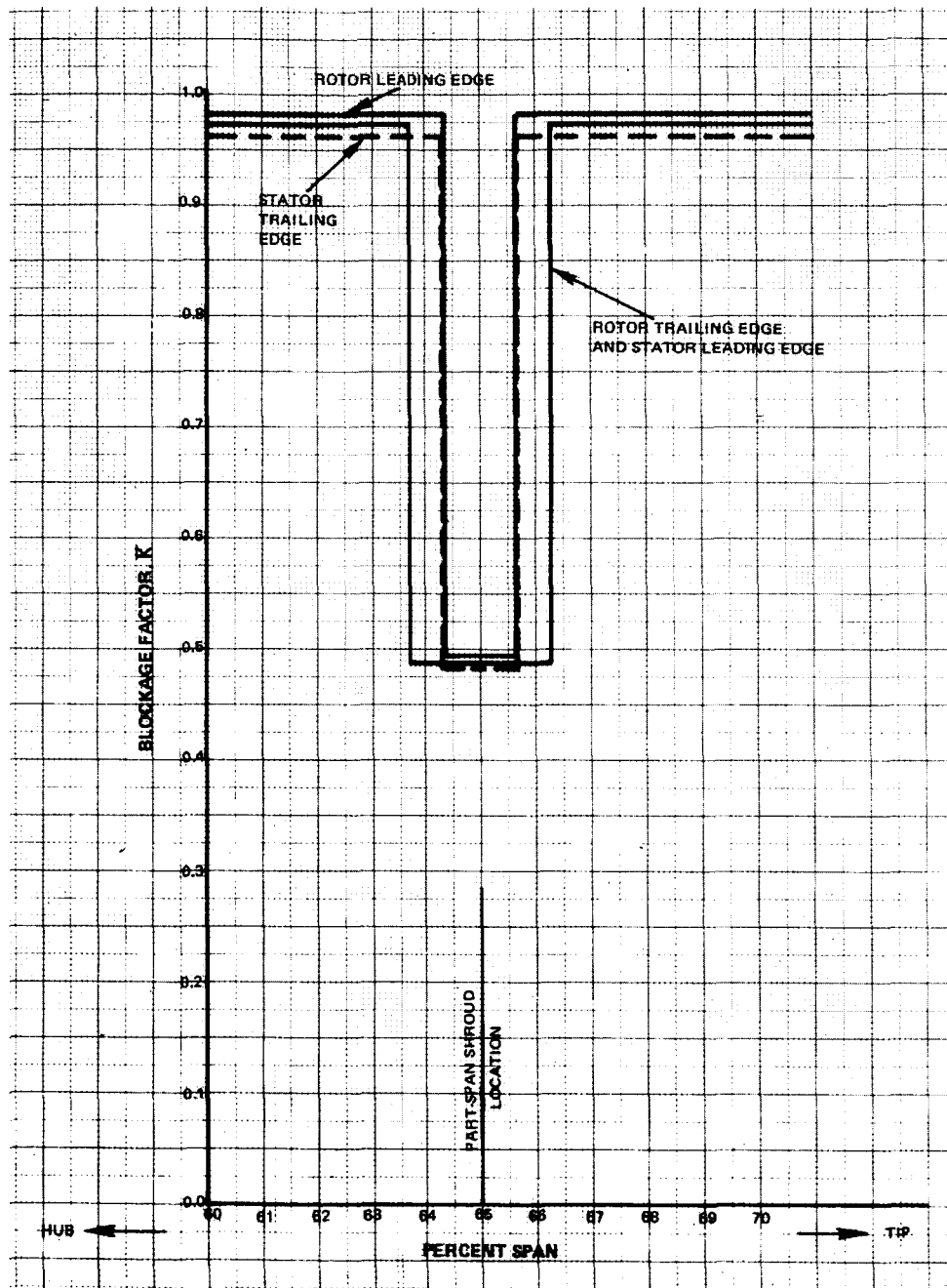


Figure 4 Spanwise Distribution of Local Blockage Factor in Vicinity of Part-Span Shroud

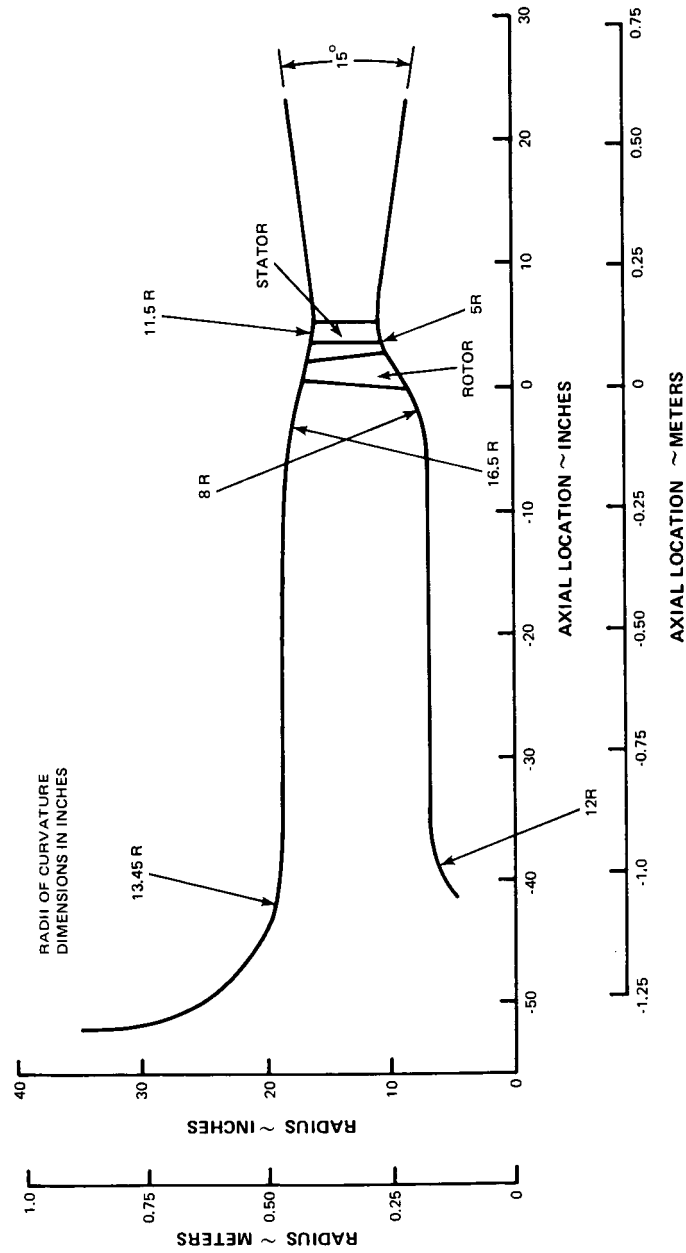


Figure 5 Flowpath

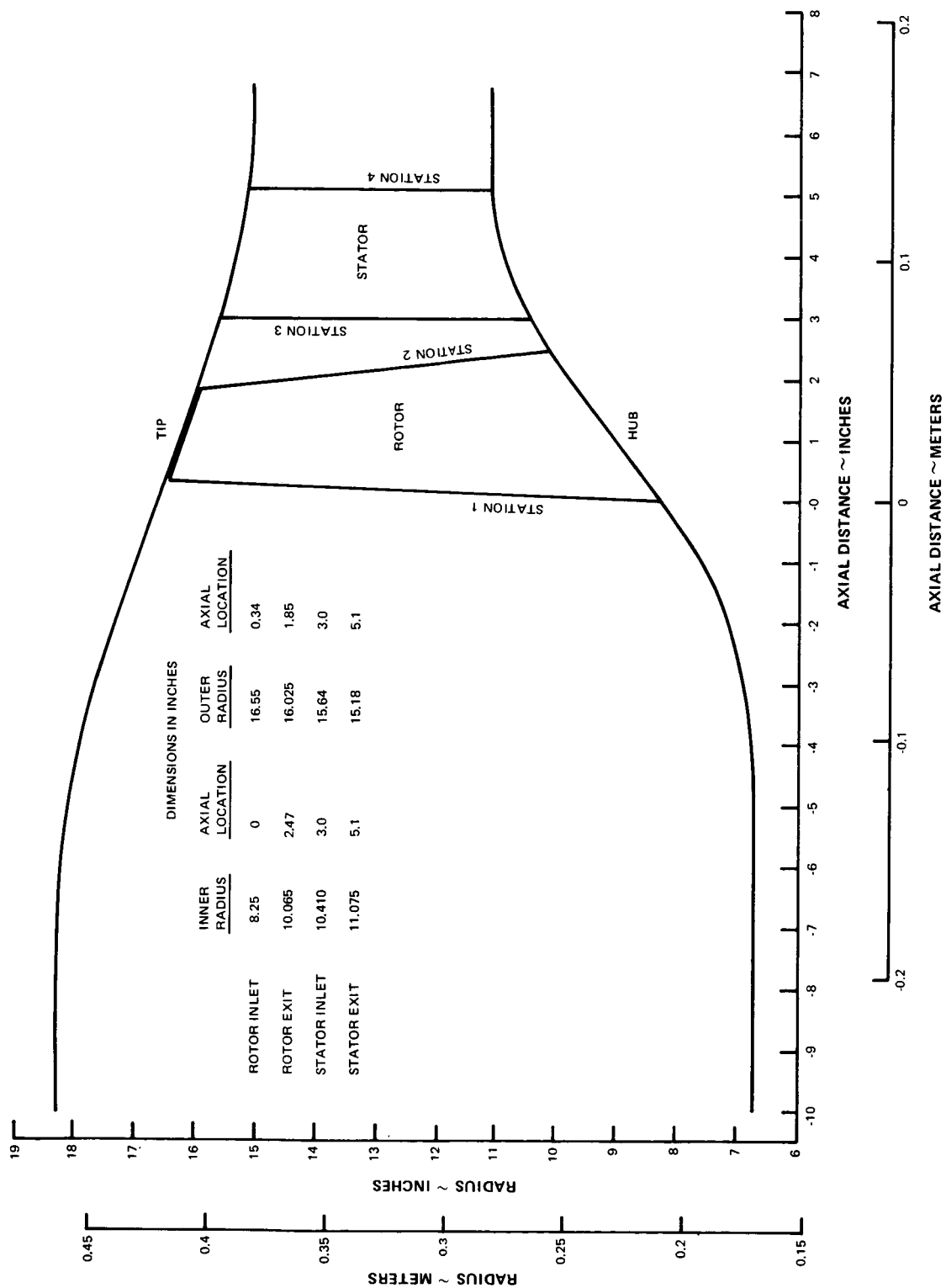


Figure 6 Rotor and Stator Portion of Flowpath

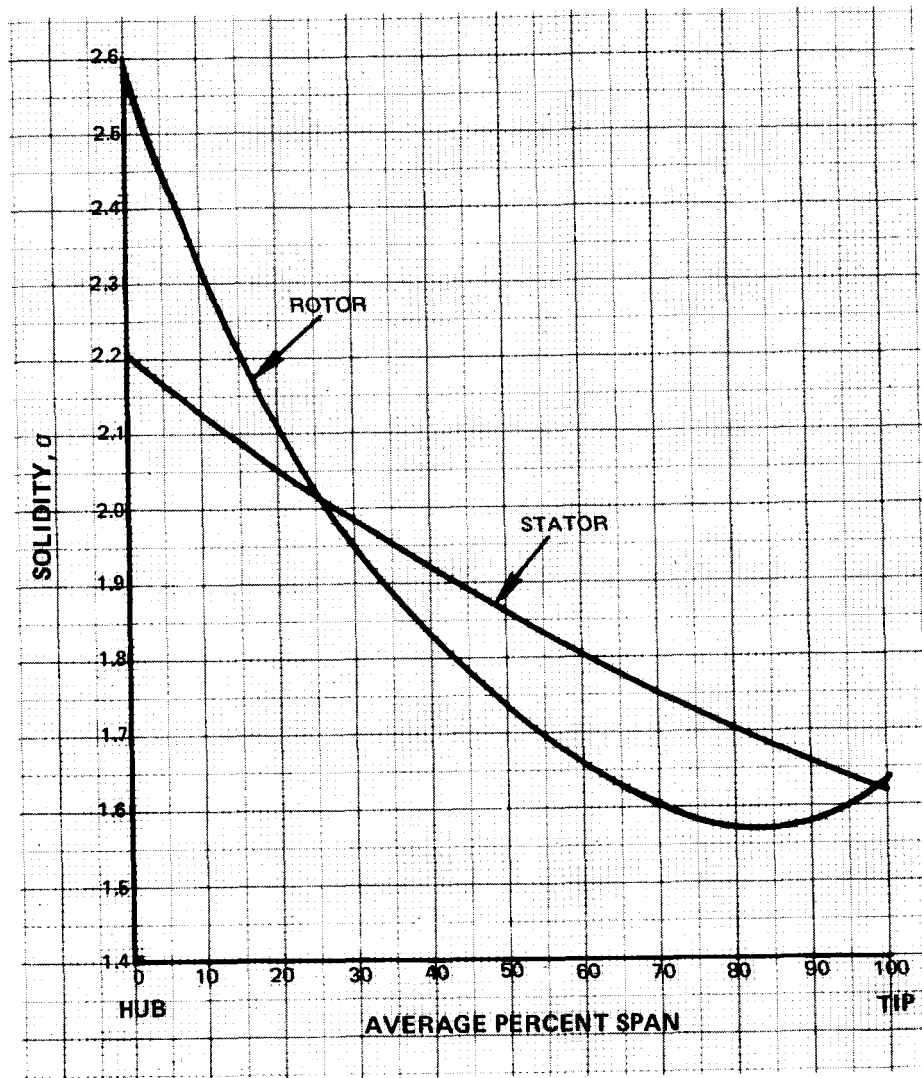


Figure 7 Rotor and Stator Solidities

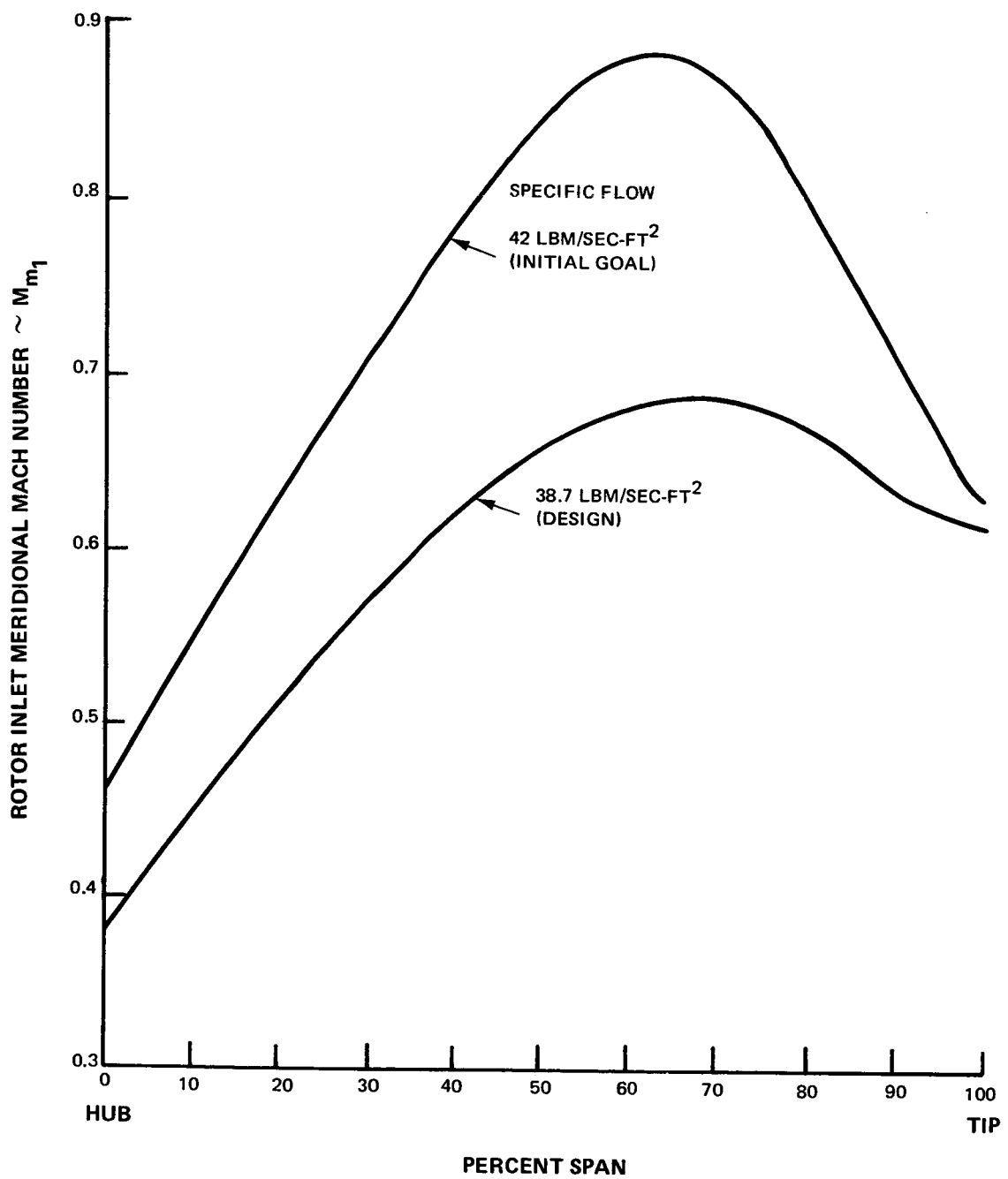


Figure 8 Rotor Inlet Meridional Mach Number Profile

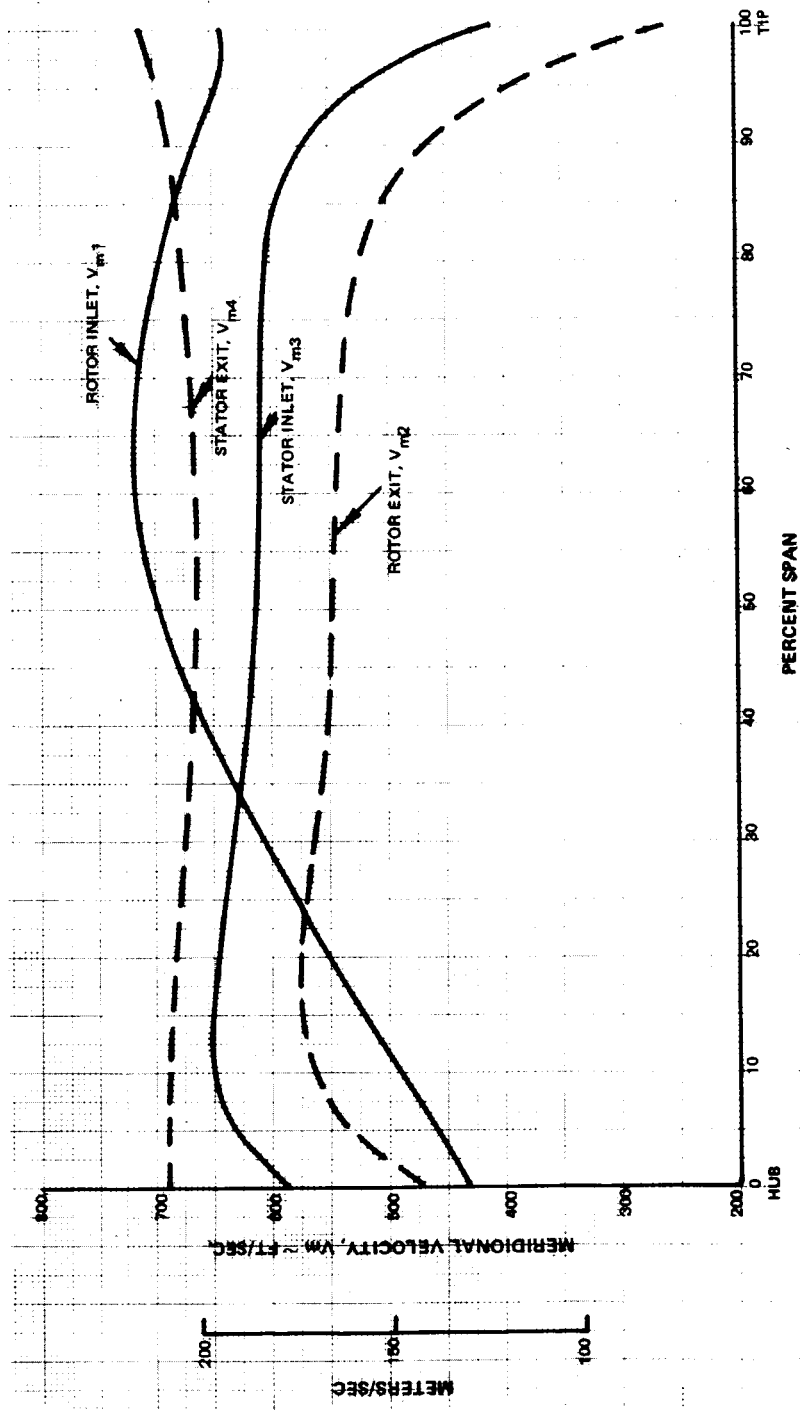


Figure 9 Rotor and Stator Inlet and Exit Meridional Velocity Profiles

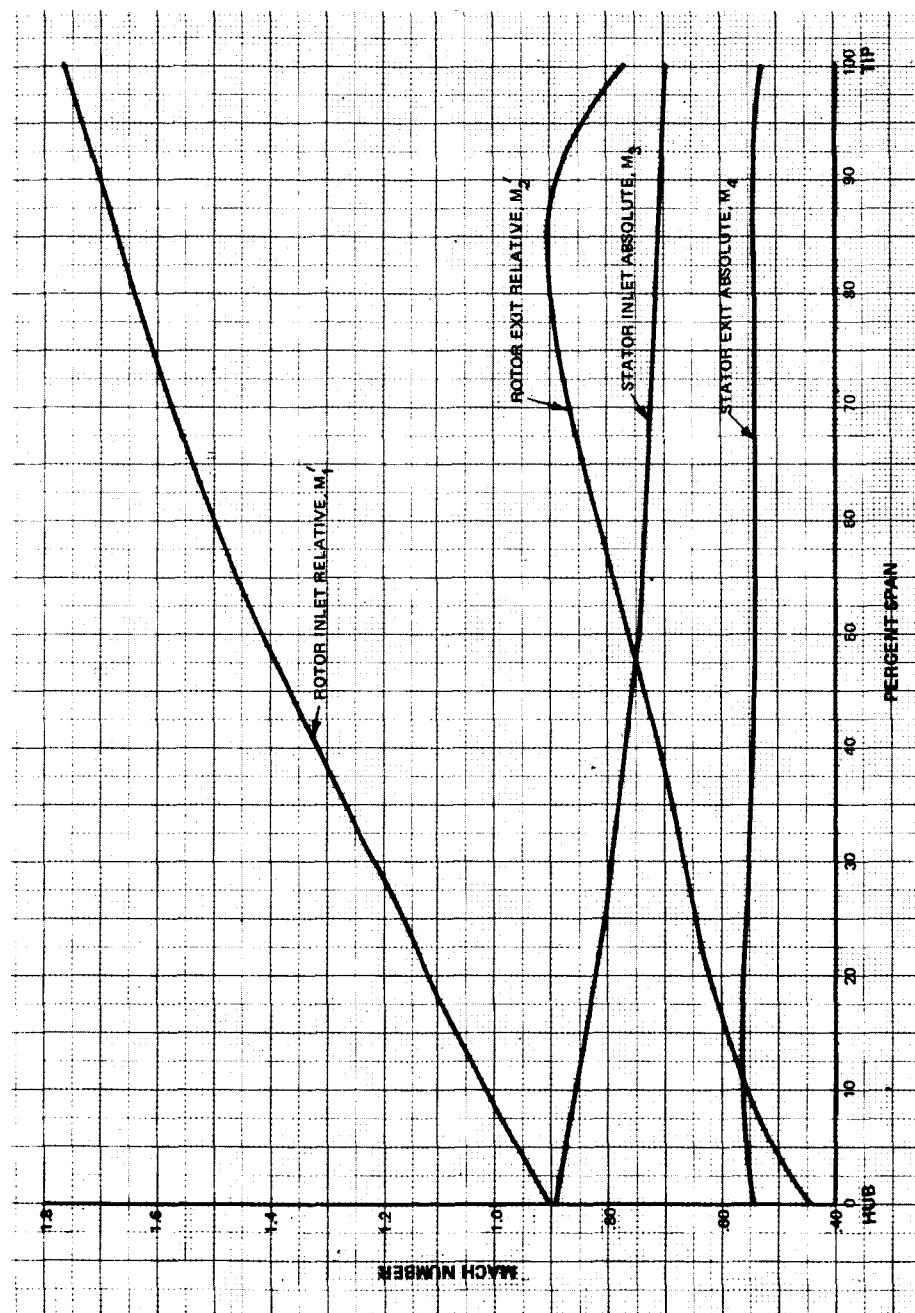


Figure 10 Rotor and Stator Mach Numbers

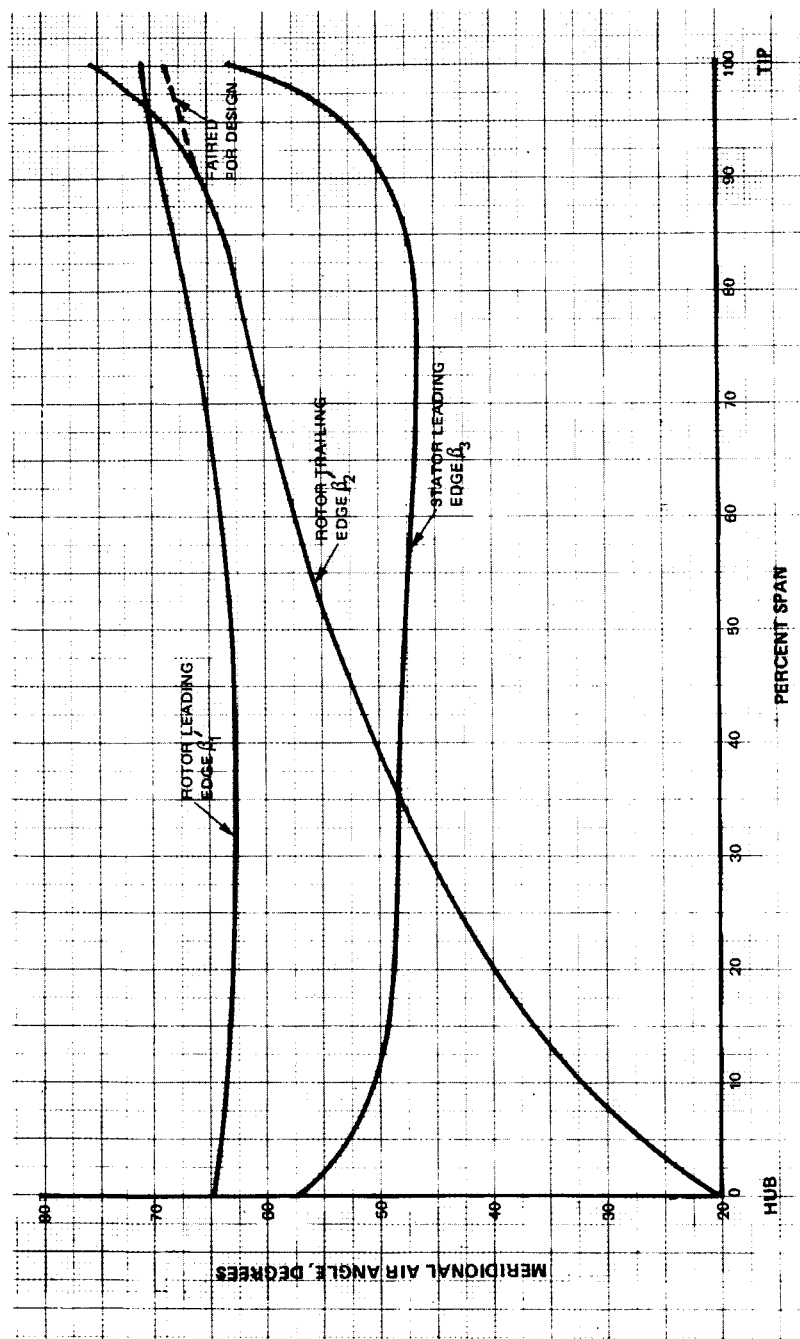


Figure 11 Rotor Inlet and Exit Relative and Stator Inlet Absolute Air Angles

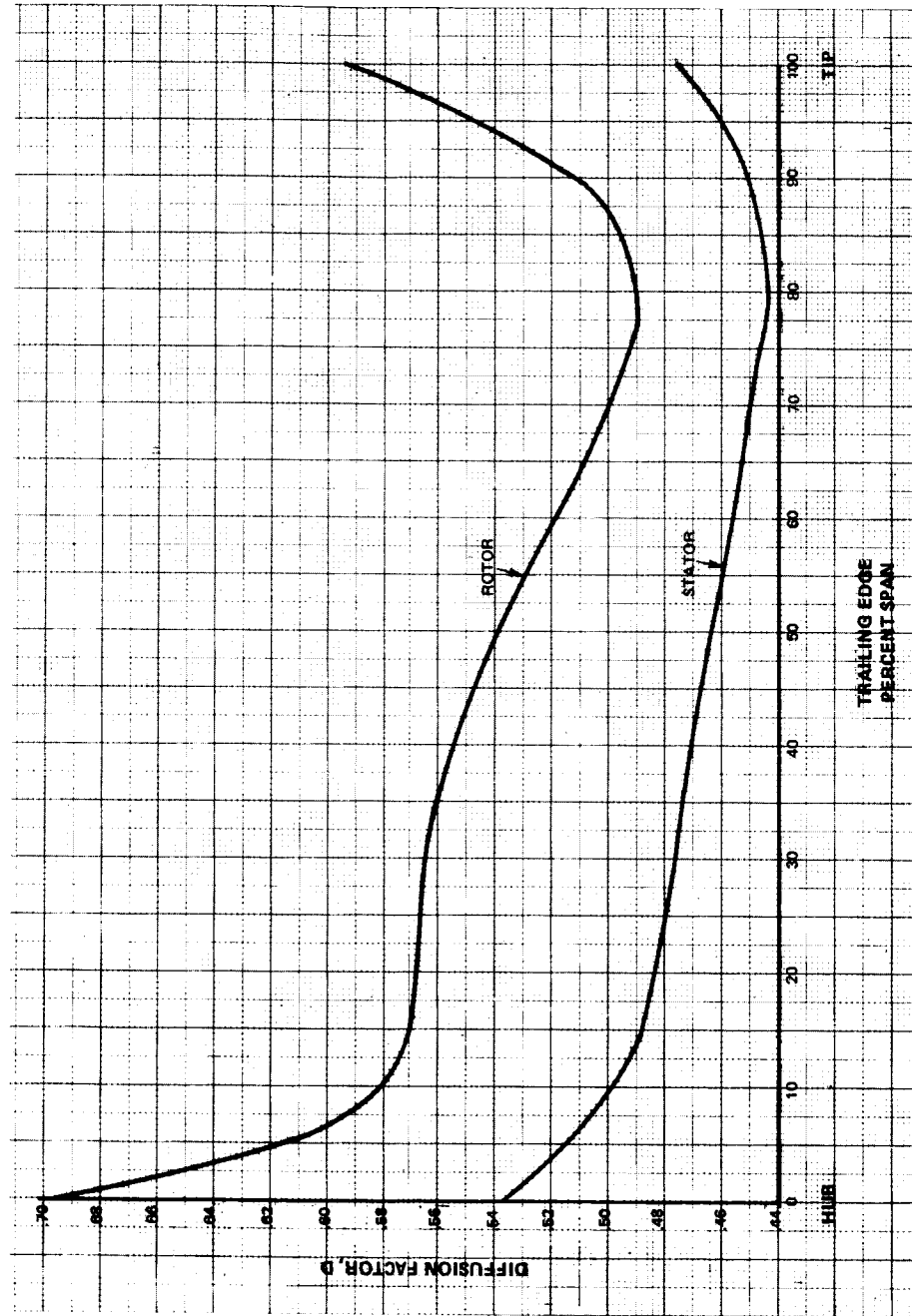


Figure 12 Rotor and Stator Diffusion Factors

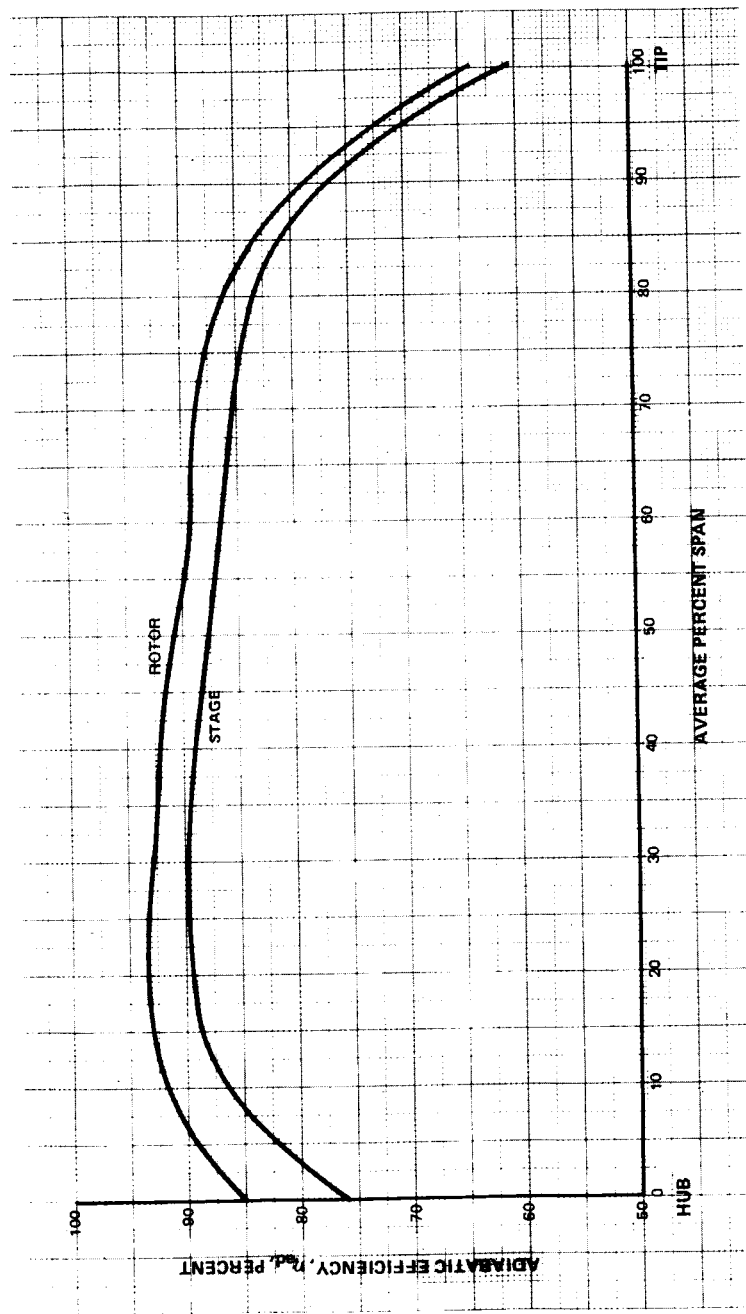


Figure 13 Rotor and Stage Efficiency

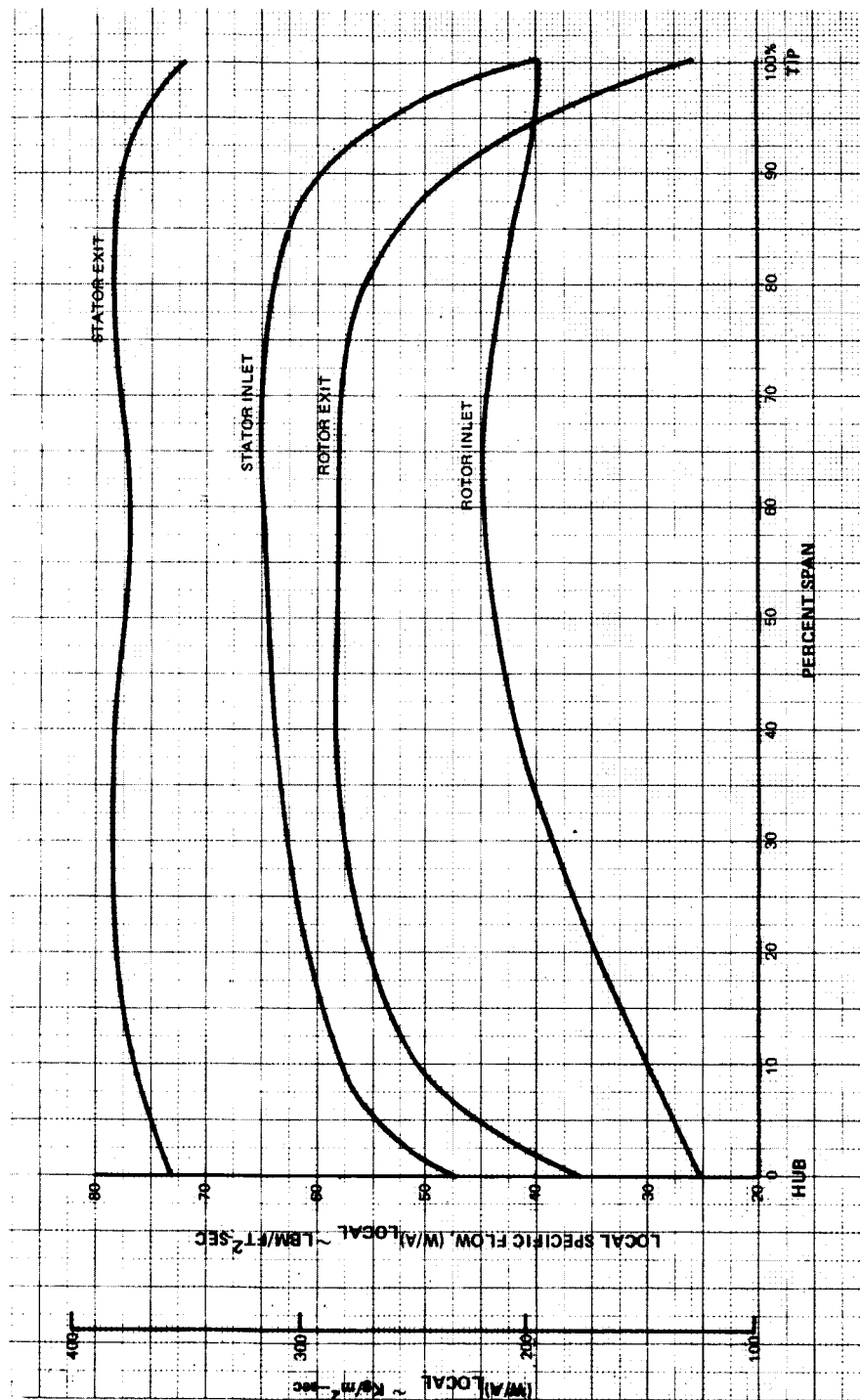


Figure 14 Rotor and Stator Spanwise Specific Flow, $W/A = \rho V_z$

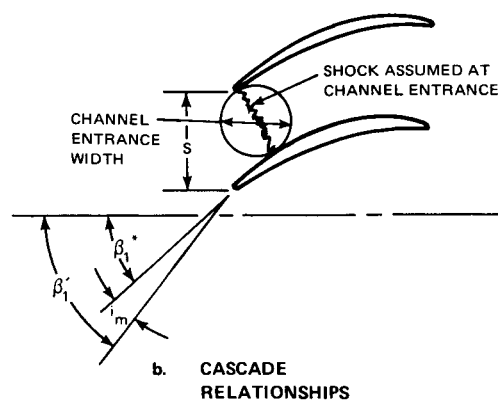
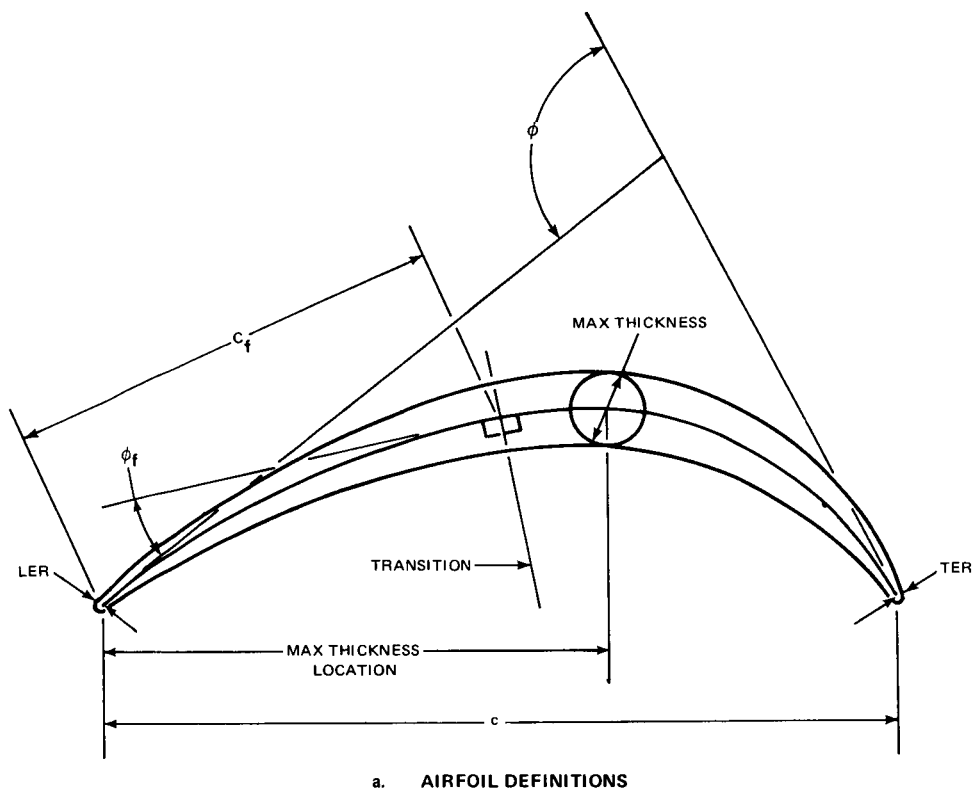


Figure 15 MCA Airfoil Definitions and Cascade Relationships

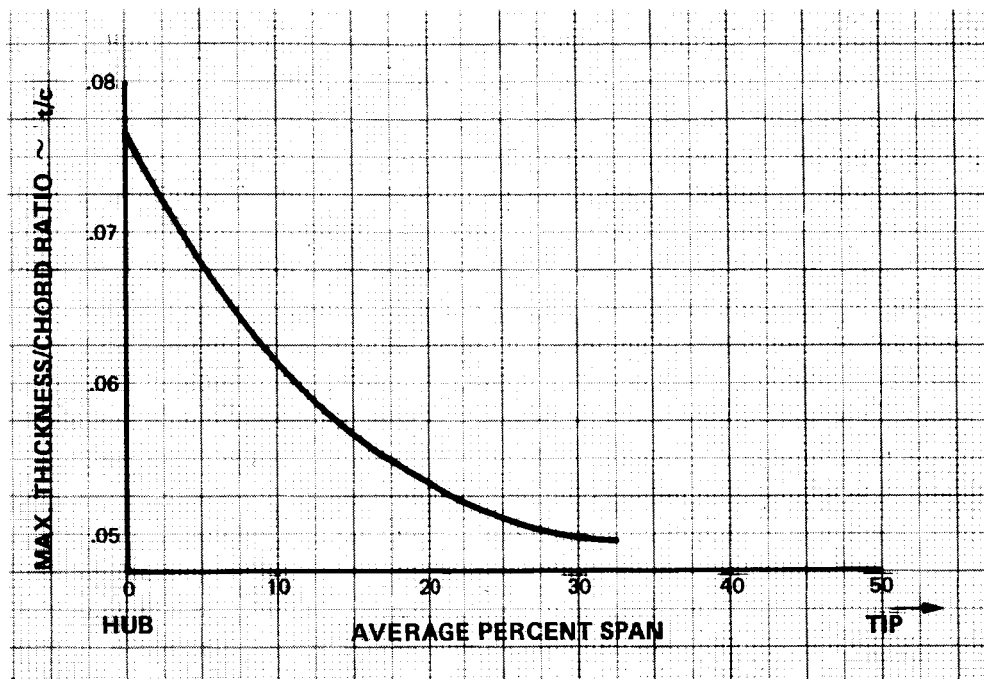


Figure 16 Maximum-Thickness to Chord Ratio for Modified MCA Rotor Blade Sections

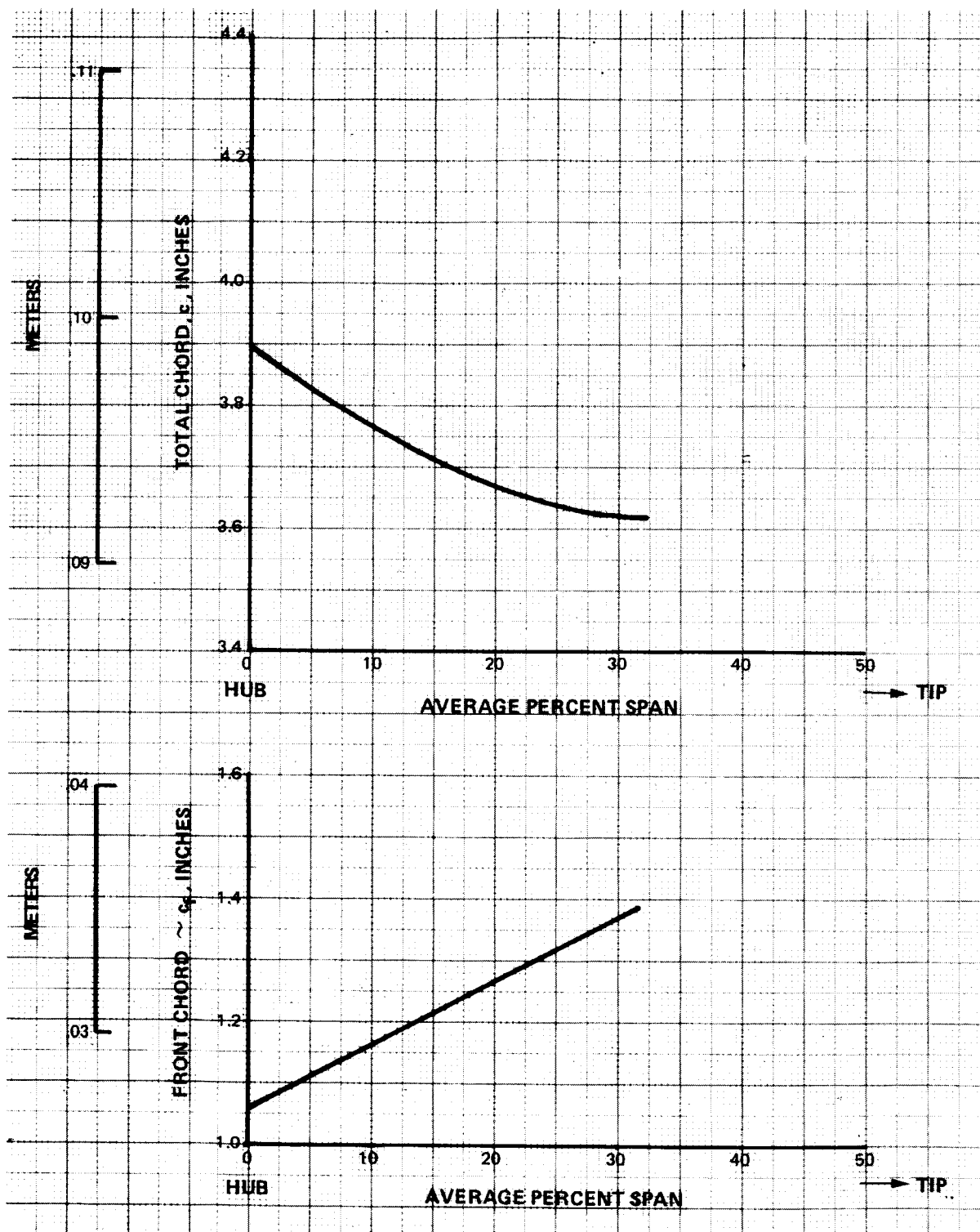


Figure 17 Total and Front Chord for Modified MCA Rotor Blade Sections

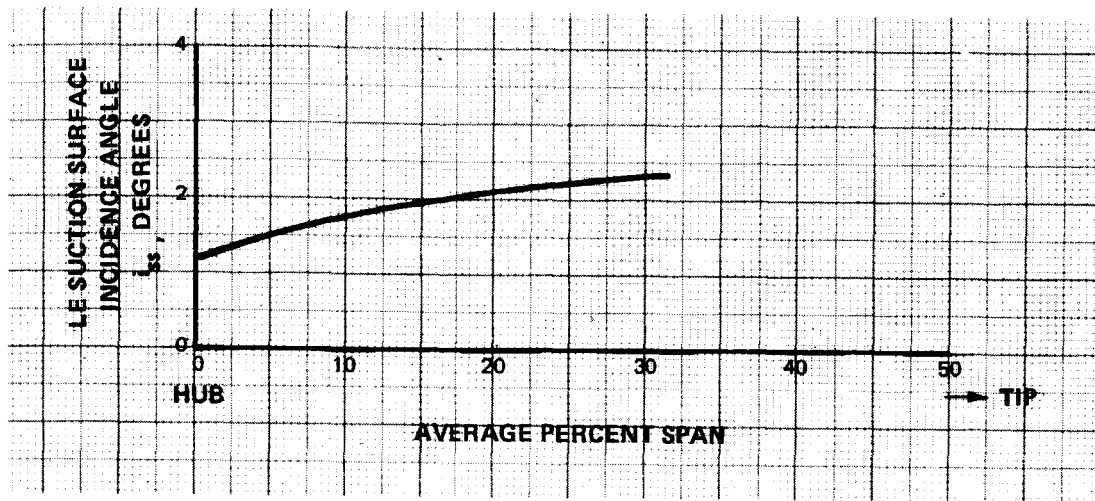


Figure 18 Suction Surface Incidence Angle for Modified MCA Rotor Blade Sections

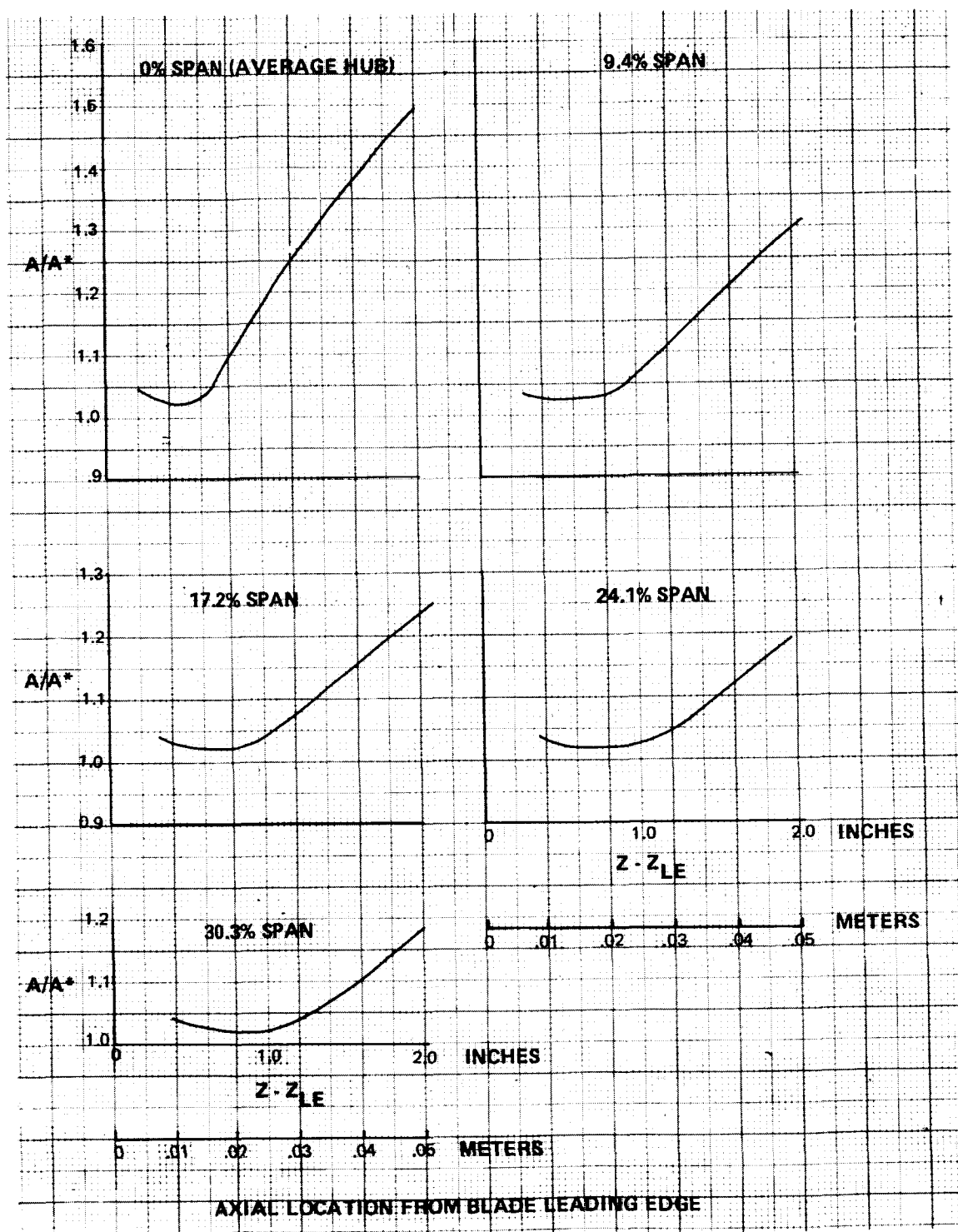


Figure 19 A/A^* Distribution for Modified MCA Rotor Blade Sections

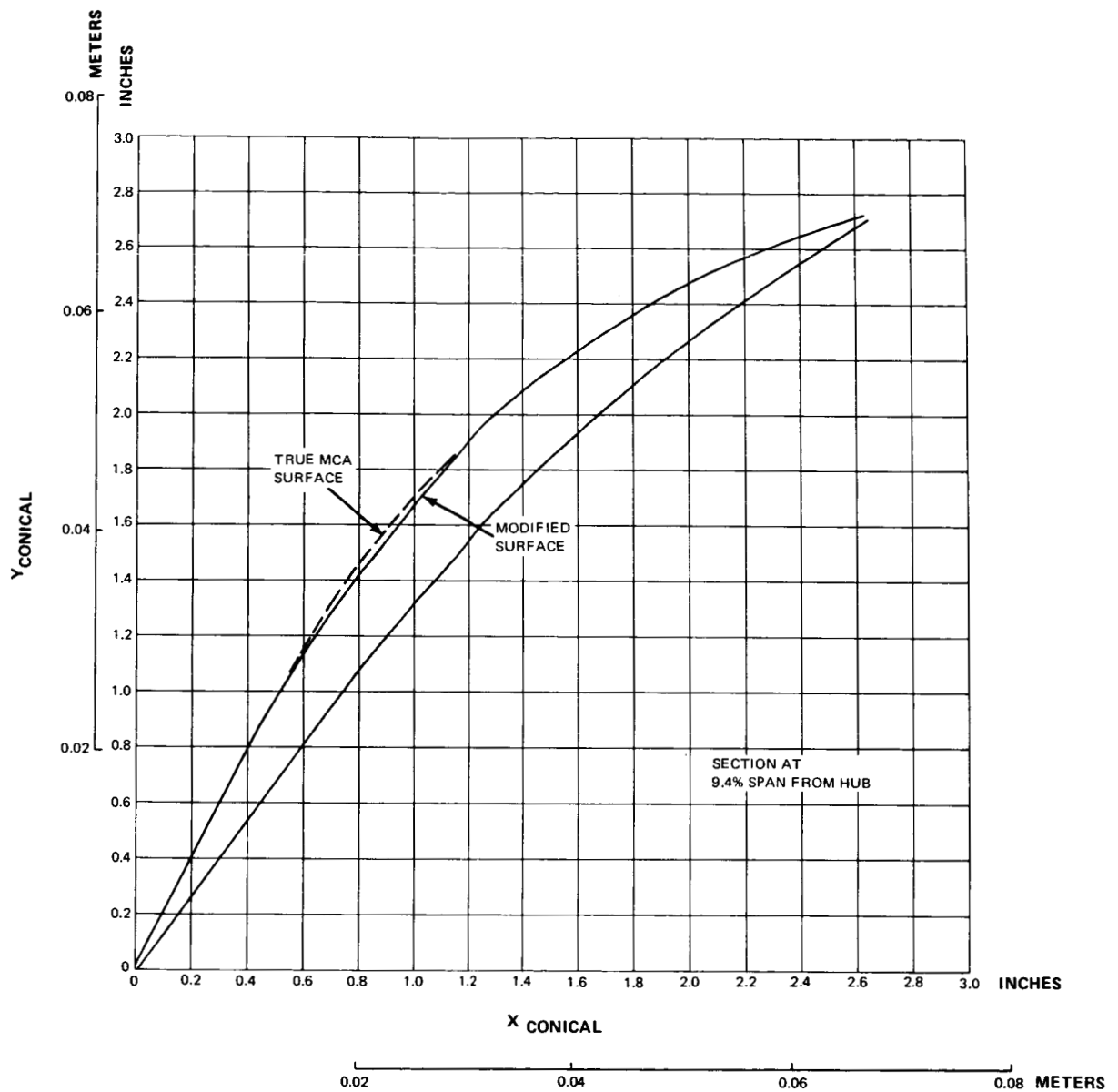


Figure 20 Modified MCA Blade Section on Unwrapped Conical Surface

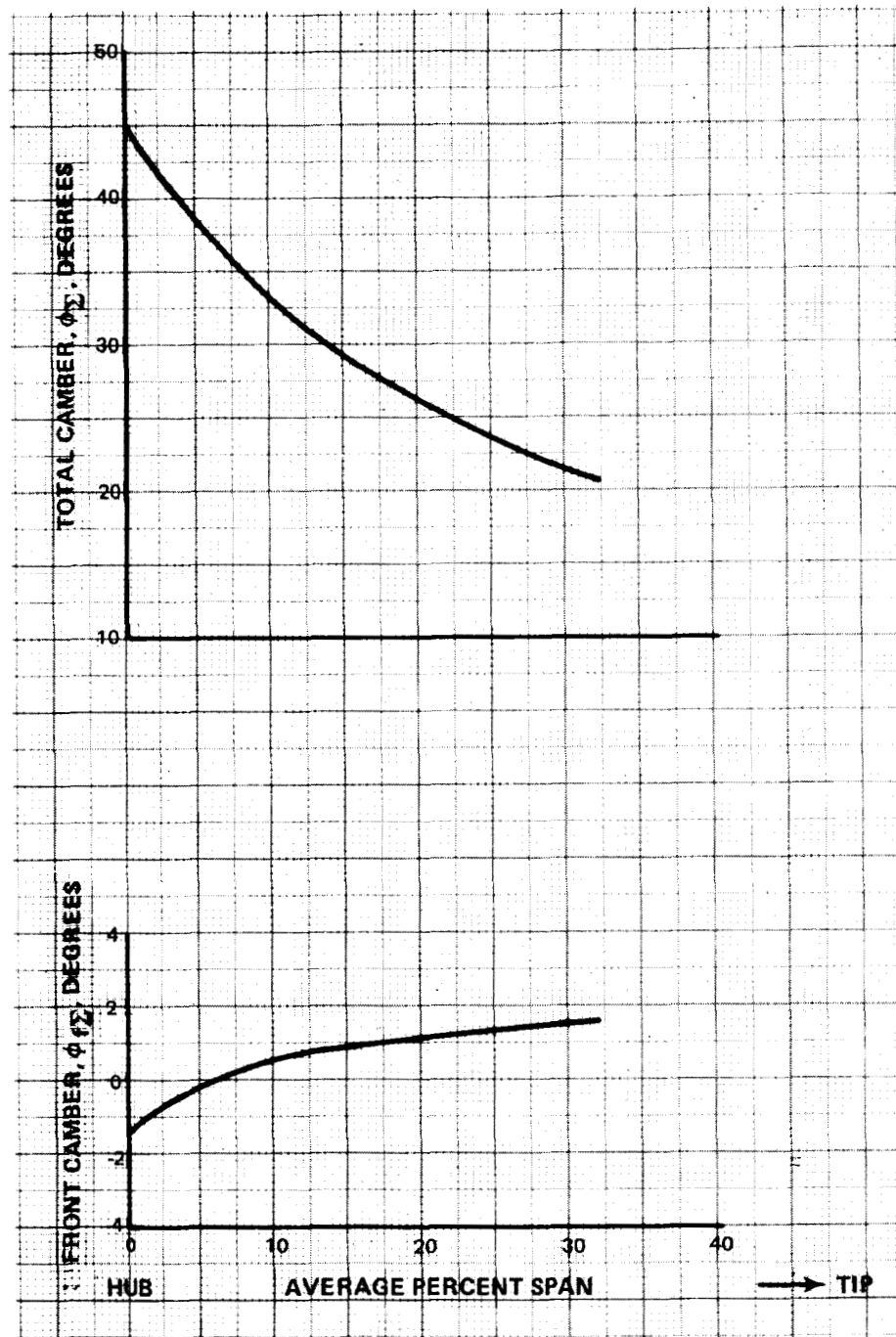


Figure 21 Total and Front Camber Angle Distributions for Modified MCA Rotor Blade Sections

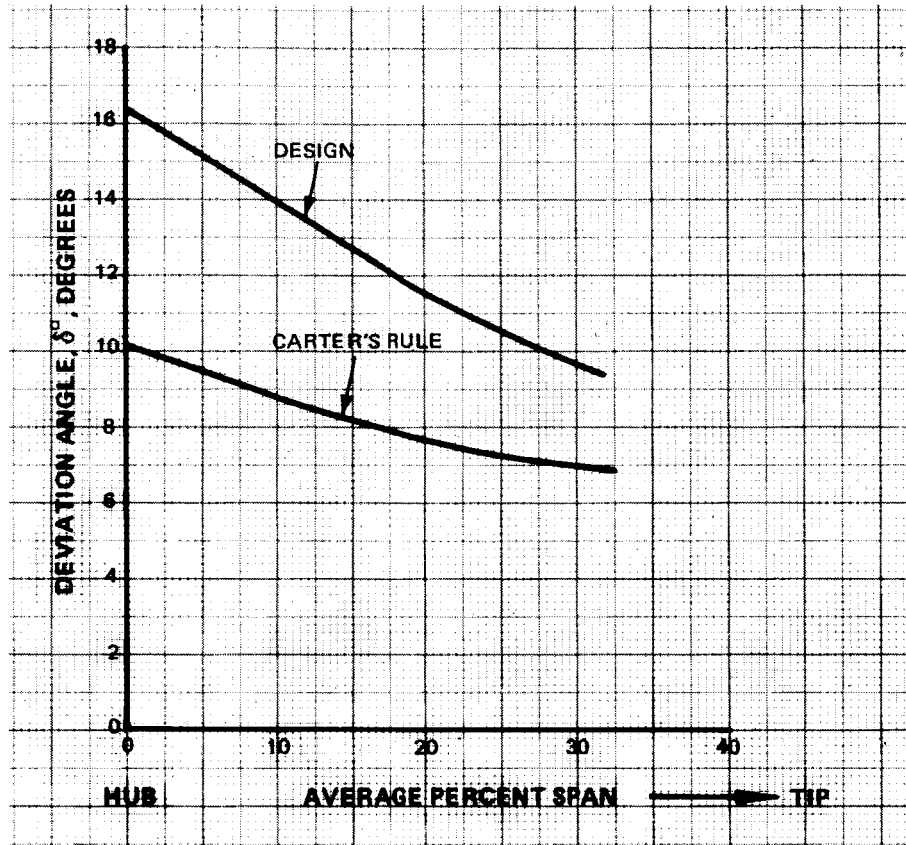


Figure 22 Deviation Angles for Modified MCA Rotor Sections and Comparison with Carter's Rule

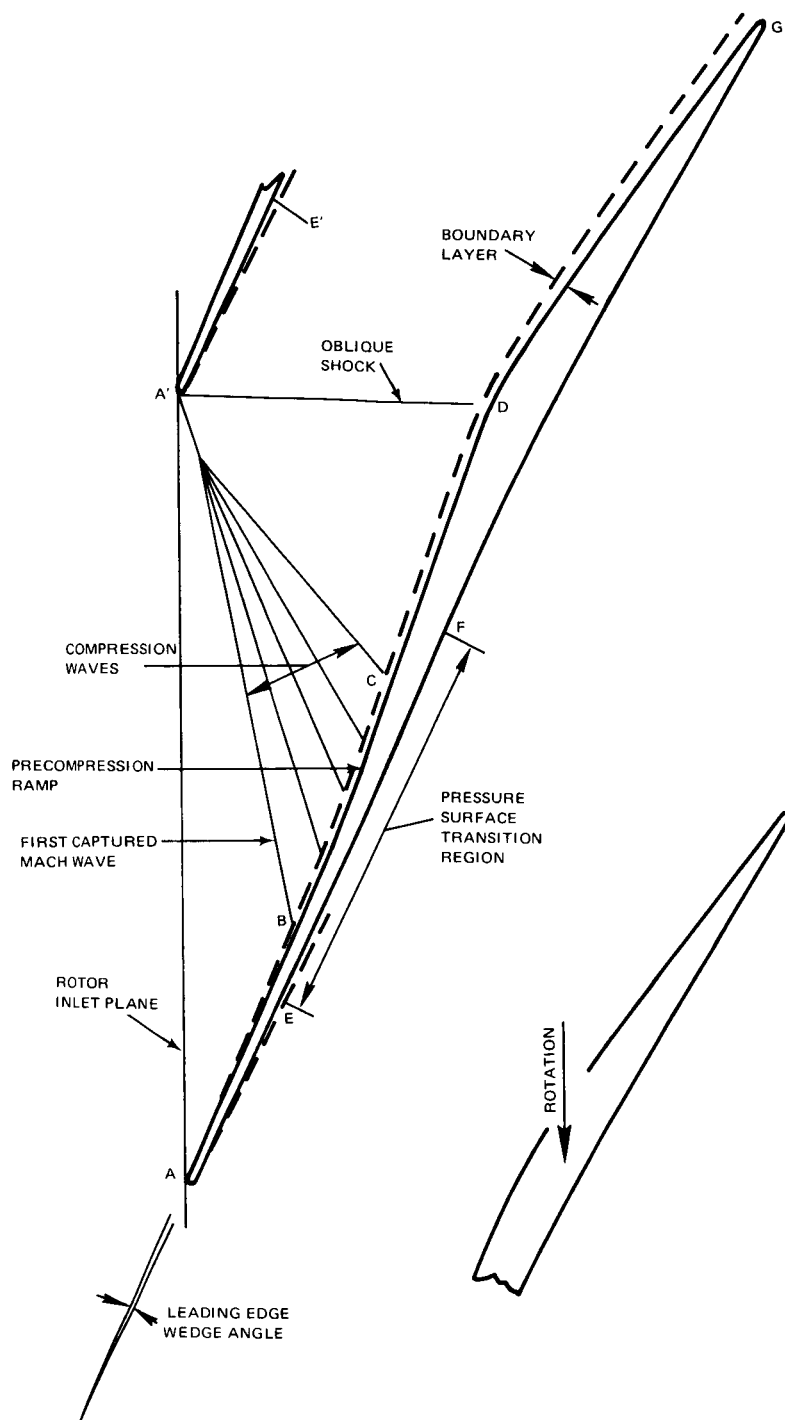


Figure 23 Precompression Blade Airfoil Terminology

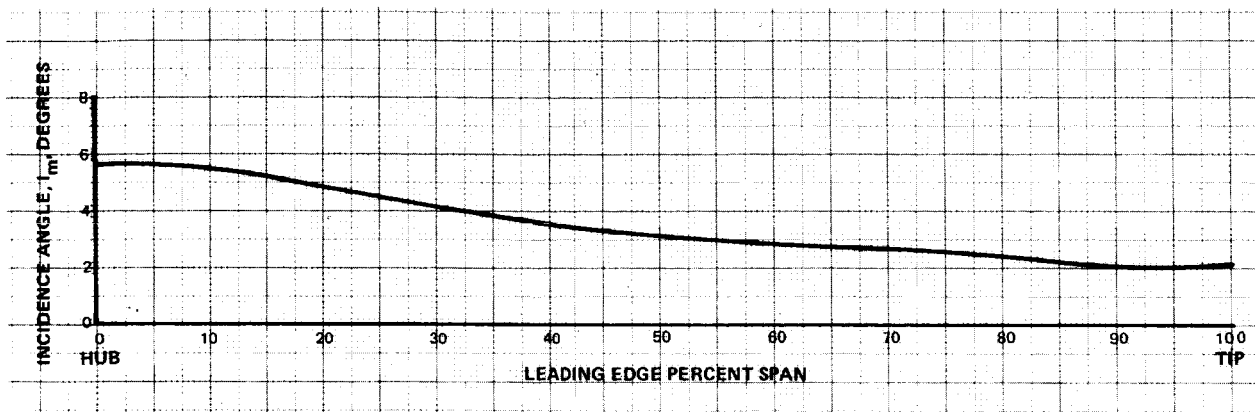


Figure 24 Rotor Blade Mean Camber Line Incidence Angle

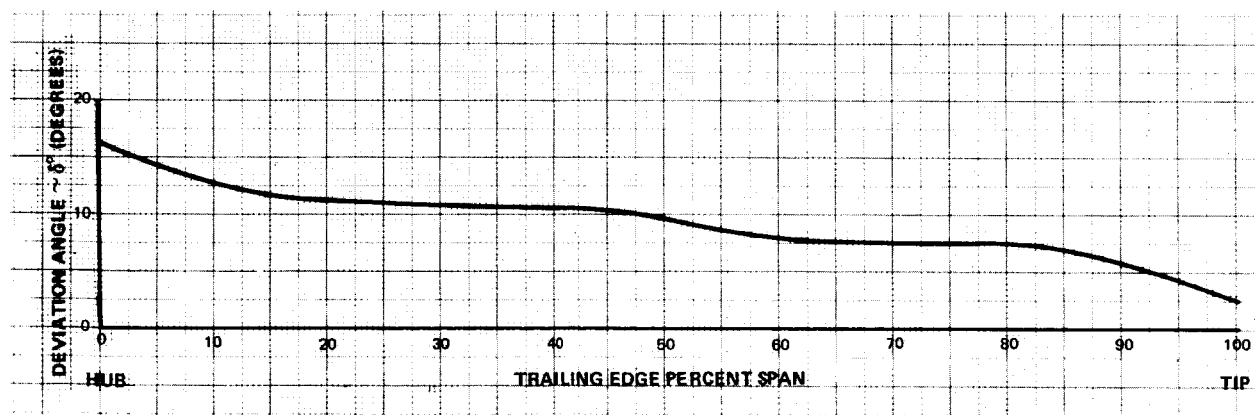


Figure 25 Rotor Blade Mean Camber Line Deviation Angle

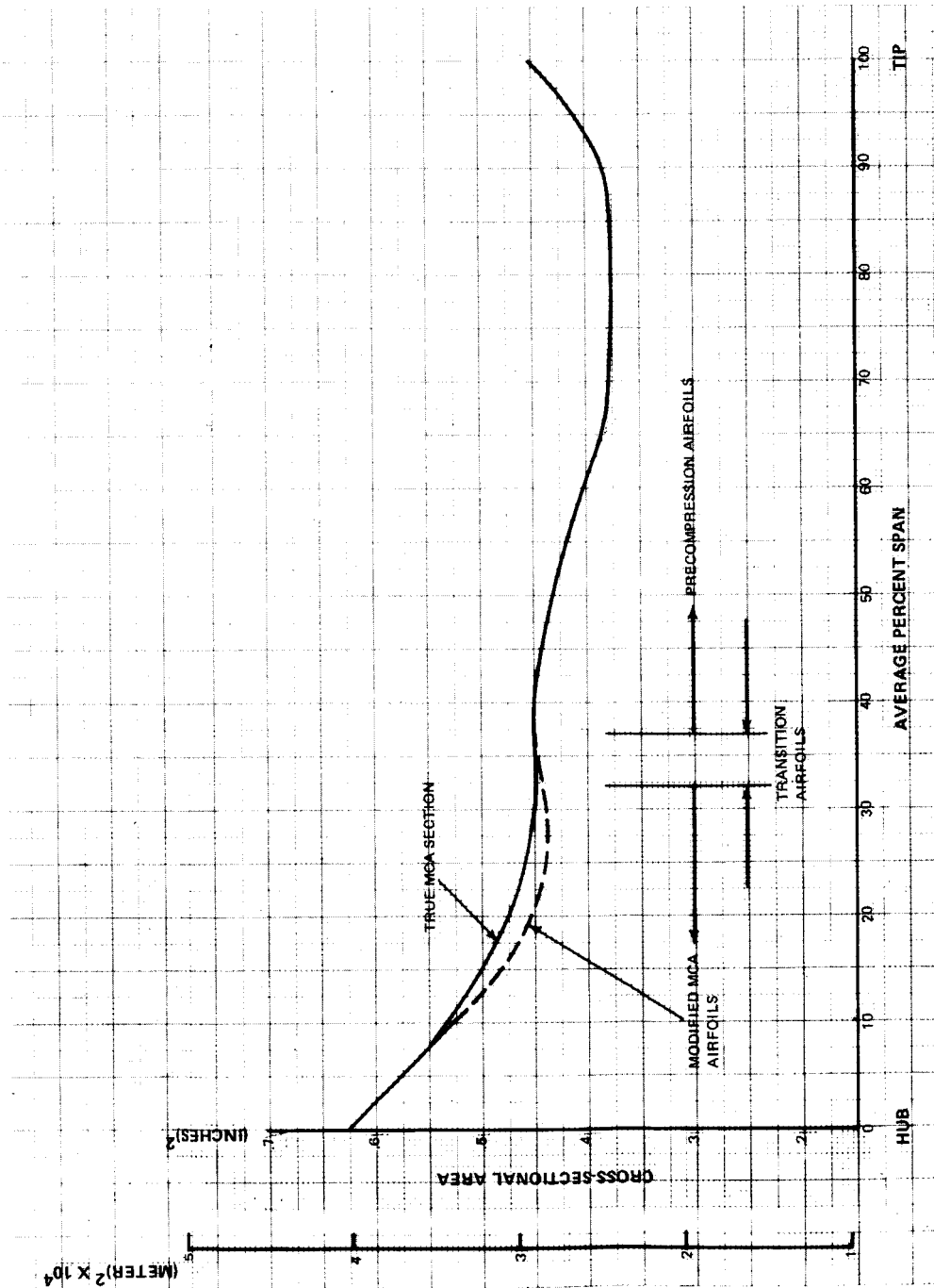


Figure 26 Rotor Blade Cross-Sectional Area Normal to Radial Line

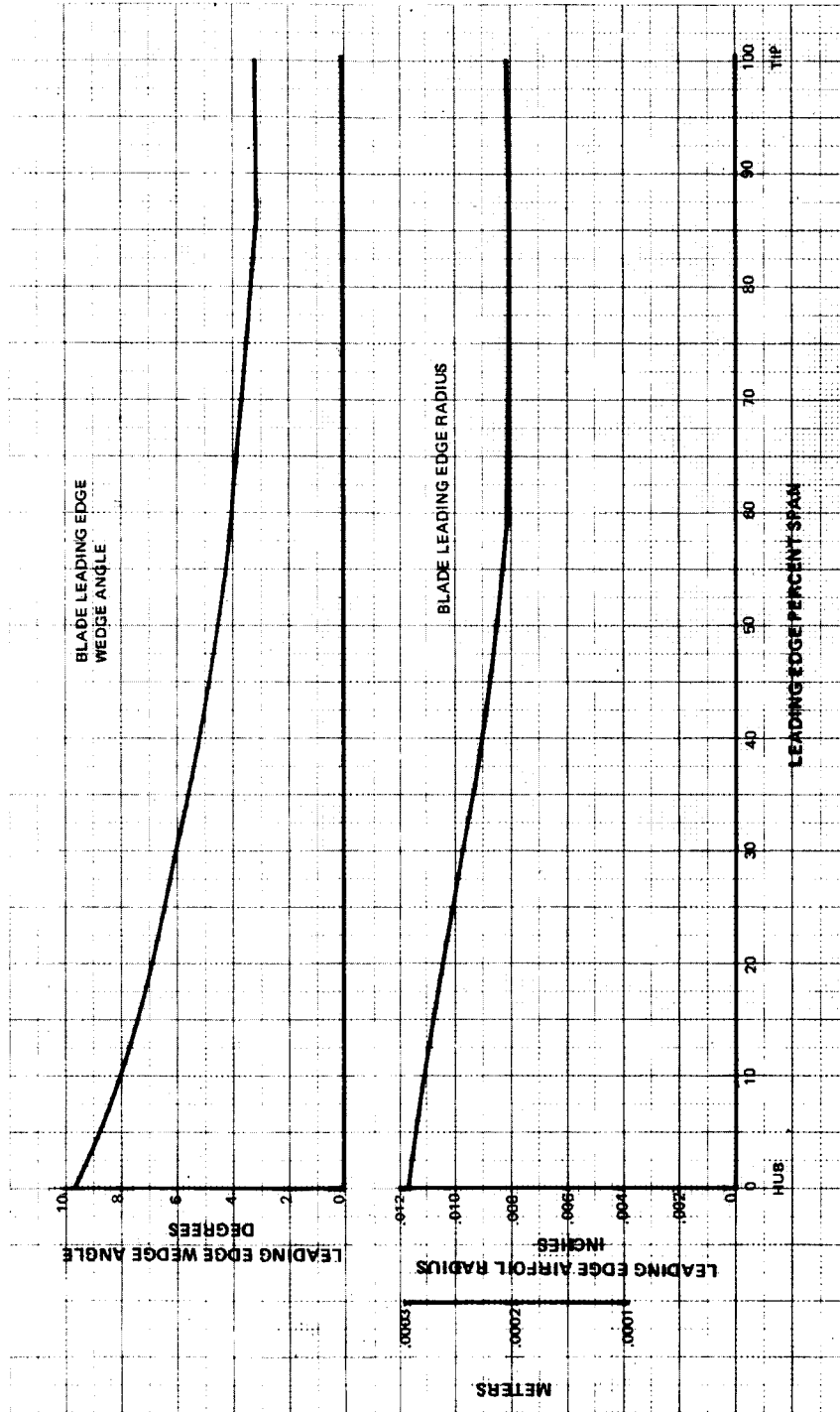


Figure 27 Rotor Blade Leading Edge Wedge Angle and Leading Edge Airfoil Radius

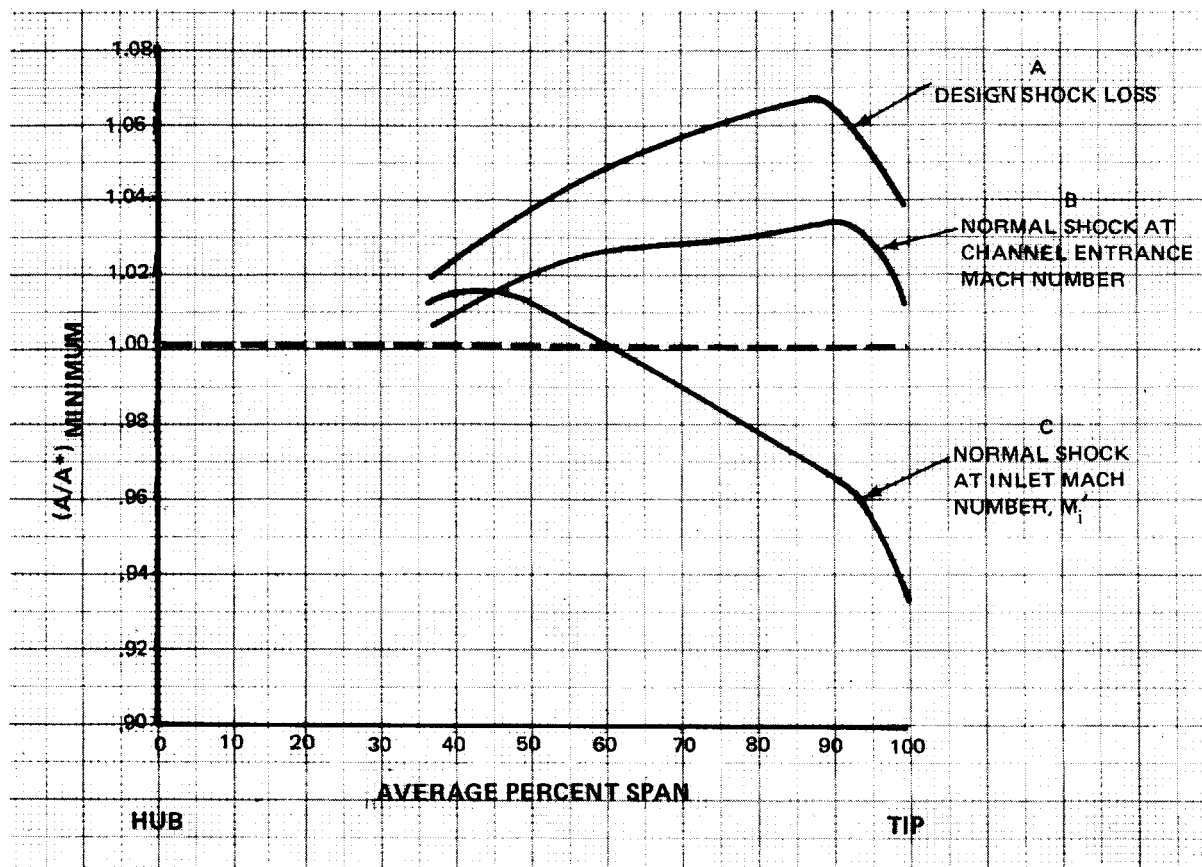


Figure 28 Rotor Blade Spanwise $(A/A^*)_{min}$ for Various Assumed Shock Losses

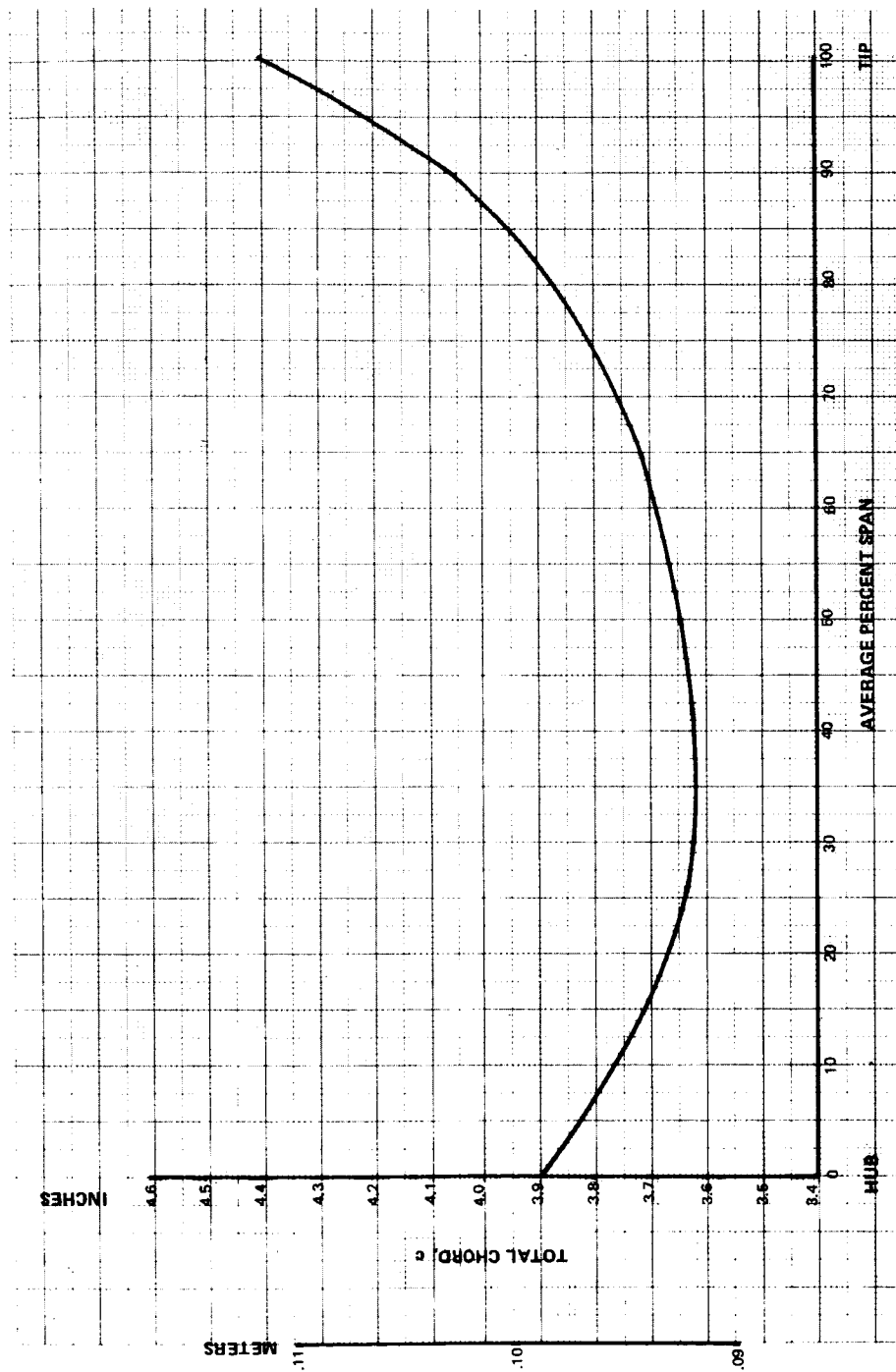


Figure 29 Rotor Blade Chord on Conical Surfaces

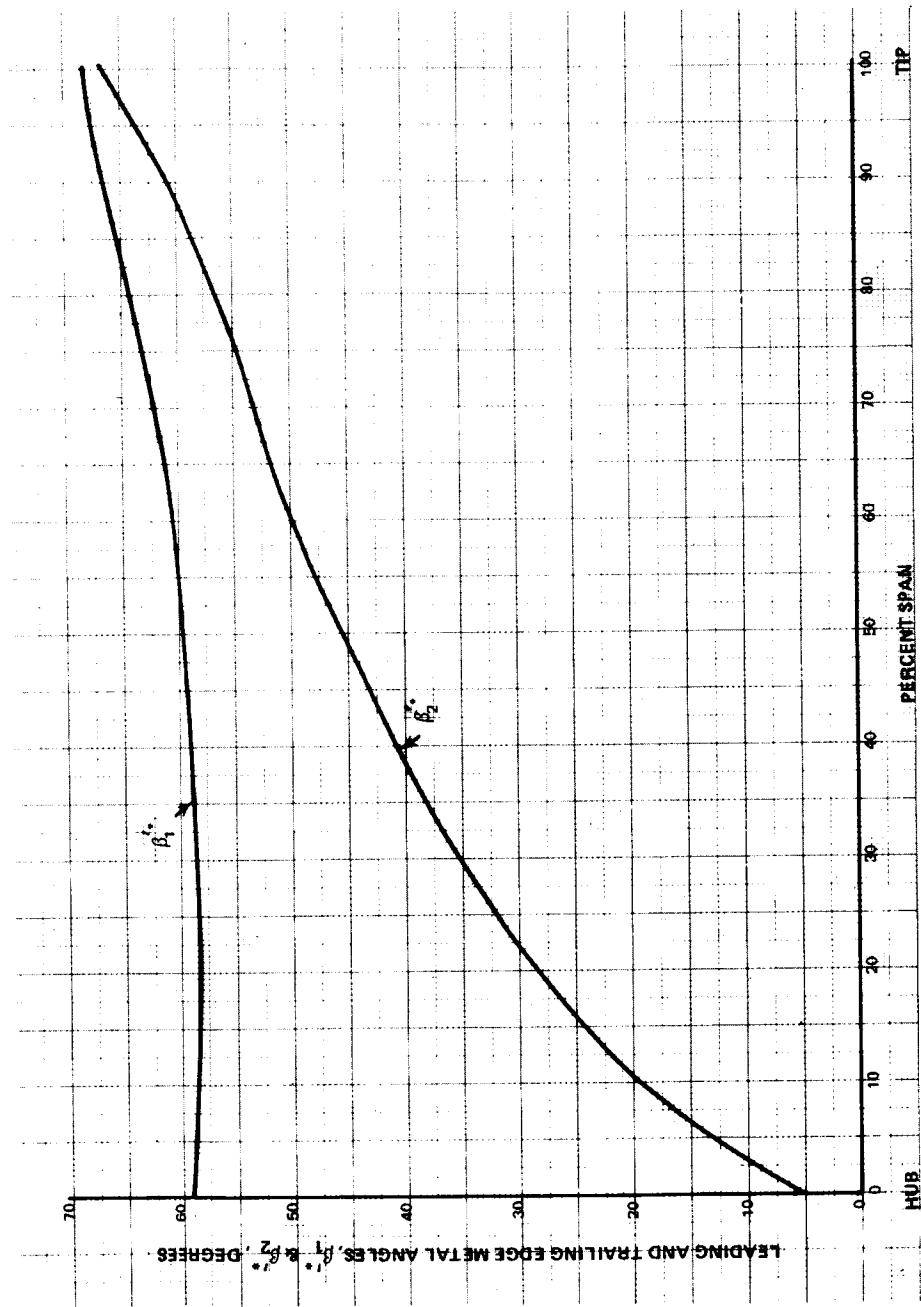


Figure 30 Rotor Blade Leading and Trailing Edge Metal Angles

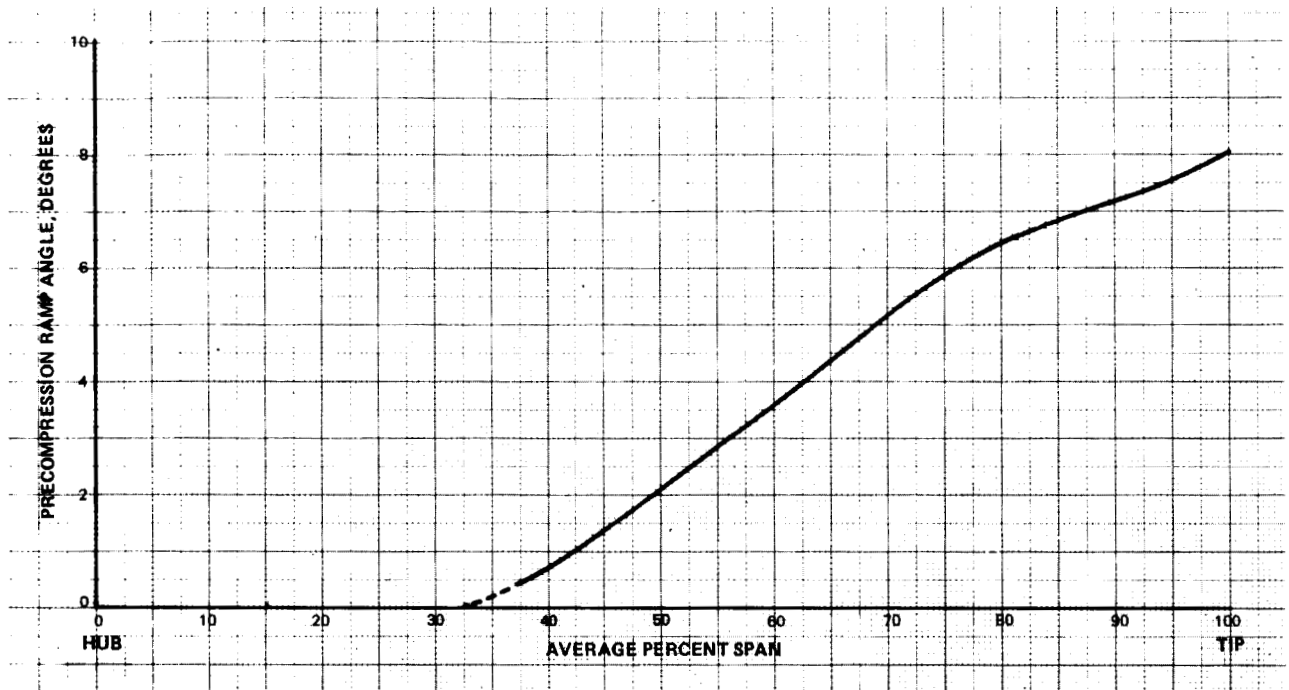


Figure 31 Rotor Blade Precompression Ramp Angle

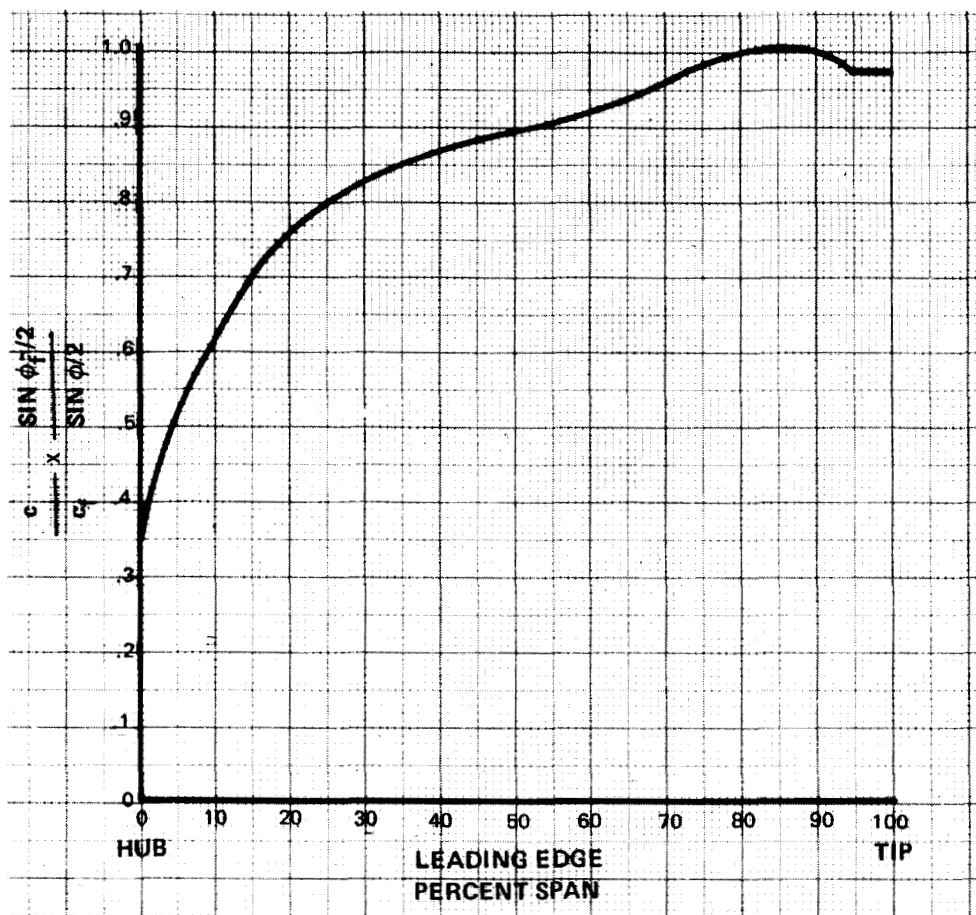


Figure 32 Chord-Camber Parameter for Stator Vane

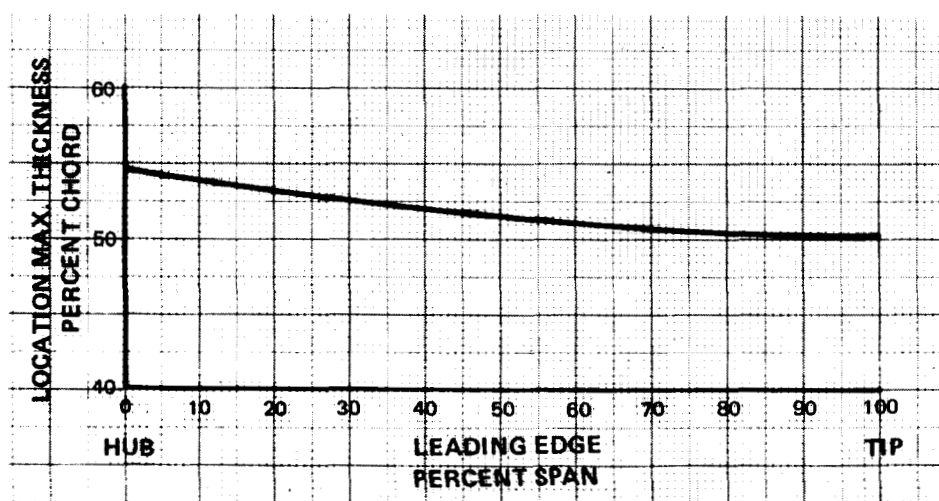


Figure 33 Location of Maximum Thickness for Stator Vane

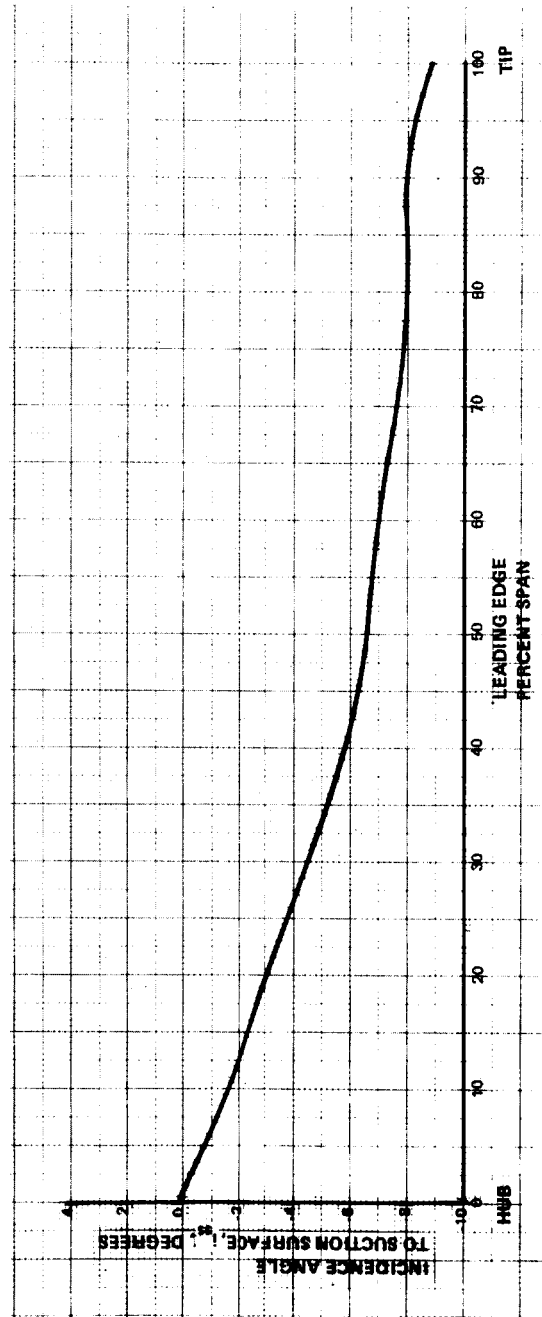


Figure 34 Stator Vane Suction Surface Incidence Angle

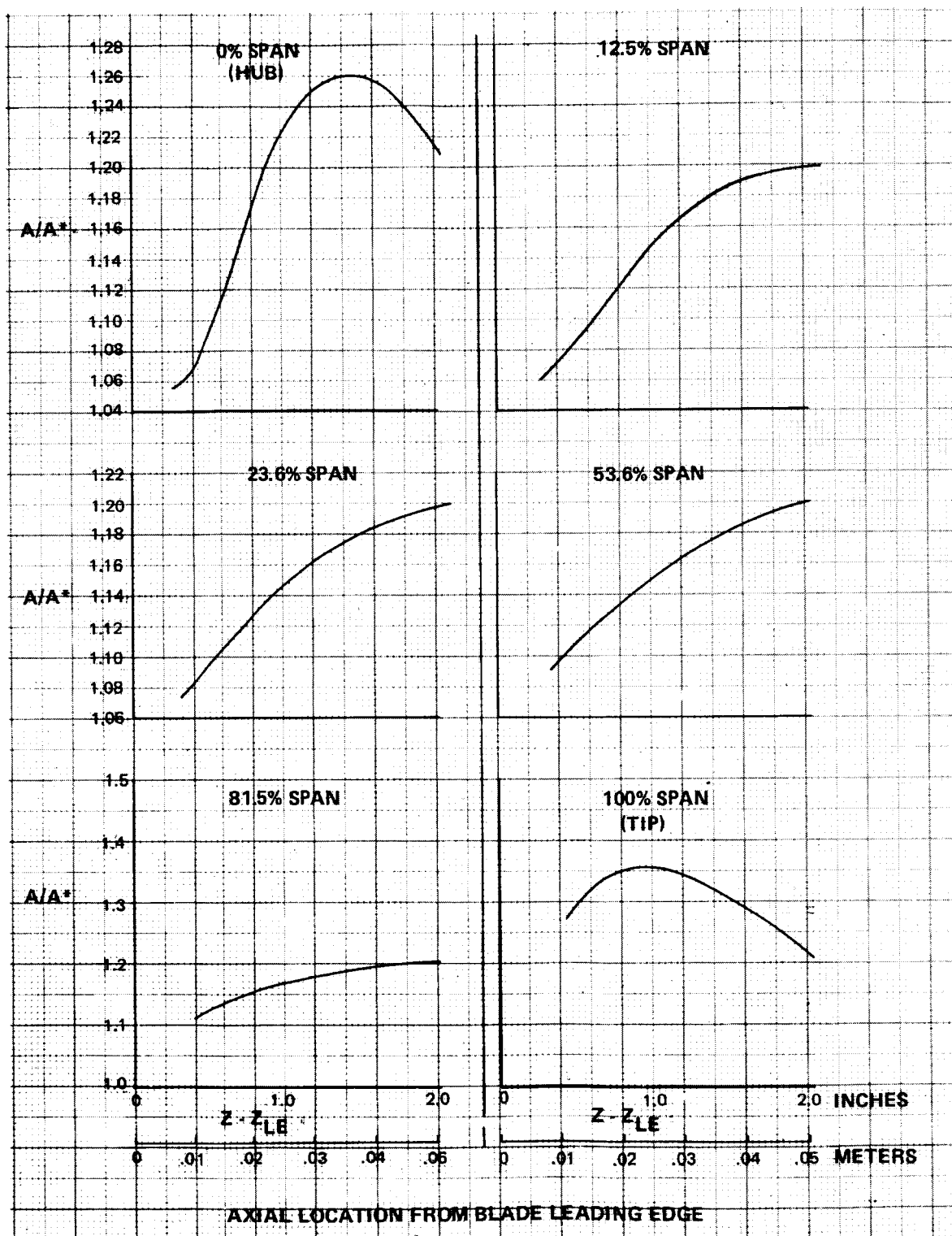


Figure 35 Stator Vane Distribution of A/A^*

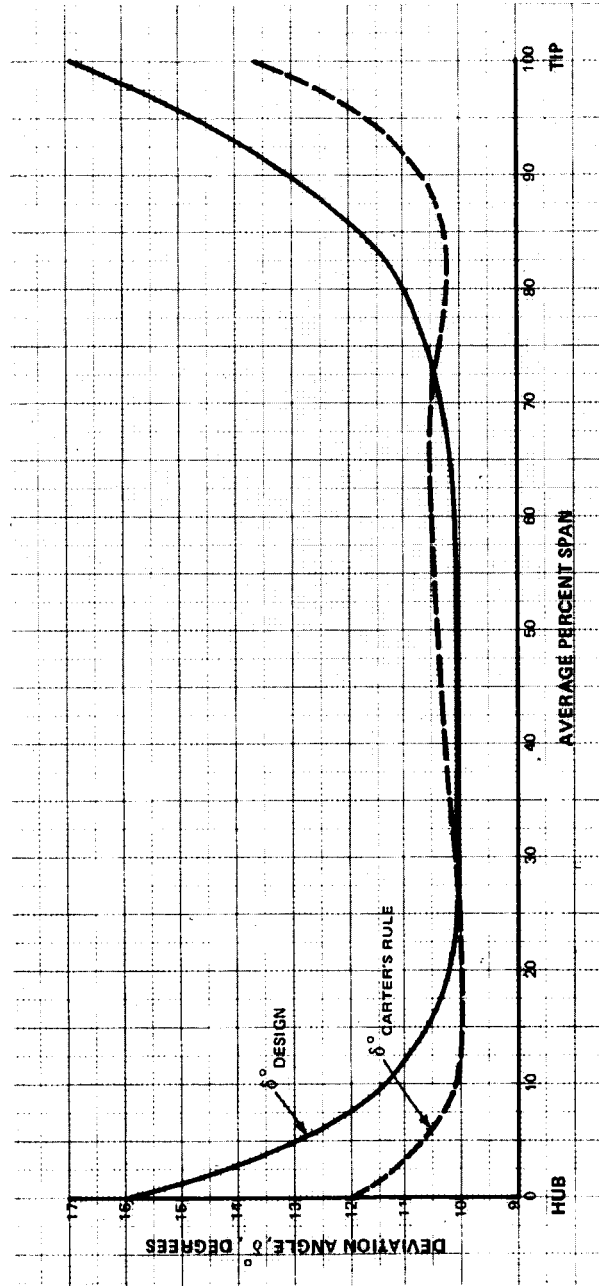


Figure 36 Stator Vane Deviation Angle and Comparison with Carter's Rule

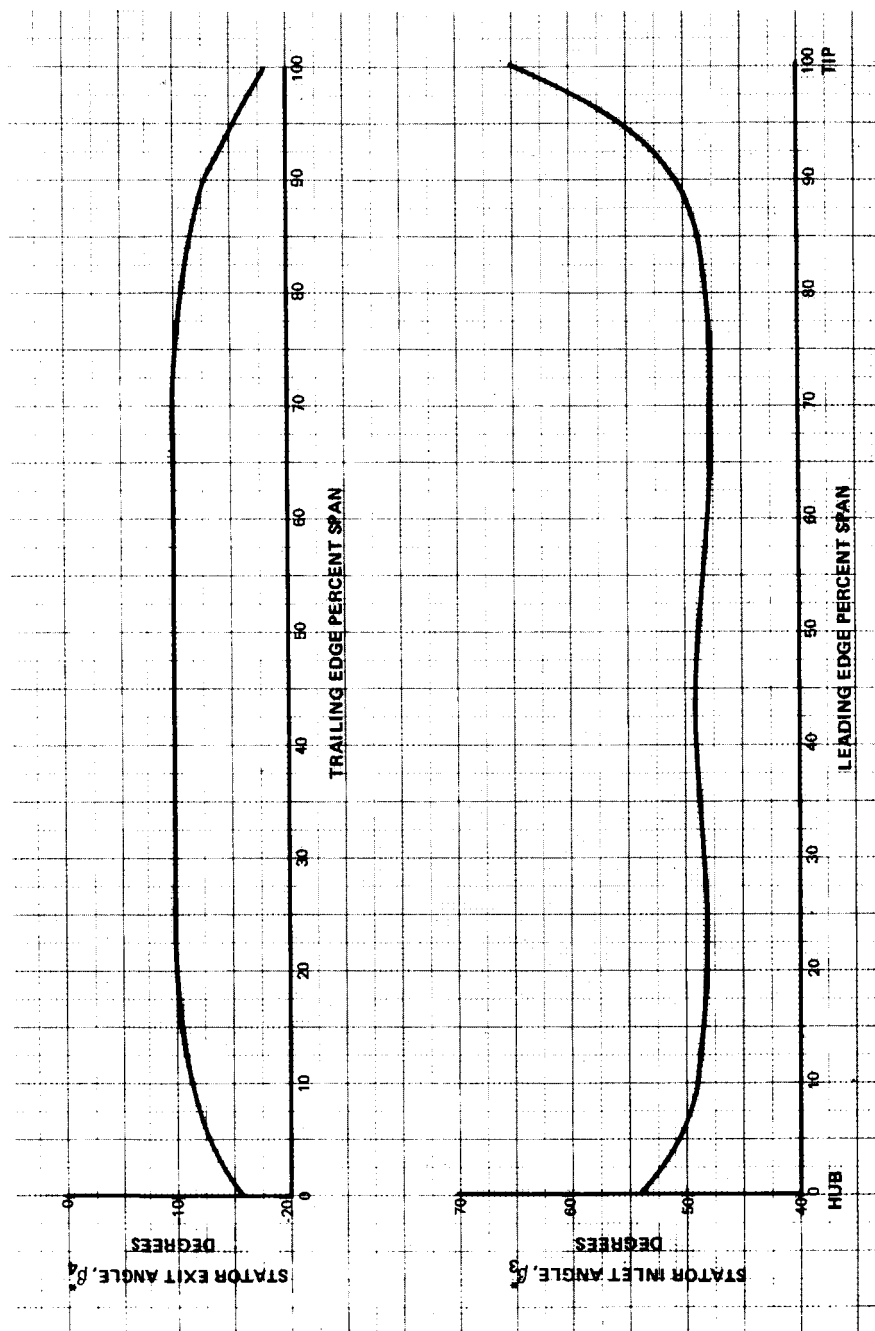


Figure 37 Stator Vane Inlet and Exit Mean Camber Line Metal Angles on Conical Surfaces

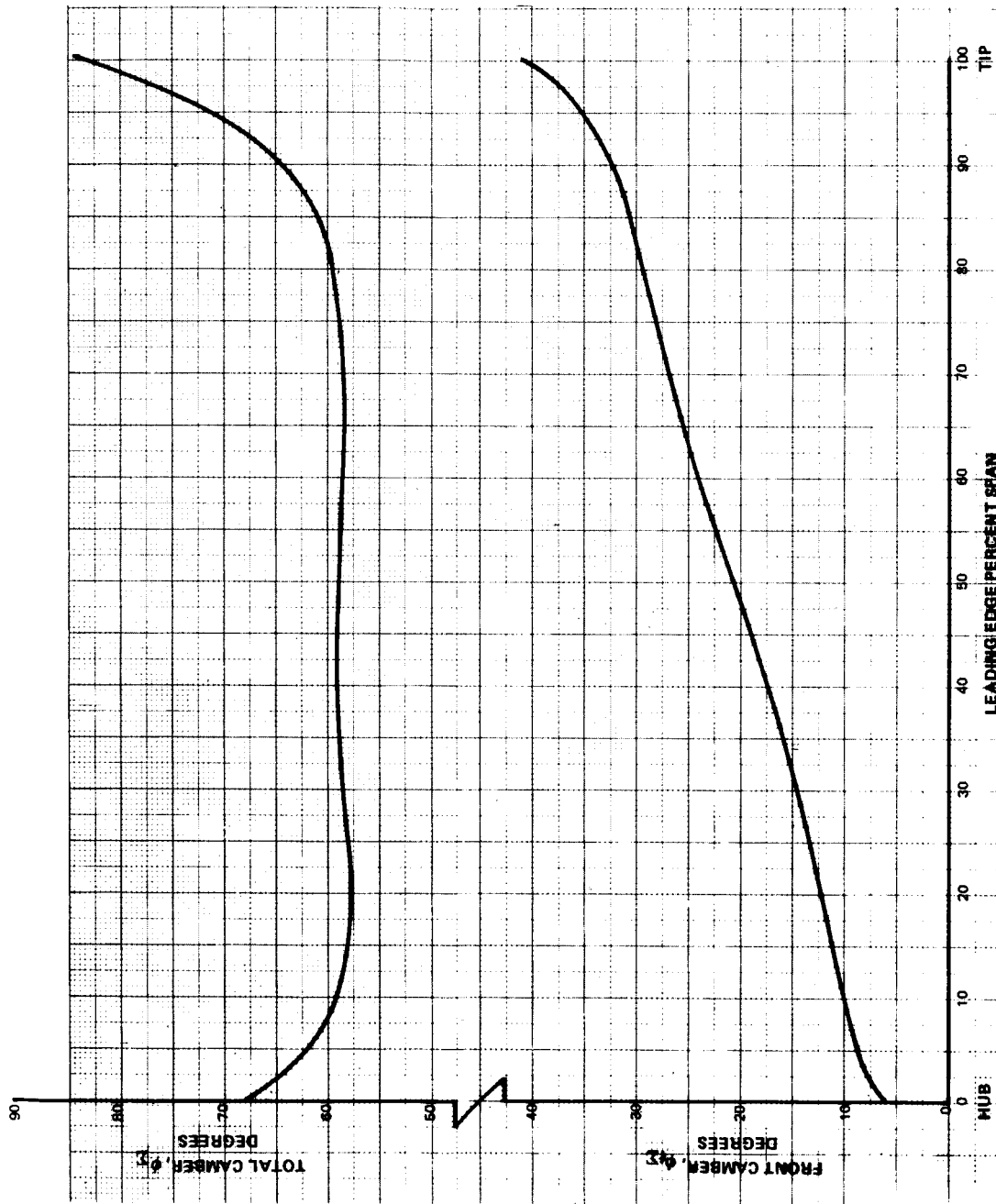


Figure 38 Stator Vane Front and Total Camber Angles

110% SPEED

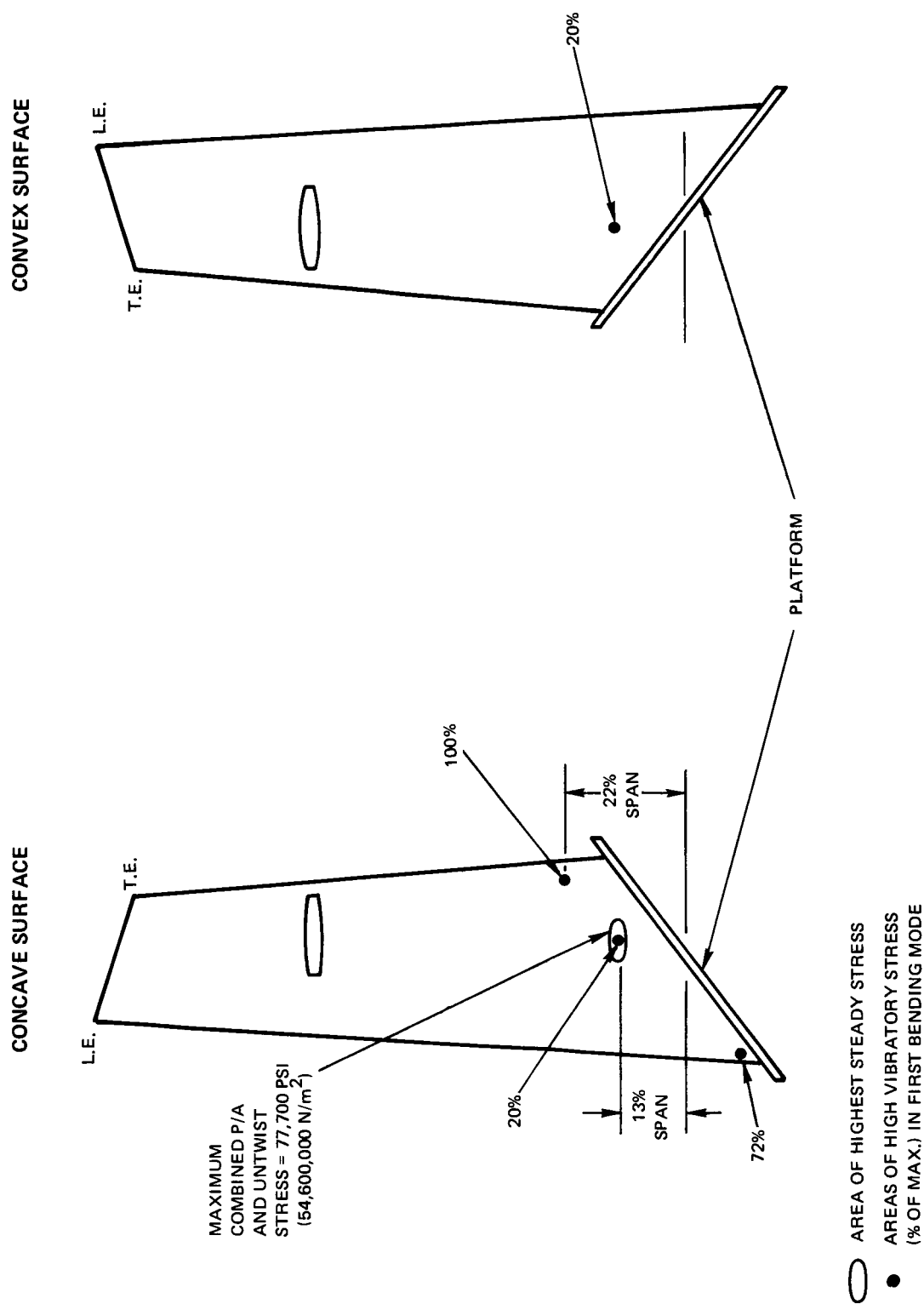


Figure 39 Rotor Blade Maximum Stress Location

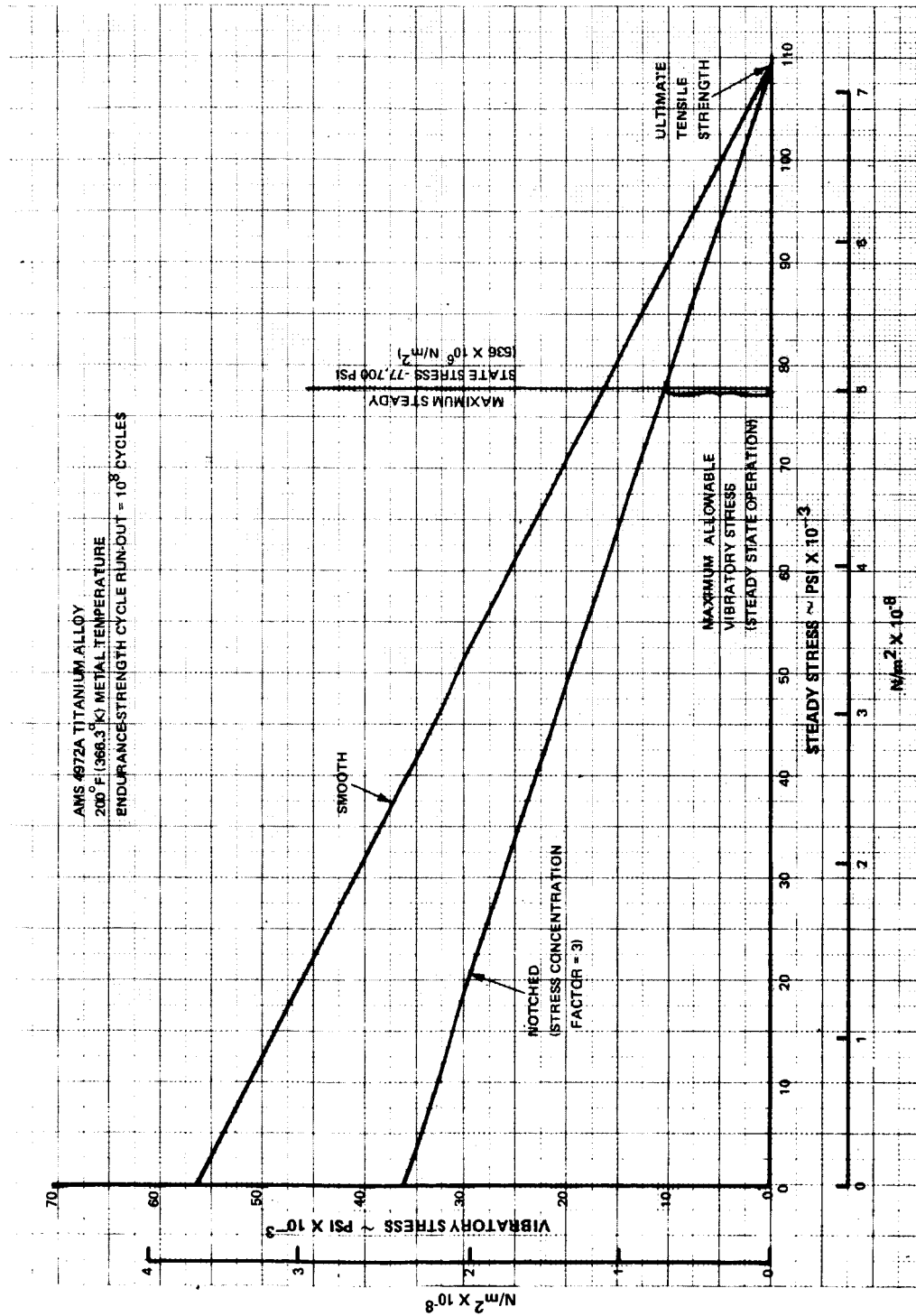


Figure 40 Rotor Modified Goodman Diagram

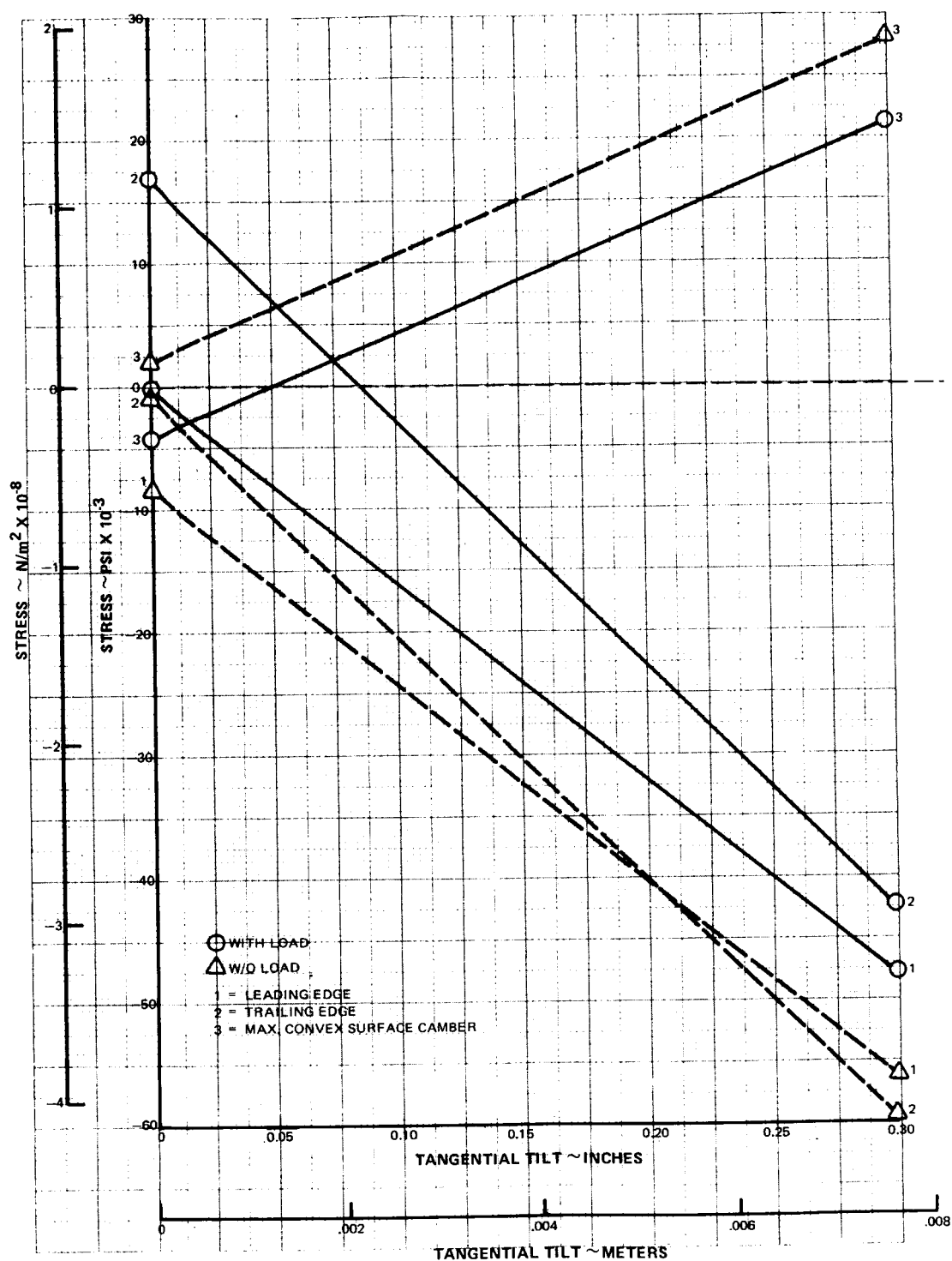


Figure 41 Effect of Tangential Tilt on Rotor Blade Gas Bending Stress

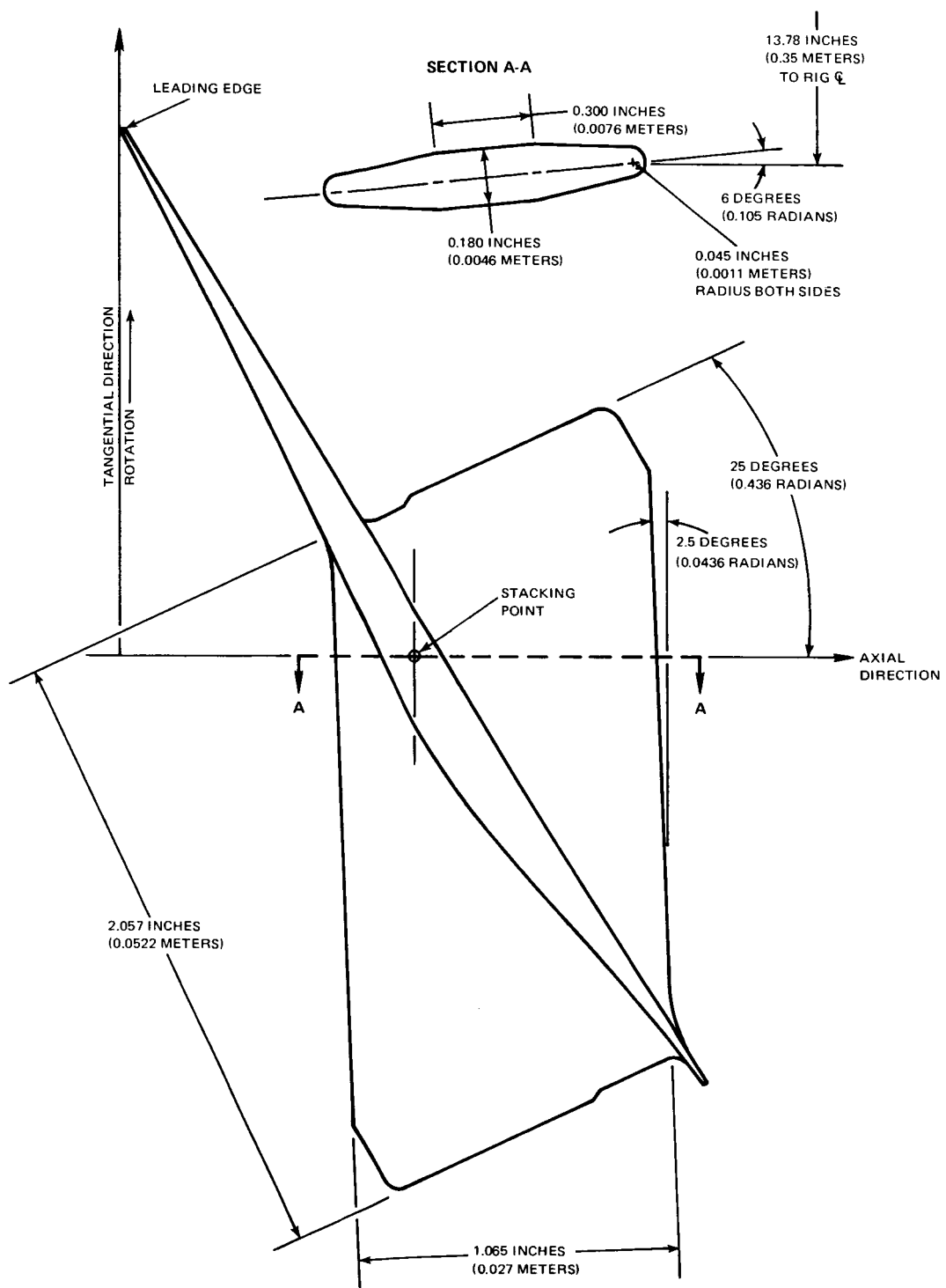


Figure 42 Top View of Rotor Blade Part-Span Shroud

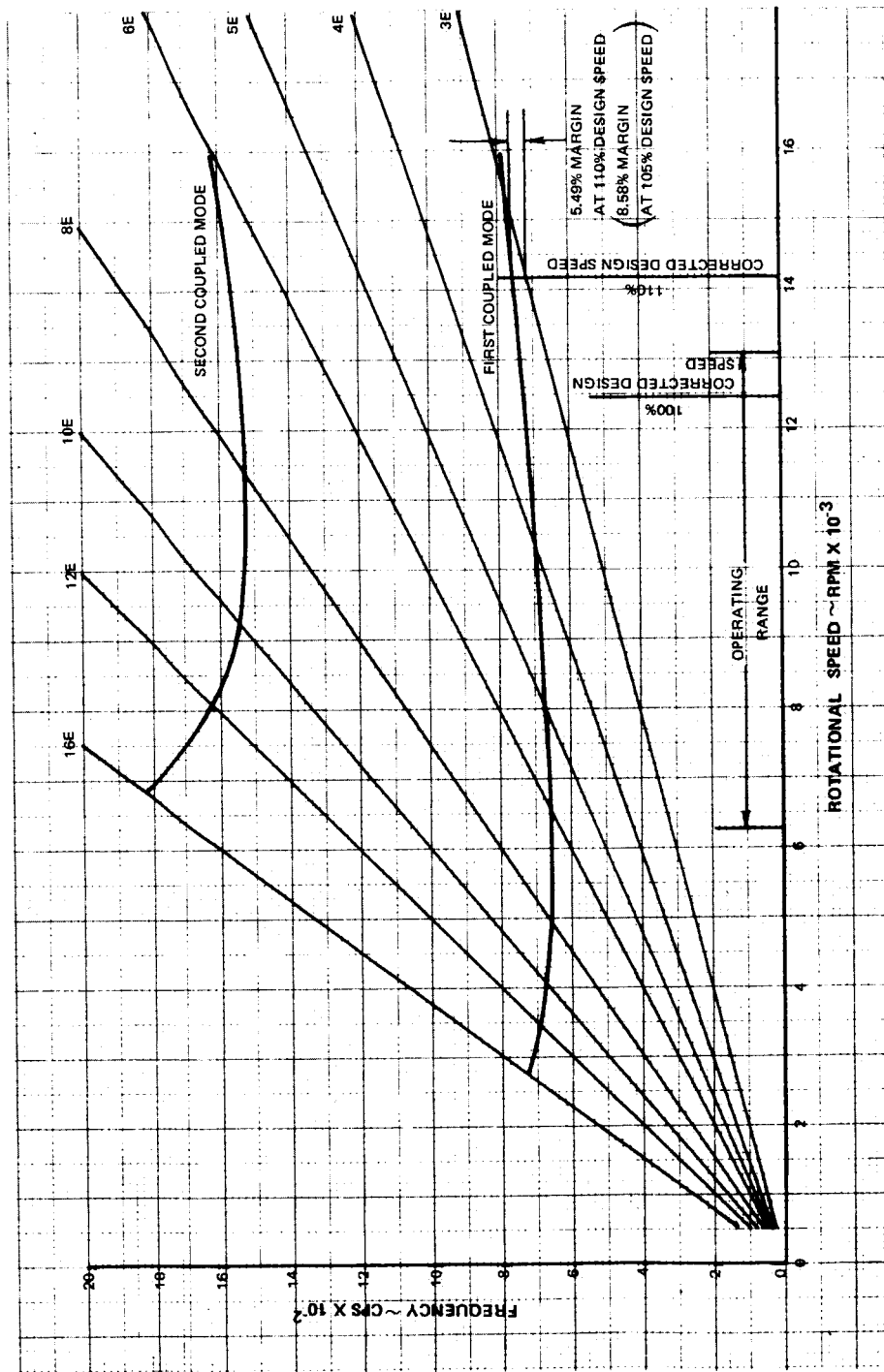


Figure 43 Resonance Diagram for Rotor Blade and Disk

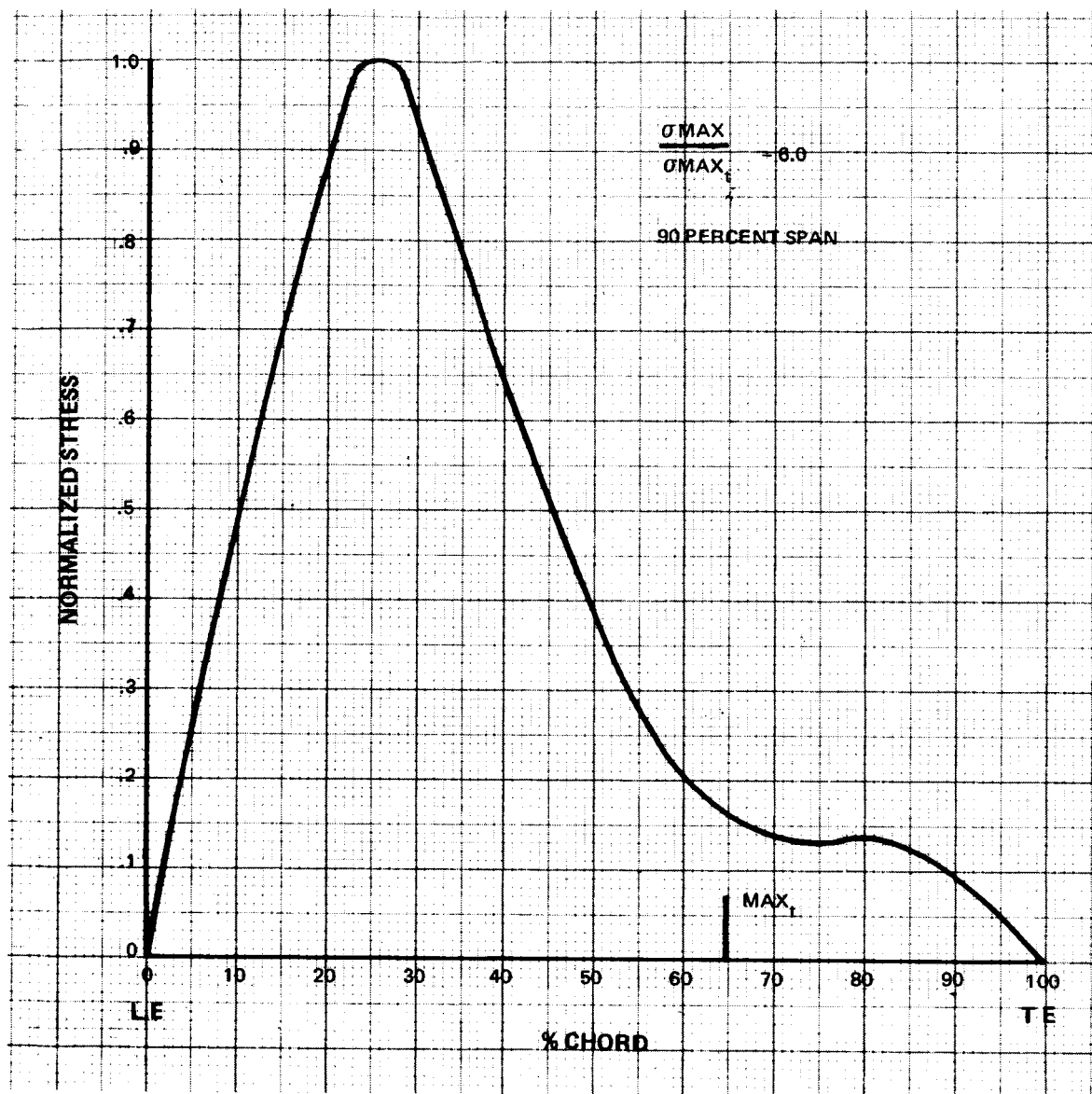


Figure 44 Rotor Blade Tip Chordwise Bending Stress Distribution

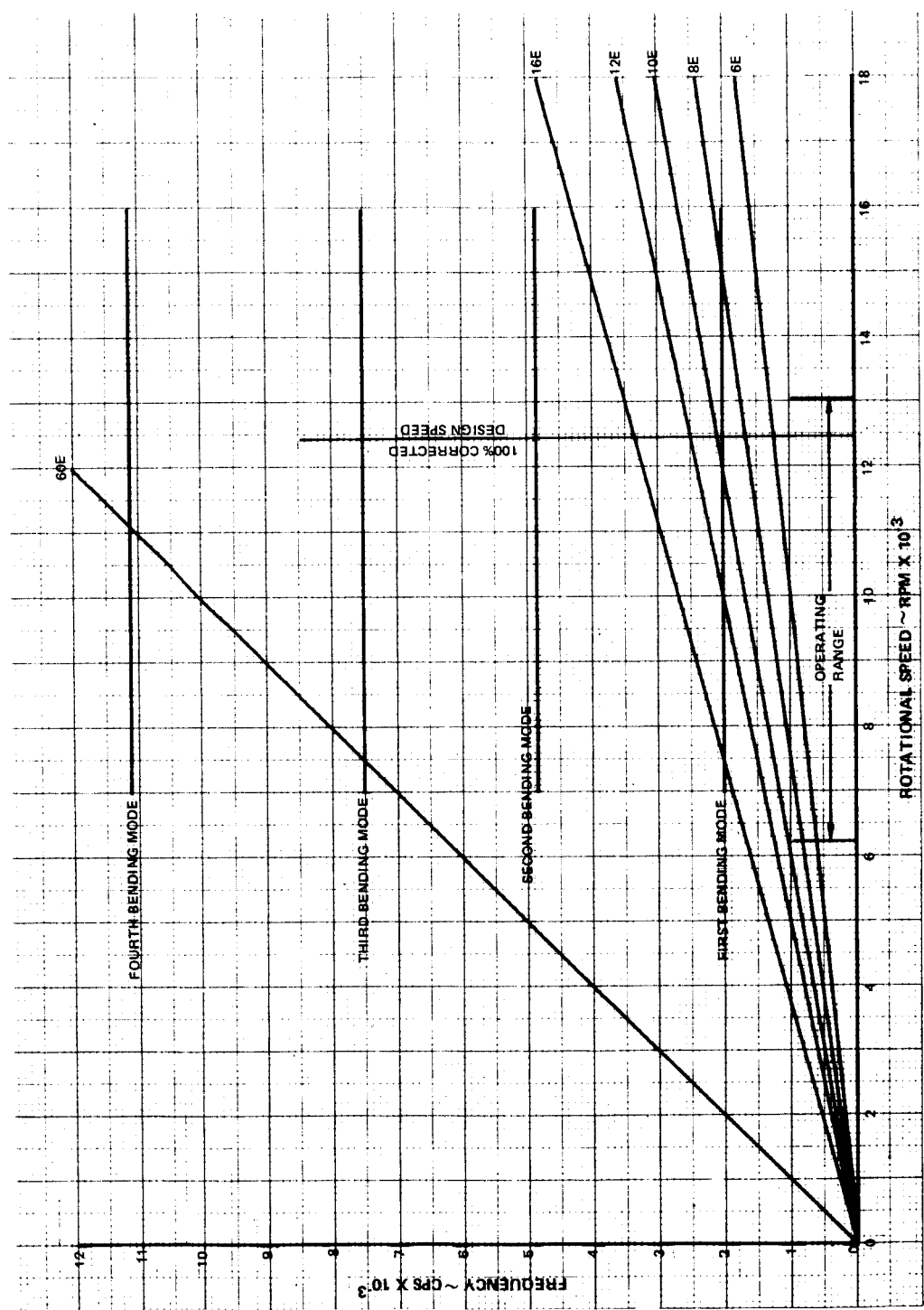


Figure 45 Resonance Diagram for Rotor Blade Tip Chordwise Bending

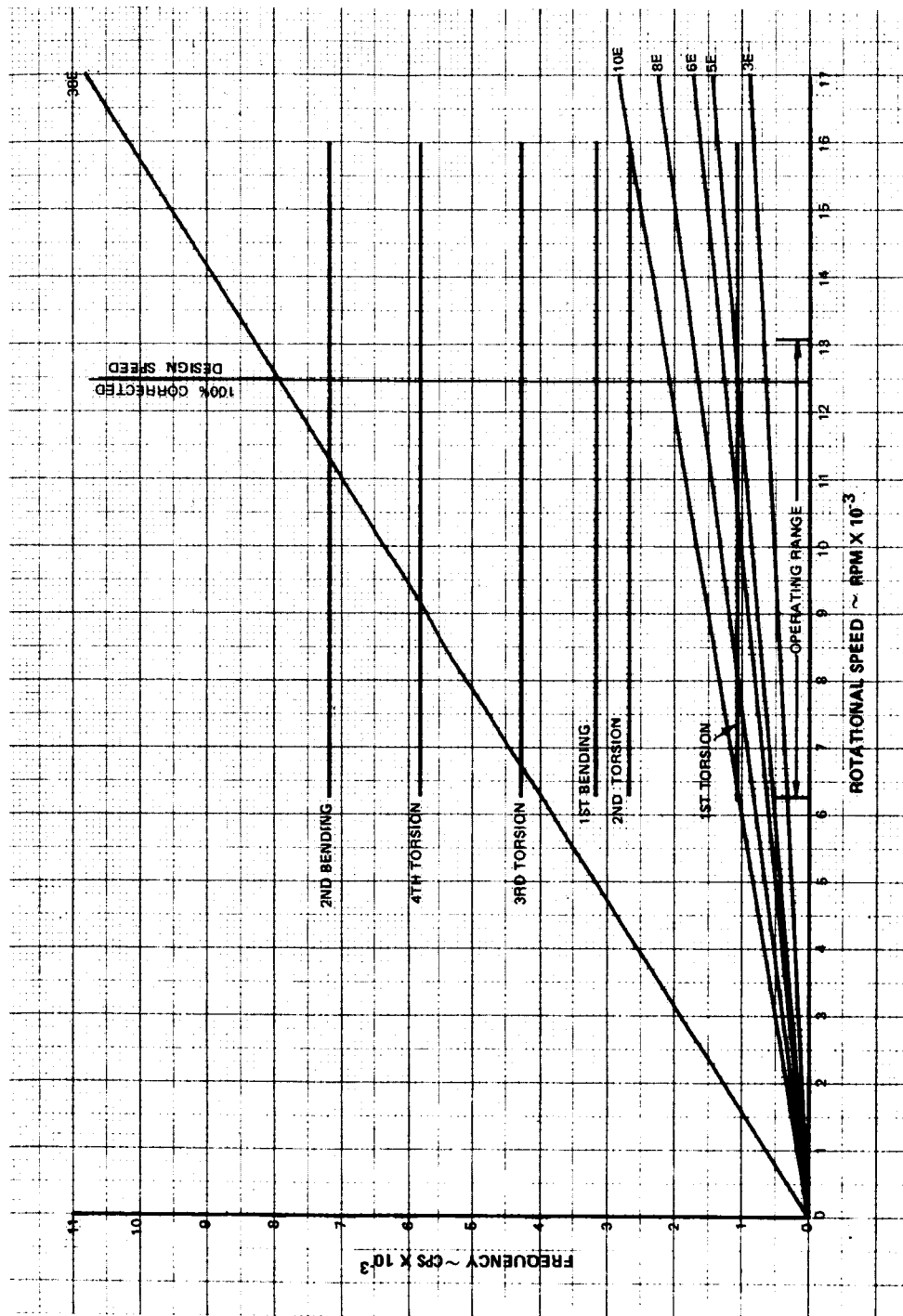


Figure 46 Resonance Diagram for Stator Vane

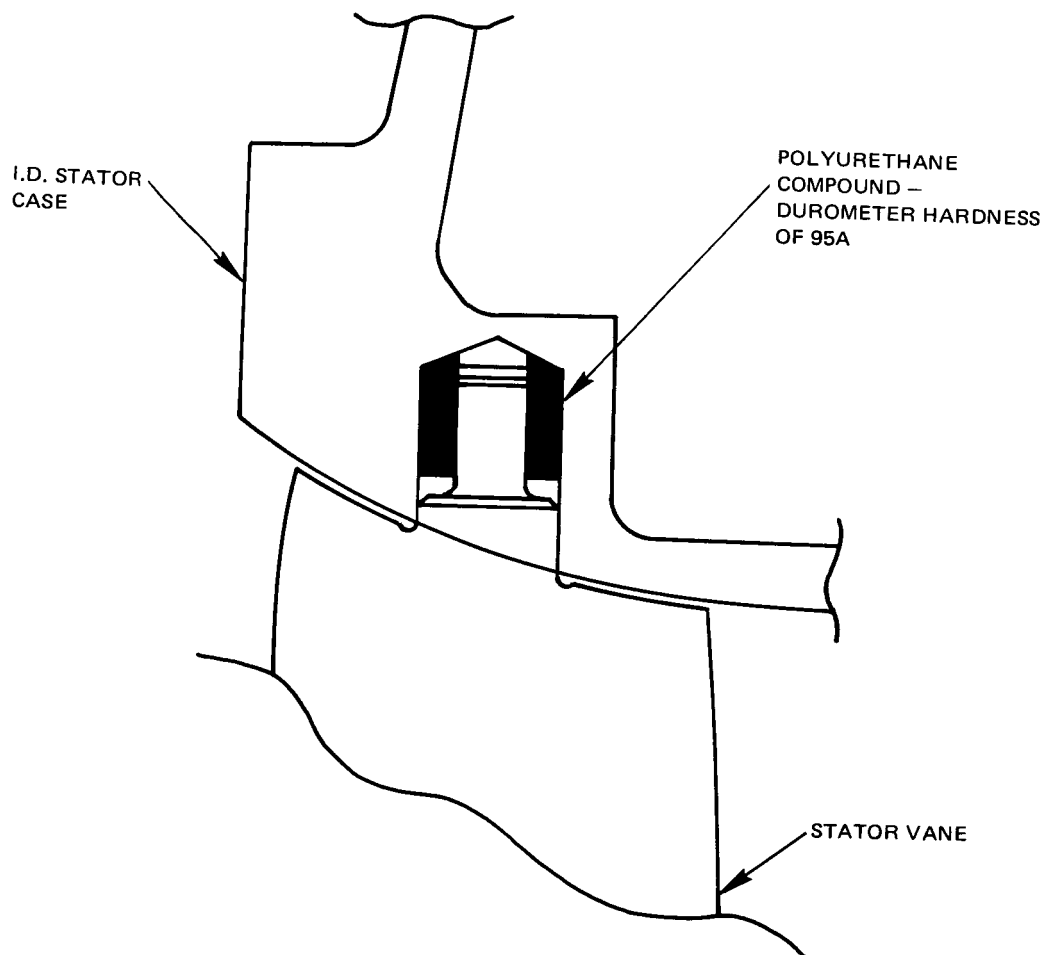


Figure 47 Stator Vane Polyurethane Bushing


$$\begin{aligned} T_1 &= 1.5 \times 10^8 \text{ (} 9.7 \times 10^8 \text{)} \\ T_2 &= 2.0 \times 10^8 \text{ (} 12.95 \times 10^8 \text{)} \\ T_3 &= 1.0 \times 10^8 \text{ (} 6.47 \times 10^8 \text{)} \\ T_4 &= 1.0 \times 10^8 \text{ (} 6.47 \times 10^8 \text{)} \end{aligned}$$

LINEAR SPRING RATES
POUNDS/INCH (N/m)

$$\begin{aligned} K_1 &= 3.0 \times 10^6 (5.25 \times 10^8) \\ K_2 &= 1.0 \times 10^6 (1.75 \times 10^8) \\ K_3 &= 0.5 \times 10^6 (0.88 \times 10^8) \\ K_4 &= 2.0 \times 10^6 (3.5 \times 10^8) \\ K_5 &= 2.0 \times 10^6 (3.5 \times 10^8) \\ K_6 &= 20.0 \times 10^6 (35.0 \times 10^8) \\ K_7 &= 10.0 \times 10^6 (17.5 \times 10^8) \\ K_8 &= 10.0 \times 10^6 (17.5 \times 10^8) \end{aligned}$$

Figure 48 Compressor Rig Spring Location and Spring Rates

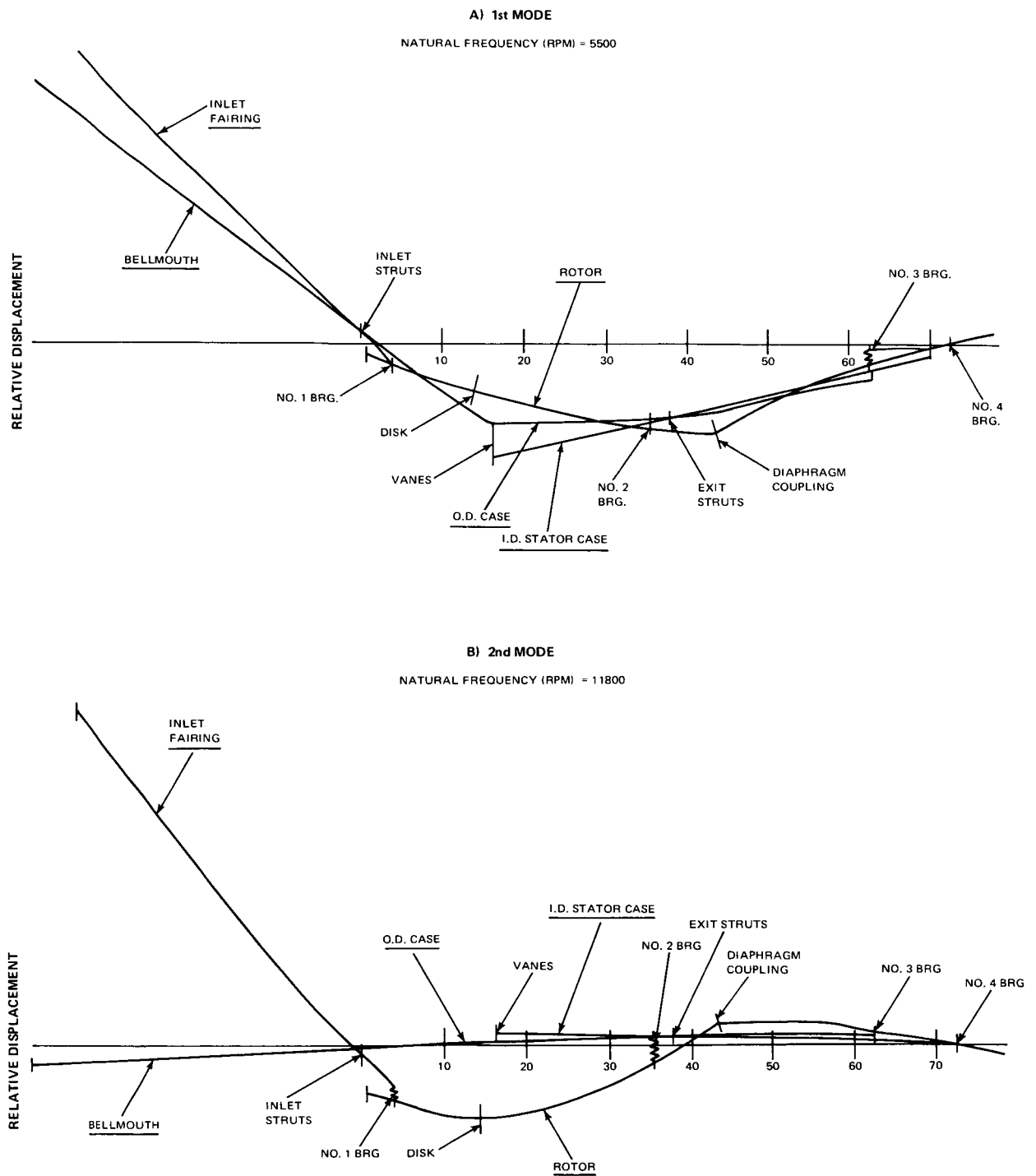
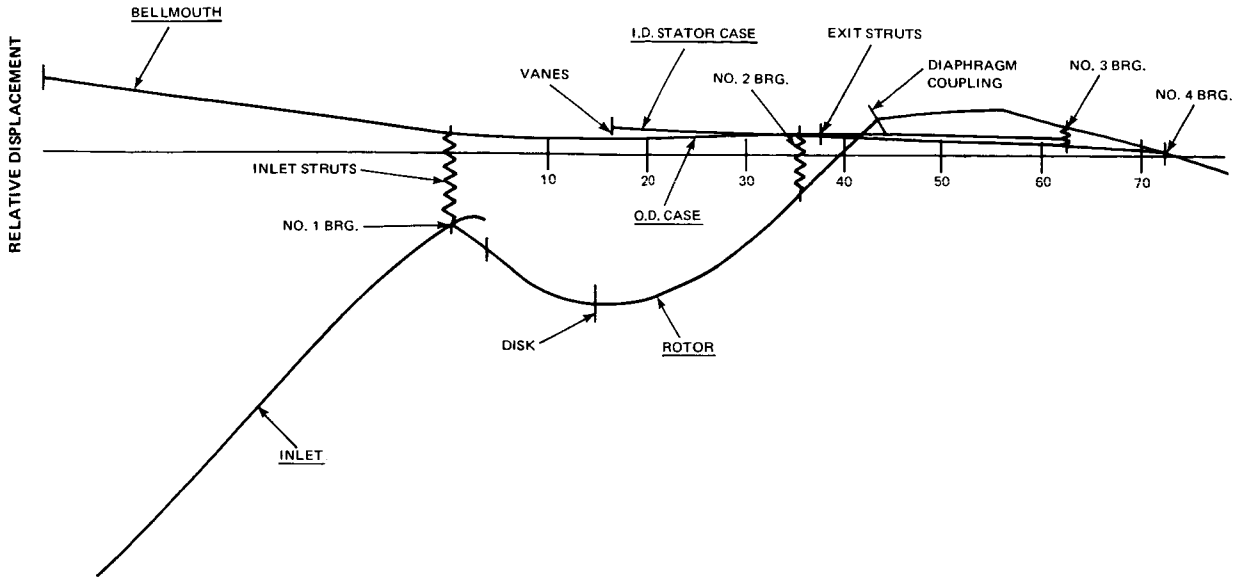


Figure 49 Critical Speed Mode Shapes

C) 3rd MODE

NATURAL FREQUENCY (RPM) = 12500



D) 4th MODE

NATURAL FREQUENCY (RPM) = 14800

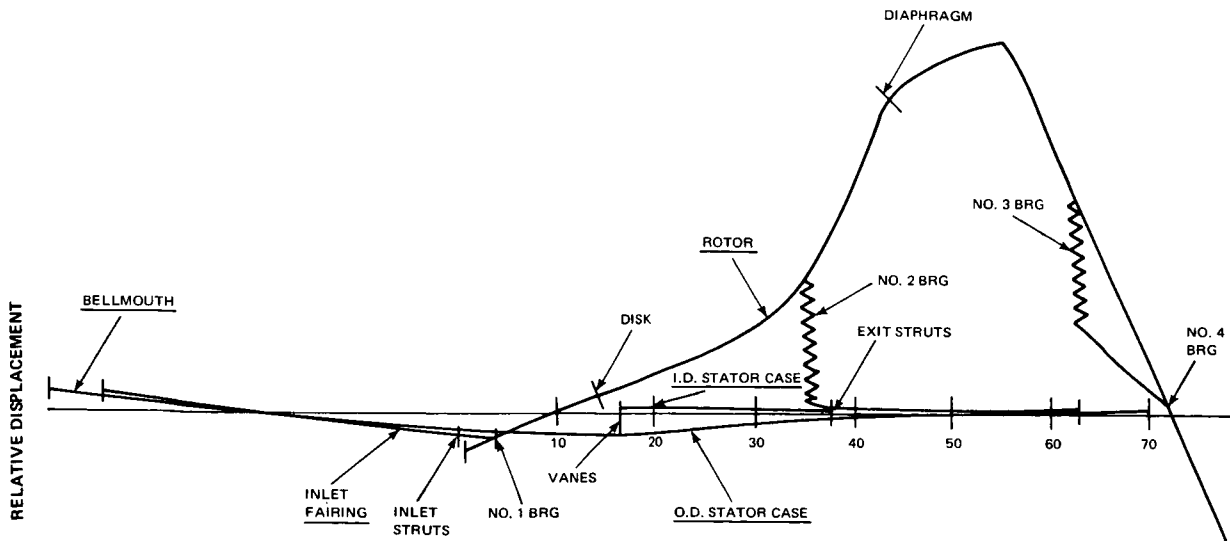


Figure 49 (Cont'd) Critical Speed Mode Shapes

APPENDIX 1

Flow Field Calculation Procedures

The aerodynamic flow field calculation used in this design assumes axisymmetric flow and uses solutions of continuity, energy, and radial equilibrium equations. These equations account for streamline curvature and radial gradients of enthalpy and entropy, but viscous terms are neglected. Calculations were performed on stations oriented at an angle λ with respect to the axial direction.

The equation of motion is in the form of:

$$\frac{1}{2} \frac{\partial V_m^2}{\partial m} \cos(\lambda - \epsilon) + \frac{V_m^2}{R_c} \sin(\lambda - \epsilon) - \frac{V_\theta^2}{r} + \frac{1}{\rho} \frac{\partial p}{\partial r} = 0$$

$$R_c = \frac{\partial \epsilon}{\partial m} = \text{streamline radius of curvature}$$

Enthalpy rise across a rotor for a streamline ψ is given by the Euler relationship

$$\Delta H_{\text{Rotor}} = (U_2 V_{\theta_2})_\psi - (U_1 V_{\theta_1})_\psi$$

Weight flow is calculated by the continuity equation

$$W = 2\pi \int_{y \text{ root}}^{y \text{ tip}} K \rho V_m \frac{\sin(\lambda - \epsilon)}{\sin \lambda} y dy$$

where K is the local blockage factor and y is the length along the calculation station from the centerline to the point of interest.

APPENDIX 2
AERODYNAMIC SUMMARY
Tables V and VI

APPENDIX 2
TABLE V
ROTOR AERODYNAMIC SUMMARY

	Percent Span	Rotor Inlet									
		10	20	30	40	50	60	70	80	90	100(Tip)
		English Units									
Total Pressure Ratio*											
Total Temperature Ratio*											
ω		1.00	1.00	1.00	1.00	1.00	1.00	1.00	1.00	1.00	1.00
D		1.00	1.00	1.00	1.00	1.00	1.00	1.00	1.00	1.00	1.00
M		0.00	0.00	0.00	0.00	0.00	0.00	0.00	0.00	0.00	0.00
M'		0.00	0.00	0.00	0.00	0.00	0.00	0.00	0.00	0.00	0.00
		.3924	.4502	.5076	.6086	.6451	.6651	.6638	.6461	.6149	.5926
		.9053	1.0082	1.1123	1.3170	1.4134	1.4999	1.5752	1.6420	1.7027	1.7696
English Units											
Diameter	Inches	16.500	18.160	19.820	21.480	23.140	24.800	26.460	28.120	29.780	31.440
V	Ft/Sec	431.62	492.78	552.77	606.13	655.71	693.15	711.92	710.63	693.19	662.06
V'	Ft/Sec	995.67	1103.66	1211.28	1315.97	1418.93	1516.33	1605.44	1686.33	1761.62	1833.43
V _m	Ft/Sec	431.52	492.78	552.77	606.13	655.71	693.15	711.92	710.63	693.19	662.06
V θ	Ft/Sec	0.00	0.00	0.00	0.00	0.00	0.00	0.00	0.00	0.00	0.00
U	Ft/Sec	-897.26	-987.53	-1077.80	-1168.07	-1258.33	-1348.60	-1438.87	-1529.14	-1619.41	-1709.68
β	Ft/Sec	897.26	987.53	1077.80	1168.07	1258.33	1348.60	1438.87	1529.14	1619.41	1709.68
β'	Degrees	0.00	0.00	0.00	0.00	0.00	0.00	0.00	0.00	0.00	0.00
β'	Degrees	64.31	63.49	62.85	62.59	62.47	62.79	63.66	65.06	66.82	68.83
ϵ	Degrees	33.99	27.60	21.70	15.25	8.80	2.70	-2.90	-7.90	-12.60	-17.40
SI Units											
Diameter	Meters	.4191	.4513	.5034	.5456	.5878	.6299	.6721	.7143	.7564	.8407
V	m/Sec	131.56	150.20	168.48	184.75	199.66	211.27	216.99	216.60	211.28	201.80
V'	m/Sec	303.48	336.40	369.20	401.11	432.49	462.18	489.34	514.00	536.94	558.83
V _m	m/Sec	131.56	150.20	168.48	184.75	199.86	211.27	216.99	216.60	211.28	201.80
V θ	m/Sec	0.00	0.00	0.00	0.00	0.00	0.00	0.00	0.00	0.00	0.00
U	m/Sec	-273.48	-301.00	-328.51	-356.03	-383.54	-411.06	-438.57	-466.08	-493.60	-521.11
β	m/Sec	273.48	301.00	328.51	356.03	383.54	411.06	438.57	466.08	493.60	521.11
β'	Radians	0.00	0.00	0.00	0.00	0.00	0.00	0.00	0.00	0.00	0.00
β'	Radians	1.1224	1.1081	1.0969	1.0924	1.0904	1.0959	1.1111	1.1355	1.1662	1.2013
ϵ	Radians	.5933	.4817	.3787	.2662	.1536	.0471	-.0506	-.1379	-.2199	-.3037

*Calculations based on an inlet pressure of 2,116 psf and an inlet temperature of 518.6°R

APPENDIX 2

TABLE V (Cont'd)

ROTOR AERODYNAMIC SUMMARY

	Percent Span	Rotor Exit									
		10	20	30	40	50	60	70	80	90	100(Tip)
		English Units									
Total Pressure Ratio*											
Total Temperature Ratio*											
$\bar{\omega}$		2.34	2.34	2.34	2.34	2.34	2.34	2.34	2.34	2.34	2.34
D		1.3228	1.2984	1.2956	1.2967	1.3001	1.3036	1.3146	1.3266	1.3576	1.4282
M		.3550	.1530	.1087	.1109	.1141	.1171	.1324	.1595	.2304	.3643
M'		.695	.581	.564	.584	.538	.519	.500	.490	.511	.594
		.8623	.8217	.7884	.7313	.7096	.6927	.6783	.6640	.6495	.6305
		.4173	.5582	.6649	.7124	.7640	.8189	.8658	.9013	.8921	.7855
English Units											
Diameter	Inches	20.130	21.322	23.706	24.898	26.090	27.282	28.474	29.666	30.858	32.050
V	Ft/Sec	1032.82	980.92	911.38	884.53	861.84	844.21	830.43	817.98	810.81	808.84
V'	Ft/Sec	499.82	666.36	739.28	800.41	861.62	927.82	998.08	1059.97	1110.40	1007.66
V ^m	Ft/Sec	468.48	563.03	567.98	551.15	544.84	543.18	538.21	519.22	463.29	254.33
V θ	Ft/Sec	920.46	803.19	754.48	691.83	667.77	645.26	634.11	631.88	665.40	767.82
V θ	Ft/Sec	-174.20	-356.28	-469.81	-662.10	-750.99	-837.32	-914.29	-981.33	-1012.64	-975.04
U	Ft/Sec	1094.65	1159.47	1224.29	1289.11	1353.93	1418.75	1483.57	1548.39	1613.21	1742.85
β	Degrees	63.03	54.97	52.01	51.46	50.79	49.95	49.78	50.59	55.15	71.67
β'	Degrees	20.40	32.31	39.35	50.21	54.04	57.03	59.60	62.11	65.42	75.38
ϵ	Degrees	34.89	26.30	19.10	12.80	7.20	-3.0	-7.40	-12.0	-16.2	-19.3
SI Units											
Diameter	Meter	.5113	.5416	.6021	.6324	.6627	.6930	.7232	.7535	.7838	.8141
V	m/Sec	314.80	299.98	277.79	269.61	262.69	257.32	253.12	249.32	247.13	246.54
V'	m/Sec	152.35	203.11	225.33	243.96	282.80	304.21	323.08	338.45	339.42	307.14
V ^m	m/Sec	142.79	171.51	173.12	167.99	166.07	165.56	163.44	158.26	141.21	77.52
V θ	m/Sec	280.56	244.81	229.97	210.87	203.54	196.98	193.28	192.60	202.81	234.03
V θ	m/Sec	-53.10	-108.59	-143.20	-201.81	-228.90	-255.22	-278.68	-299.11	-308.65	-297.19
U	m/Sec	333.65	353.41	373.17	412.68	432.44	452.19	471.95	491.71	511.47	531.22
β	Radians	1.100	.9594	.9252	.8981	.8864	.8718	.8688	.8830	.9626	1.2509
β'	Radians	.3560	.5639	.6868	.7941	.8763	.9431	1.0403	1.0840	1.1417	1.3156
ϵ	Radians	.6090	.4590	.3334	.2234	.1257	-.0524	-.1292	-.2094	-.2828	-.3370

* Calculations based on an inlet pressure of 2.116 psf and an inlet temperature of 518.6°R

APPENDIX 2

TABLE VI

STATOR AERODYNAMIC SUMMARY

	Percent Span	Stator Inlet										
		O(Hub)	10	20	30	40	50	60	70	80	90	100(Tip)
		English Units										
Total Pressure Ratio*												
Total Temperature Ratio*												
$\frac{W}{D}$		2.34	2.34	2.34	2.34	2.34	2.34	2.34	2.34	2.34	2.34	2.34
D		1.3228	1.2983	1.2956	1.2966	1.2999	1.3032	1.3067	1.3135	1.3234	1.3524	1.4282
M		0.00	0.00	0.00	0.00	0.00	0.00	0.00	0.00	0.00	0.00	0.00
M'		0.00	0.00	0.00	0.00	0.00	0.00	0.00	0.00	0.00	0.00	0.00
		.8924	.8557	.8229	.7924	.7681	.7481	.7337	.7237	.7159	.7092	.6940
		.5296	.6439	.6869	.7215	.7573	.7987	.8444	.8852	.9205	.9119	.7845
English Units												
Diameter	Inches	20.820	21.866	22.912	23.953	25.004	25.050	27.096	28.142	29.188	30.234	31.280
V	Ft/Sec	1063.98	1016.45	981.01	949.25	924.32	903.90	889.37	880.61	875.20	877.23	883.54
V'	Ft/Sec	631.44	764.79	819.06	864.31	911.93	964.99	1023.54	1077.17	1125.47	1127.88	998.80
V _m	Ft/Sec	583.13	648.06	642.72	629.32	615.82	608.84	607.32	605.39	601.28	566.99	402.15
V θ	Ft/Sec	889.95	783.04	741.11	710.66	688.39	668.09	649.71	639.52	635.89	669.16	786.72
U	Ft/Sec	-242.23	-406.02	-504.82	-592.16	-671.30	-748.49	-823.74	-890.82	-951.33	-974.94	-914.26
β	Ft/Sec	1132.13	1189.06	1245.94	1302.82	1359.70	1416.58	1473.46	1530.34	1587.22	1644.10	1700.98
β'	Degrees	56.77	50.39	49.06	48.47	48.14	47.66	46.93	46.57	46.00	49.72	62.93
ϵ	Degrees	22.56	32.06	38.00	43.24	47.40	50.86	53.58	55.78	57.70	59.82	66.26
	Degrees	30.42	22.20	16.10	10.80	6.50	2.90	-0.10	-3.7	-7.0	-10.1	-17.05
SI Units												
Diameter	Meters	.5288	.5554	.5820	.6085	.6351	.6617	.6882	.7148	.7414	.7680	.7945
V	m/Sec	324.30	309.82	299.01	289.33	281.73	275.51	271.08	268.41	266.76	267.38	269.30
V'	m/Sec	192.46	233.11	249.65	263.44	277.96	294.13	311.98	328.32	343.04	343.78	304.44
V _m	m/Sec	177.74	197.53	195.90	191.32	188.01	185.57	185.11	183.27	172.82	172.82	122.57
V θ	m/Sec	271.26	238.67	225.85	216.61	209.82	203.63	198.03	194.93	193.82	203.96	239.79
V θ'	m/Sec	-73.83	-123.75	-153.87	-180.49	-204.61	-228.14	-251.08	-271.52	-289.97	-297.10	-278.67
U	m/Sec	345.09	362.43	379.76	397.10	414.44	431.77	449.11	466.45	483.79	501.12	518.46
β	m/Sec	.9907	.8794	.8582	.8317	.8402	.8317	.8191	.8128	.8134	.8678	1.0983
β'	Radians	.3937	.5596	.6633	.7547	.8272	.8876	.9352	.9736	1.0071	1.0441	1.1564
ϵ	Radians	.5309	.3875	.2810	.1885	.1135	.0506	-.0018	-.0646	-.1222	-.1763	-.2976

* Calculations based on all inlet pressure of 2.116 psf and an inlet temperature of 518.6°R

APPENDIX 2

TABLE VI (Cont'd)

STATOR AERODYNAMIC SUMMARY

	Percent Span	Stator Exit										
		0(Hub)	10	20	30	40	50	60	70	80	90	100(Tip)
		English Units										
Total Pressure Ratio*												
Total Temperature Ratio*												
$\bar{\omega}$		2.1861	2.2427	2.2669	2.2792	2.2900	2.2956	2.3002	2.3032	2.3035	2.2969	2.2860
		1.3228	1.2977	1.2957	1.2968	1.3001	1.3033	1.3066	1.3132	1.3215	1.3487	1.4282
D		.1629	.1094	.0871	.0787	.0662	.0612	.0565	.0535	.0540	.0646	.0640
		.538	.499	.484	.476	.471	.464	.456	.450	.444	.451	.476
M		.5528	.5571	.5514	.5419	.5384	.5356	.5353	.5369	.5399	.5427	.5486
M'		1.1138	1.1559	1.1854	1.2118	1.2412	1.2710	1.3023	1.3332	1.3641	1.3865	1.3886
English Units												
Diameter	Inches	22.150	22.971	23.792	24.613	25.434	26.255	27.076	27.897	28.718	29.539	30.360
V	Ft/Sec	688.54	687.04	679.97	669.17	665.85	663.38	663.92	667.47	673.08	683.15	709.96
V'	Ft/Sec	1387.41	1425.62	1461.77	1496.40	1535.03	1574.33	1615.15	1657.38	1700.54	1745.54	1797.13
V _m	Ft/Sec	686.54	687.04	679.97	669.17	665.85	663.38	663.92	667.47	673.08	683.15	709.96
V _θ	Ft/Sec	0.00	0.00	0.00	0.00	0.00	0.00	0.00	0.00	0.00	0.00	0.00
U	Ft/Sec	-1204.50	-1249.14	-1293.79	-1338.44	-1383.08	-1427.73	-1472.37	-1517.02	-1561.66	-1606.31	-1660.95
β	Degrees	1204.50	1249.14	1293.79	1338.44	1383.08	1472.73	1472.37	1517.02	1561.66	1606.31	1660.95
β'	Degrees	0.00	0.00	0.00	0.00	0.00	0.00	0.00	0.00	0.00	0.00	0.00
ε	Degrees	60.25	61.19	62.26	63.44	64.29	65.08	65.73	66.25	66.68	66.96	66.73
	Degrees	5.51	5.00	4.10	3.10	2.10	0.80	-0.50	-2.2	-3.6	-5.1	-6.72
SI Units												
Diameter	Meters	.5625	.5835	.6043	.6252	.6460	.6669	.6877	.7086	.7294	.7503	.7712
V	m/Sec	209.87	209.41	207.26	203.96	202.95	202.20	202.36	203.46	205.16	208.22	216.40
V'	m/Sec	422.88	434.53	445.55	456.10	467.88	479.86	492.30	505.17	518.33	532.04	547.77
V _m	m/Sec	209.87	209.41	207.26	203.95	202.95	202.20	202.36	203.45	205.16	208.22	215.40
V _θ	m/Sec	0.00	0.00	0.00	0.00	0.00	0.00	0.00	0.00	0.00	0.00	0.00
U	m/Sec	-367.13	-380.74	-394.35	-407.96	-421.56	-435.17	-448.78	-462.39	-476.00	-489.60	-503.21
β	m/Sec	367.13	380.74	394.35	407.96	421.56	435.17	448.78	462.39	476.00	489.60	503.21
β'	Radians	0.00	0.00	0.00	0.00	0.00	0.00	0.00	0.00	0.00	0.00	0.00
β'	Radians	1.0515	1.0679	1.0866	1.1072	1.1221	1.1358	1.1471	1.1563	1.1638	1.1687	1.1647
ε	Radians	.0962	.0873	.0716	.0541	.0367	.0140	-.0087	-.0384	-.0628	-.0890	-.1173

* Calculations based on an inlet pressure of 2.116 psf and an inlet temperature of 518.6°R

APPENDIX 3

COSINE VARIATION OF BLADE CHANNEL AREA

The suction surface D-G of Figure 23 is obtained by knowing the pressure surface shape and the local channel areas determined by the equation

$$A = A_D + (A_G - A_D) \left[1 - \cos \left(\frac{\pi}{2} \frac{Z - Z_D}{Z_G - Z_D} \right) \right]$$

where $A_D = A_D(Z)$

This function is calculated assuming constant corrected specific flow from core-flow conditions downstream of the oblique shock at D

and $A_G = A_G(Z)$

This function is calculated assuming constant corrected specific flow from exit core-flow conditions

APPENDIX 4

BLADE AIRFOIL GEOMETRY ON CONICAL SURFACES

TABLES VII AND VIII

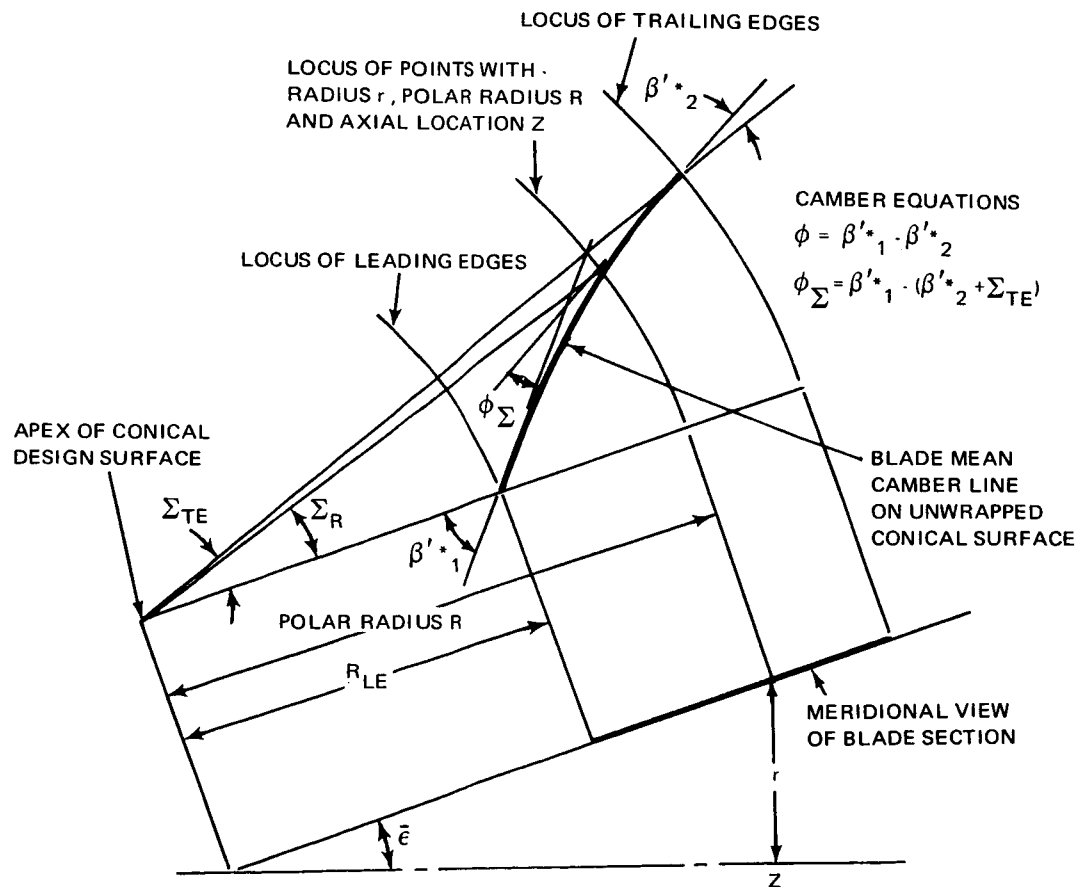


Figure 50 Unwrapped Conical Surface Definitions

APPENDIX 4
TABLE VII
ROTOR BLADE GEOMETRY ON CONICAL SURFACES

38 Blades

Inlet Hub Diameter 16.5 Inches (.419m) Inlet Tip Diameter 33.0 Inches (.838m)
Exit Hub Diameter 20.13 Inches (.511m) Exit Tip Diameter 32.11 Inches (.816m)

Diameter LE Inches	Diameter TE Inches	c Inches	c _f Inches	LER Inches	TER Inches	β_1^* Degrees	β_2^* Degrees	W.A. Degrees	ϕ_2 Degrees	ϕ_2 Degrees	Precompression Ramp Angle Degrees	τ Degrees	Σ Degrees	Precompression Blade Pressure Surface Points F C	U/c Max.	Location U/c Max.	θ
16.500	20.130	3.900	1.055	.0117	.0102	58.75	4.85	9.7	44.92	-1.34		36.30	8.98		0.770	53.7	2.576
18.042	20.966	3.800	1.140	.0111	.0099	58.25	15.65	8.1	34.90	.42		31.05	7.70		0.638	54.5	2.357
19.344	21.684	3.720	1.218	.0106	.0096	58.19	22.90	7.1	28.82	1.00		26.23	6.47		0.563	55.0	2.194
20.480	22.359	3.660	1.302	.0101	.0094	58.17	27.66	6.5	25.10	1.20		22.05	5.41		0.520	55.5	2.067
21.499	23.001	3.620	1.344	.0097	.0091	58.25	31.90	5.9	22.00	1.50		18.25	4.35		0.498	56.0	1.968
24.152	24.706	3.640		.0086	.0124	59.15	38.98	4.6	18.30		1.68	8.09	1.87	.230	0.567	59.1	1.802
24.944	25.279	3.660		.0084	.0080	59.43	41.47	4.4	16.80		2.41	5.06	1.16	.173	0.606	60.2	1.763
25.704	25.843	3.665		.0082	.0083	59.87	44.42	4.1	14.95		3.15	2.17	50	.161	0.585	61.5	1.720
26.437	26.399	3.677		.0081	.0079	60.36	46.43	3.9	14.06		3.81	.61	-13	.160	0.564	62.7	1.684
27.147	26.948	3.690		.0080	.0083	60.90	48.74	3.8	12.96		4.38	-3.30	74	.162	0.549	63.6	1.650
27.861	27.489	3.720		.0080	.0097	61.55	50.87	3.6	12.11		4.93	-6.34	-1.43	.169	0.536	64.4	1.626
28.571	28.024	3.750		.0080	.0076	62.38	51.85	3.4	12.69		5.45	-9.57	-2.16	.179	0.523	65.0	1.603
29.231	28.586	3.790		.0080	.0111	63.23	52.94	3.2	12.90		5.91	-11.61	-3.03	.188	0.512	65.5	1.586
29.879	29.152	3.842		.0080	.0081	64.13	53.78	3.0	13.38		6.34	-13.48	-4.15	.199	0.502	65.9	1.575
31.148	30.217	3.983		.0080	.0064	65.88	56.53	3.0	13.50		6.94	-18.19	-4.74	.225	0.485	66.5	1.570
31.772	30.775	4.084		.0080	.0080	66.79	59.07	3.0	12.46		7.22	-20.42	-5.24	.239	0.481	66.5	1.580
32.391	31.328	4.220		.0080	.0076	67.50	62.59	3.0	10.15		7.54	-22.02	-5.24	.252	0.478	66.3	1.602
33.000	32.11	4.400		.0080	.0067	67.73	66.42	3.0	6.15		7.97	-19.60	-4.84	.263	0.475	65.5	1.635

Diameter LE Meters	Diameter TE Meters	c Meters	c _f Meters	LER Meters	TER Meters	β_1^* Radians	β_2^* Radians	W.A. Radians	ϕ_2 Radians	ϕ_2 Radians	Precompression Ramp Angle Radians	τ Radians	Σ Radians
.4191	.5113	.09906	.03680	.000297	.000259	1.0252	.0846	.1693	.7839	-.0234		.6334	1.567
.4583	.5325	.09652	.03896	.000282	.000251	1.0165	.2731	.1413	.6090	.0073		.5418	1.344
.4913	.5508	.09449	.03094	.000269	.000244	1.0134	.3997	.1239	.5029	.01745		.4577	1.130
.5202	.5679	.09296	.03307	.000257	.000239	1.0151	.4827	.1134	.4380	.0309		.3848	.0944
.5461	.5842	.09195	.03414	.000246	.000231	1.0165	.5567	.1030	.3839	.0262		.3185	.0760
.6135	.6275	.09246		.000218	.000315	1.0322	.6803	.0803	.3193		.0293	.1412	.0326
.6336	.6421	.09296		.000213	.000203	1.0371	.7237	.0768	.2932		.0421	.0883	.0202
.6529	.6541	.09309		.000208	.000211	1.0447	.7752	.0715	.2609		.0550	.0379	.0087
.6715	.6705	.09340		.000206	.000201	1.0533	.8103	.0681	.2453		.0665	-.0106	-.0023
.6895	.6845	.09373		.000203	.000211	1.0627	.8506	.0663	.2262		.0764	-.0576	-.0129
.7077	.6982	.09449		.000203	.000246	1.0740	.8878	.0628	.2113		.0860	-.1106	-.0250
.7257	.7118	.09525		.000203	.000193	1.0885	.9049	.0593	.2214		.0951	-.1670	-.0377
.7425	.7261	.09627		.000203	.000282	1.1034	.9239	.0558	.2251		.1031	-.2026	-.0456
.7589	.7405	.09759		.000203	.000206	1.1191	.9386	.0524	.2335		.1106	-.2352	-.0529
.7912	.7675	.10117		.000203	.000163	1.1496	.9866	.0524	.2356		.1211	-.3174	-.0724
.8070	.7817	.10373		.000203	.000203	1.1655	1.0309	.0524	.2374		.1260	-.3563	-.0827
.8227	.7957	.10719		.000203	.000193	1.1779	1.0923	.0524	.2384		.1316	-.3842	-.0915
.8382	.8156	.11278		.000203	.000170	1.1819	1.1592	.0524	.2373		.1391	-.4240	-.0845

APPENDIX 4
TABLES VIII
STATOR VANE GEOMETRY ON CONICAL SURFACES

60 Vanes

Inlet Hub Diameter 20.82 Inches (.529m) Inlet Tip Diameter 31.28 Inches (.7945m)
Exit Hub Diameter 22.172 Inches (.563m) Exit Tip Diameter 30.252 Inches (.768m)

Diameter LE Inches	Diameter TE Inches	c Inches	c _f Inches	LER Inches	TER Inches	β_3^* Degrees	β_4^* Degrees	W.A. Degrees	ϕ_Σ Degrees	ϕ_Σ Degrees	τ Degrees	Σ Degrees	t/c Max.	Location of t/c Max. (% c)	a/c	σ
20.82	22.17	2.480	.727	.00500	.00500	54.0	-16.00	5.80	68.28	6.0	17.57	1.72	.0500	54.4	.532	2.204
21.51	22.72	2.490	.709	.00520	.00520	49.8	-12.50	6.21	61.01	9.2	15.19	1.29	.0513	54.0	.521	2.151
22.13	23.30	2.496	.708	.00538	.00538	48.5	-11.00	6.80	58.44	10.5	13.26	1.06	.0525	53.6	.517	2.103
22.72	23.66	2.502	.719	.00553	.00553	48.2	-10.30	7.35	57.61	11.9	11.57	.89	.0536	53.3	.513	2.061
23.29	24.10	2.510	.736	.00570	.00570	48.4	-10.00	8.03	57.65	13.1	10.00	.75	.0546	52.9	.511	2.023
24.38	24.96	2.520	.810	.00600	.00600	48.9	-10.00	9.21	58.39	15.6	7.06	.51	.0567	52.4	.509	1.951
25.42	25.78	2.532	.920	.00630	.00630	49.0	-10.00	10.40	58.70	18.6	4.36	.30	.0587	51.8	.509	1.889
26.43	26.58	2.545	1.060	.00660	.00660	48.5	-10.12	11.34	58.50	21.8	1.77	.12	.0606	51.3	.510	1.834
27.41	27.34	2.556	1.180	.00687	.00687	47.5	-10.60	12.01	58.15	24.8	-.82	-.05	.0625	50.9	.508	1.783
28.42	28.11	2.569	1.250	.00715	.00715	47.8	-10.30	12.53	58.31	27.6	-.368	-.21	.0644	50.5	.499	1.736
29.35	28.83	2.580	1.280	.00741	.00741	48.0	-11.25	12.86	59.58	29.6	-.612	-.33	.0660	50.2	.491	1.694
30.27	29.53	2.590	1.300	.00768	.00768	50.8	-13.40	13.12	64.66	32.5	-.866	-.46	.0679	50.0	.489	1.655
30.74	29.89	2.595	1.300	.00781	.00781	55.2	-16.00	13.06	71.76	35.1	-10.00	-.56	.0688	50.0	.493	1.635
31.28	30.25	2.600	1.300	.00800	.00800	65.0	-18.00	12.75	83.79	41.0	-12.36	-.79	.0700	50.0	.488	1.614

Diameter LE Meters	Diameter TE Meters	c Meters	c _f Meters	LER Meters	TER Meters	β_3^* Radians	β_4^* Radians	W.A. Radians	ϕ_Σ Radians	ϕ_Σ Radians	τ Radians	Σ Radians
.5288	.5631	.06300	.01847	.000127	.000127	.9423	-.2792	.1012	1.1915	.1047	.3066	.030
.5464	.5771	.06325	.01801	.000132	.000132	.8690	-.2182	.1084	1.0646	.1605	.2651	.023
.5621	.5893	.06340	.01798	.000137	.000137	.8463	-.1920	.1187	1.0198	.1832	.2314	.019
.5771	.6009	.06355	.01826	.000140	.000140	.8411	-.1798	.1283	1.0053	.2077	.2019	.016
.5916	.6121	.06375	.01869	.000145	.000145	.8446	-.1745	.1401	1.0060	.2286	.1745	.013
.6193	.6340	.06401	.02057	.000152	.000152	.8533	-.1745	.1607	1.0189	.2722	.1232	.009
.6457	.6548	.06431	.02337	.000160	.000160	.8551	-.1745	.1815	1.0243	.3246	.0761	.005
.6713	.6751	.06464	.02692	.000168	.000168	.8463	-.1766	.1979	1.0208	.3804	.0309	.002
.6962	.6944	.06492	.02997	.000174	.000174	.8289	-.1850	.2096	1.0147	.4328	-.0143	-.0009
.7219	.7140	.06525	.03175	.000182	.000182	.8341	-.1798	.2186	1.0175	.4816	-.0642	-.003
.7455	.7323	.06553	.03251	.000188	.000188	.8376	-.1963	.2244	1.0397	.5165	-.1068	-.006
.7689	.7501	.06579	.03302	.000195	.000195	.8865	-.2339	.2289	1.1283	.5671	-.1511	-.008
.7808	.7592	.06591	.03302	.000198	.000198	.9632	-.2792	.2279	1.2522	.6125	-.1745	-.010
.7945	.7684	.06604	.03302	.000203	.000203	1.1343	-.3141	.2225	1.4621	.7155	-.2157	-.014

APPENDIX 5

MANUFACTURING COORDINATES FOR SECTIONS
NORMAL TO STACKING LINE

TABLES IX AND X

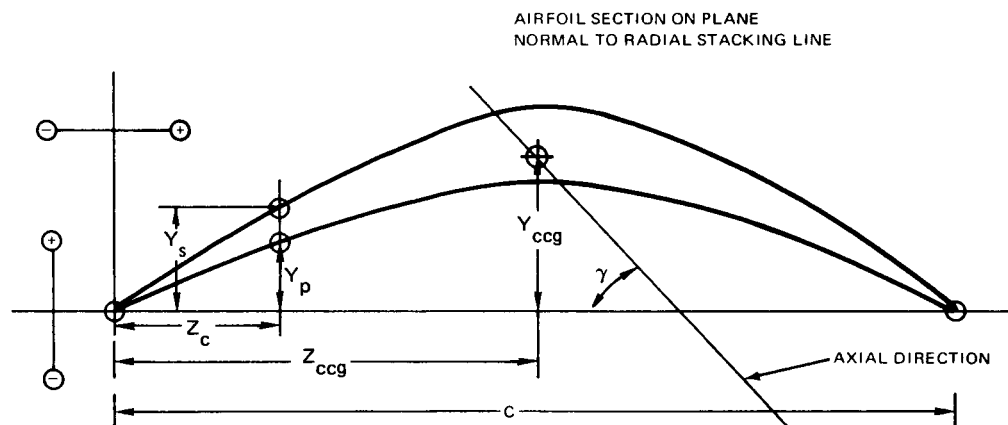


Figure 51 Airfoil Coordinate Labels for Manufacturing Sections

TABLE IX
 ROTOR MANUFACTURING COORDINATES
 FOR SECTIONS NORMAL TO STACKING LINE

A				B			
INCHES		METERS		INCHES		METERS	
ZC	YP	YS		ZC	YP	YS	
-.0000	-.0117	.0127	-.0000	-.0000	-.0105	.0111	.0003
.0948	.0499	.1011	.0024	.0997	.0341	.0753	.0019
.1896	.1120	.1902	.0048	.1993	.0787	.1396	.0035
.2844	.1742	.2799	.0072	.2990	.1231	.2041	.0052
.3793	.2369	.3700	.0096	.3987	.1674	.2687	.0068
.4741	.3000	.4631	.0120	.4984	.2116	.3341	.0085
.5689	.3639	.5579	.0145	.5980	.2560	.4002	.0102
.6637	.4283	.6482	.0169	.6977	.3006	.4658	.0118
.7585	.4931	.7254	.0193	.7974	.3456	.5285	.0134
.8533	.5572	.7976	.0217	.8970	.3904	.5871	.0149
.9480	.6176	.8691	.0241	.9967	.4336	.6404	.0163
1.0430	.6732	.9376	.0265	1.0964	.4742	.6903	.0175
1.1378	.7252	1.0066	.0289	1.1961	.5122	.7392	.0182
1.2326	.7727	1.0770	.0313	1.2957	.5470	.7883	.0200
1.3274	.8160	1.1428	.0337	1.3954	.5788	.8348	.0212
1.4222	.8549	1.2025	.0361	1.4951	.6072	.8779	.0223
1.5170	.8895	1.2504	.0385	1.5948	.6325	.9160	.0233
1.6119	.9194	1.2836	.0409	1.6944	.6542	.9463	.0240
1.7067	.9438	1.3038	.0433	1.7941	.6719	.9694	.0246
1.8015	.9631	1.3152	.0458	1.8938	.6856	.9841	.0250
1.8963	.9764	1.3228	.0482	1.9934	.6992	.9933	.0252
1.9911	.9830	1.3286	.0506	2.0931	.6992	.9975	.0253
2.0859	.9826	1.3273	.0530	2.1928	.6981	.9963	.0253
2.1808	.9738	1.3170	.0554	2.2925	.6908	.9881	.0251
2.2756	.9549	1.2965	.0578	2.3921	.6761	.9719	.0247
2.3704	.9242	1.2632	.0602	2.4918	.6526	.9459	.0240
2.4652	.8789	1.2138	.0626	2.5915	.6185	.9077	.0231
2.5600	.8144	1.1440	.0650	2.6911	.5705	.8540	.0217
2.6548	.7233	1.0441	.0674	2.7908	.5037	.7787	.0198
2.7497	.5898	.8974	.0698	2.8905	.4082	.6699	.0170
2.8445	.3710	.6516	.0722	2.9902	.2623	.4955	.0126
2.9393	.0141	-.0343	.0747	3.0898	-.0029	.0075	.0002
RADIUS (INCHES) = 7.984				RADIUS (INCHES) = 8.684			
CHORD (INCHES) = 2.939				CHORD (INCHES) = 3.090			
ZCSL (INCHES) = 1.6835				ZCSL (INCHES) = 1.8001			
YCSL (INCHES) = .8995				YCSL (INCHES) = .6574			
LER (INCHES) = .0105				LER (INCHES) = .0102			
TER (INCHES) = .0044				TER (INCHES) = .0014			
X-AREA (SQ. IN.) = .7910				X-AREA (SQ. IN.) = .6900			
GAMMA-CHORD (DEG.) = 24.56				GAMMA-CHORD (DEG.) = 32.40			
RADIUS (METERS) = 2.028				RADIUS (METERS) = 2.206			
CHORD (METERS) = .0747				CHORD (METERS) = .0785			
ZCSL (METERS) = .0428				ZCSL (METERS) = .0457			
YCSL (METERS) = .0228				YCSL (METERS) = .0167			
LER (METERS) = .000267				LER (METERS) = .000259			
TER (METERS) = .000112				TER (METERS) = .000036			
X-AREA (SQ. METERS) = .000510				X-AREA (SQ. METERS) = .000445			
GAMMA-CHORD (RAD.) = .4287				GAMMA-CHORD (RAD.) = .5656			

TABLE IX

ROTOR MANUFACTURING COORDINATES
FOR SECTIONS NORMAL TO STACKING LINE

C				METERS				INCHES				D				METERS				
INCHES		METERS		INCHES		METERS		INCHES		METERS		INCHES		METERS		INCHES		METERS		
ZC	YP	YS	ZC	YP	YS	ZC	YP	YS	ZC	YP	YS	ZC	YP	YS	ZC	YP	YS	ZC	YP	YS
-.0000	-.0102	.0104	.0000	-.0003	.0003	-.0000	-.0097	.0101	-.0000	-.0097	.0101	.0000	-.0002	.0003	.0000	-.0002	.0003	.0000	-.0002	.0003
.1031	.0268	.0640	.0026	.0007	.0016	.0026	.0194	.0546	.1061	.0194	.0546	.0027	.0005	.0014	.0027	.0005	.0014	.0027	.0005	.0014
.2062	.0637	.1177	.0052	.0016	.0030	.0052	.0494	.0991	.2122	.0494	.0991	.0122	.0091	.0025	.0122	.0091	.0025	.0122	.0091	.0025
.3092	.1002	.1712	.0079	.0025	.0043	.0079	.0786	.1435	.3183	.0786	.1435	.0183	.0020	.0036	.0183	.0020	.0036	.0183	.0020	.0036
.4123	.1363	.2246	.0105	.0035	.0057	.0105	.1075	.1876	.4244	.1075	.1876	.0244	.0027	.0048	.0244	.0027	.0048	.0244	.0027	.0048
.5154	.1720	.2776	.0131	.0044	.0071	.0131	.1360	.2314	.5306	.1360	.2314	.0306	.0035	.0059	.0306	.0035	.0059	.0306	.0035	.0059
.6185	.2072	.3304	.0157	.0053	.0094	.0157	.1641	.2751	.6367	.1641	.2751	.0367	.0042	.0070	.0367	.0042	.0070	.0367	.0042	.0070
.7216	.2420	.3839	.0183	.0061	.0098	.0183	.1918	.3194	.7428	.1918	.3194	.0428	.0049	.0081	.0428	.0049	.0081	.0428	.0049	.0081
.8246	.2770	.4381	.0209	.0070	.0111	.0209	.2194	.3635	.8489	.2194	.3635	.0489	.0056	.0092	.0489	.0056	.0092	.0489	.0056	.0092
.9277	.3117	.4888	.0236	.0079	.0124	.0236	.2465	.4044	.9550	.2465	.4044	.0550	.0063	.0103	.0550	.0063	.0103	.0550	.0063	.0103
1.0308	.3454	.5319	.0262	.0088	.0135	.0262	.2731	.4414	1.0611	.2731	.4414	.0611	.0069	.0112	.0611	.0069	.0112	.0611	.0069	.0112
1.1339	.3774	.5716	.0288	.0096	.0145	.0288	.2979	.4739	1.1672	.2979	.4739	.0672	.0076	.0120	.0672	.0076	.0120	.0672	.0076	.0120
1.2370	.4070	.6092	.0314	.0103	.0155	.0314	.3207	.5030	1.2733	.3207	.5030	.0733	.0081	.0128	.0733	.0081	.0128	.0733	.0081	.0128
1.3400	.4342	.6453	.0340	.0110	.0164	.0340	.3433	.5298	1.3794	.3433	.5298	.0789	.0087	.0135	.0789	.0087	.0135	.0789	.0087	.0135
1.4431	.4586	.6795	.0367	.0116	.0173	.0367	.3595	.5544	1.4856	.3595	.5544	.0844	.0091	.0141	.0844	.0091	.0141	.0844	.0091	.0141
1.5462	.4805	.7116	.0393	.0122	.0181	.0393	.3752	.5783	1.5917	.3752	.5783	.0900	.0095	.0147	.0900	.0095	.0147	.0900	.0095	.0147
1.6493	.4995	.7421	.0419	.0127	.0188	.0419	.3888	.6016	1.6978	.3888	.6016	.0957	.0099	.0153	.0957	.0099	.0153	.0957	.0099	.0153
1.7524	.5157	.7683	.0445	.0131	.0195	.0445	.3999	.6231	1.8039	.3999	.6231	.1014	.0102	.0158	.1014	.0102	.0158	.1014	.0102	.0158
1.8554	.5285	.7895	.0471	.0134	.0201	.0471	.4136	.6408	1.8510	.4136	.6408	.1052	.0105	.0163	.1052	.0105	.0163	.1052	.0105	.0163
1.9585	.5379	.8041	.0497	.0137	.0204	.0497	.4272	.6528	1.9161	.4272	.6528	.1098	.0106	.0166	.1098	.0106	.0166	.1098	.0106	.0166
2.0616	.5435	.8120	.0524	.0138	.0206	.0524	.4407	.6582	2.1222	.4407	.6582	.1144	.0105	.0165	.1144	.0105	.0165	.1144	.0105	.0165
2.1647	.5448	.8138	.0550	.0138	.0207	.0550	.4536	.6585	2.2283	.4536	.6585	.1190	.0104	.0164	.1190	.0104	.0164	.1190	.0104	.0164
2.2678	.5416	.8098	.0576	.0138	.0206	.0576	.4661	.6480	2.2944	.4661	.6480	.1236	.0102	.0161	.1236	.0102	.0161	.1236	.0102	.0161
2.3709	.5331	.7995	.0602	.0135	.0203	.0602	.4786	.6352	2.3606	.4786	.6352	.1282	.0098	.0156	.1282	.0098	.0156	.1282	.0098	.0156
2.4739	.5184	.7820	.0628	.0132	.0199	.0628	.4909	.6160	2.4467	.4909	.6160	.1328	.0093	.0150	.1328	.0093	.0150	.1328	.0093	.0150
2.5770	.4966	.7558	.0655	.0126	.0192	.0655	.5032	.5895	2.5498	.5032	.5895	.1374	.0086	.0141	.1374	.0086	.0141	.1374	.0086	.0141
2.6801	.4660	.7191	.0681	.0118	.0183	.0681	.5155	.5541	2.6528	.5155	.5541	.1420	.0077	.0129	.1420	.0077	.0129	.1420	.0077	.0129
2.7832	.4243	.6691	.0707	.0108	.0170	.0707	.5278	.5072	2.7599	.5278	.5072	.1466	.0065	.0113	.1466	.0065	.0113	.1466	.0065	.0113
2.8863	.3679	.6005	.0733	.0083	.0153	.0733	.5401	.4449	2.8650	.5401	.4449	.1512	.0049	.0092	.1512	.0049	.0092	.1512	.0049	.0092
2.9893	.2900	.5042	.0759	.0074	.0128	.0759	.5524	.3666	2.9711	.5524	.3666	.1558	.0028	.0051	.1558	.0028	.0051	.1558	.0028	.0051
3.0924	.1766	.3562	.0785	.0045	.0090	.0785	.5647	.2387	3.0772	.5647	.2387	.1604	.0003	.0005	.1604	.0003	.0005	.1604	.0003	.0005
3.1955	-.0097	.0207	.0812	-.0002	.0005	.0812	.5770	.0210	3.2895	.5770	.0210	.1650	-.0003	.0005	.1650	-.0003	.0005	.1650	-.0003	.0005
				RADIUS (INCHES) = 9.144				RADIUS (METERS) = .2323				RADIUS (INCHES) = 9.594				RADIUS (METERS) = .2437				
				CHORD (INCHES) = 3.196				CHORD (METERS) = .0812				CHORD (INCHES) = 3.289				CHORD (METERS) = .0836				
				ZCSL (INCHES) = 1.8461				ZCSL (METERS) = .0469				ZCSL (INCHES) = 1.8697				ZCSL (METERS) = .0475				
				YCSL (INCHES) = .5242				YCSL (METERS) = .0133				YCSL (INCHES) = .4110				YCSL (METERS) = .0104				
				LER (INCHES) = .0101				LER (METERS) = .00257				LER (INCHES) = .0100				LER (METERS) = .00254				
				TER (INCHES) = .0060				TER (METERS) = .000152				TER (INCHES) = .0099				TER (METERS) = .00251				
				X-AREA (SQ. IN.) = .6209				X-AREA (SQ. METERS) = .000401				X-AREA (SQ. IN.) = .5570				X-AREA (SQ. METERS) = .000359				
				GAMMA-CHORD(DEG.) = 36.80				GAMMA-CHORD(DEG.) = .6423				GAMMA-CHORD(DEG.) = 40.55				GAMMA-CHORD(DEG.) = .7078				

TABLE IX

ROTOR MANUFACTURING COORDINATES
FOR SECTIONS NORMAL TO STACKING LINE

E			F		
INCHES			INCHES		
ZC	YP	YS	ZC	YP	YS
-.0000	-.0088	.0101	-.0000	-.0086	.0099
.1085	.0142	.0471	.1098	.0084	.0393
.2171	.0370	.0838	.2197	.0249	.0684
.3256	.0594	.1201	.3296	.0410	.0970
.4342	.0815	.1560	.4394	.0564	.1250
.5427	.1032	.1916	.5493	.0713	.1526
.6512	.1245	.2270	.6591	.0855	.1796
.7598	.1455	.2624	.7690	.0991	.2059
.8683	.1663	.2970	.8788	.1125	.2319
.9769	.1870	.3304	.9887	.1259	.2582
1.0854	.2075	.3622	1.0985	.1398	.2851
1.1939	.2269	.3908	1.2084	.1532	.3092
1.3025	.2448	.4142	1.3182	.1657	.3300
1.4110	.2605	.4339	1.4281	.1767	.3467
1.5196	.2742	.4518	1.5379	.1860	.3596
1.6281	.2858	.4686	1.6478	.1937	.3697
1.7366	.2951	.4845	1.7576	.1997	.3774
1.8452	.3022	.4994	1.8675	.2040	.3835
1.9537	.3068	.5111	1.9774	.2065	.3882
2.0623	.3089	.5195	2.0872	.2071	.3923
2.1708	.3083	.5251	2.1971	.2056	.3942
2.2793	.3049	.5234	2.3069	.2020	.3918
2.3879	.2987	.5119	2.4168	.1960	.3839
2.4964	.2885	.4957	2.5266	.1873	.3698
2.6050	.2751	.4744	2.6365	.1758	.3486
2.7135	.2575	.4474	2.7463	.1611	.3218
2.8220	.2349	.4134	2.8562	.1428	.2901
2.9306	.2065	.3706	2.9660	.1214	.2520
3.0391	.1708	.3168	3.0759	.0961	.2070
3.1476	.1255	.2478	3.1857	.0667	.1536
3.2562	.0669	.1553	3.2956	.0314	.0893
3.3647	-.0119	.0167	3.4054	-.0097	.0110
METERS			METERS		
ZC	YP	YS	ZC	YP	YS
-.0000	-.0002	.0003	.0000	-.0002	.0003
.0028	.0004	.0012	.0028	.0002	.0010
.0055	.0009	.0021	.0056	.0006	.0017
.0083	.0015	.0031	.0084	.0010	.0025
.0110	.0021	.0040	.0112	.0014	.0032
.0138	.0026	.0049	.0140	.0018	.0039
.0165	.0032	.0058	.0167	.0022	.0046
.0193	.0037	.0067	.0195	.0025	.0052
.0221	.0042	.0075	.0223	.0029	.0059
.0248	.0047	.0084	.0251	.0032	.0066
.0276	.0053	.0092	.0279	.0036	.0072
.0303	.0058	.0099	.0307	.0039	.0079
.0331	.0062	.0105	.0335	.0042	.0084
.0358	.0066	.0110	.0363	.0045	.0088
.0386	.0070	.0115	.0391	.0047	.0091
.0414	.0073	.0119	.0419	.0049	.0094
.0441	.0075	.0123	.0446	.0051	.0096
.0469	.0077	.0127	.0474	.0052	.0097
.0496	.0078	.0130	.0502	.0052	.0099
.0524	.0078	.0132	.0530	.0053	.0100
.0551	.0078	.0133	.0558	.0052	.0100
.0579	.0077	.0133	.0586	.0051	.0100
.0607	.0076	.0130	.0614	.0050	.0098
.0634	.0073	.0126	.0642	.0048	.0094
.0662	.0070	.0120	.0670	.0045	.0089
.0689	.0065	.0114	.0698	.0041	.0082
.0717	.0060	.0105	.0725	.0036	.0074
.0744	.0052	.0094	.0753	.0031	.0064
.0772	.0043	.0080	.0781	.0024	.0053
.0800	.0032	.0063	.0809	.0017	.0039
.0827	.0017	.0039	.0837	.0008	.0023
.0855	-.0003	.0004	.0865	-.0002	.0003
RADIUS (INCHES)			RADIUS (INCHES)		
10.044	10.044	10.044	10.504	10.504	10.504
3.365	3.365	3.365	3.405	3.405	3.405
1.8755	1.8755	1.8755	1.8631	1.8631	1.8631
.3160	.3160	.3160	.2295	.2295	.2295
.0097	.0097	.0097	.0096	.0096	.0096
.0116	.0116	.0116	.0104	.0104	.0104
.4994	.4994	.4994	.4488	.4488	.4488
43.86	43.86	43.86	47.15	47.15	47.15
RADIUS (METERS)			RADIUS (METERS)		
.2688	.2688	.2688	.2688	.2688	.2688
.0865	.0865	.0865	.0865	.0865	.0865
.0473	.0473	.0473	.0473	.0473	.0473
.0058	.0058	.0058	.0058	.0058	.0058
.00244	.00244	.00244	.00244	.00244	.00244
.000264	.000264	.000264	.000264	.000264	.000264
.000290	.000290	.000290	.000290	.000290	.000290
.8229	.8229	.8229	.8229	.8229	.8229

TABLE IX

ROTOR MANUFACTURING COORDINATES
FOR SECTIONS NORMAL TO STACKING LINE

INCHES			METERS			INCHES			METERS		
ZC	YP	YS	ZC	YP	YS	ZC	YP	YS	ZC	YP	YS
-.0000	-.0086	.0090	.0000	-.0002	.0002	-.0000	-.0086	.0087	.0000	-.0002	.0002
.1162	.0040	.0321	.0030	.0001	.0008	.1160	.0024	.0293	.0029	.0001	.0007
.2324	.0161	.0548	.0059	.0004	.0014	.2321	.0128	.0494	.0059	.0003	.0013
.3485	.0275	.0767	.0089	.0007	.0019	.3481	.0226	.0685	.0088	.0006	.0017
.4647	.0381	.0978	.0118	.0010	.0025	.4641	.0316	.0867	.0118	.0008	.0022
.5809	.0480	.1182	.0148	.0012	.0030	.5802	.0398	.1038	.0147	.0010	.0026
.6971	.0571	.1376	.0177	.0015	.0035	.6962	.0474	.1196	.0177	.0012	.0030
.8133	.0654	.1572	.0207	.0017	.0040	.8122	.0542	.1357	.0206	.0014	.0034
.9294	.0728	.1768	.0236	.0018	.0045	.9283	.0602	.1533	.0236	.0015	.0039
1.0456	.0795	.1960	.0266	.0020	.0050	1.0443	.0654	.1710	.0265	.0017	.0043
1.1618	.0857	.2151	.0295	.0022	.0055	1.1603	.0697	.1884	.0295	.0018	.0048
1.2780	.0916	.2342	.0325	.0023	.0059	1.2764	.0731	.2054	.0324	.0019	.0052
1.3941	.0971	.2535	.0354	.0025	.0064	1.3924	.0754	.2220	.0354	.0019	.0056
1.5103	.1017	.2705	.0384	.0026	.0069	1.5084	.0767	.2382	.0383	.0019	.0060
1.6265	.1060	.2839	.0413	.0027	.0072	1.6245	.0781	.2534	.0413	.0020	.0064
1.7427	.1102	.2935	.0443	.0028	.0075	1.7405	.0803	.2668	.0442	.0020	.0068
1.8589	.1143	.3039	.0472	.0029	.0077	1.8565	.0835	.2833	.0472	.0021	.0072
1.9750	.1177	.3071	.0502	.0030	.0078	1.9726	.0872	.2964	.0501	.0023	.0075
2.0912	.1196	.3042	.0531	.0030	.0078	2.0886	.0901	.3007	.0531	.0023	.0076
2.2074	.1189	.2980	.0561	.0030	.0076	2.2046	.0894	.2955	.0560	.0023	.0075
2.3236	.1168	.2920	.0590	.0030	.0074	2.3207	.0852	.2852	.0589	.0020	.0072
2.4398	.1138	.2843	.0620	.0029	.0072	2.4367	.0802	.2727	.0619	.0020	.0069
2.5559	.1100	.2749	.0649	.0028	.0070	2.5527	.0746	.2577	.0648	.0019	.0065
2.6721	.1051	.2639	.0679	.0027	.0067	2.6688	.0684	.2406	.0678	.0017	.0061
2.7883	.0992	.2511	.0708	.0025	.0064	2.7848	.0615	.2212	.0707	.0016	.0056
2.9045	.0912	.2346	.0738	.0023	.0060	2.9008	.0539	.1995	.0737	.0014	.0051
3.0207	.0807	.2114	.0767	.0020	.0054	3.0168	.0455	.1753	.0766	.0012	.0045
3.1368	.0681	.1823	.0797	.0017	.0046	3.1329	.0363	.1498	.0796	.0009	.0038
3.2530	.0532	.1478	.0826	.0014	.0038	3.2489	.0264	.1228	.0825	.0007	.0031
3.3692	.0358	.1020	.0856	.0009	.0027	3.3649	.0156	.0934	.0855	.0004	.0024
3.4854	.0158	.0627	.0885	.0004	.0016	3.4810	.0039	.0612	.0884	.0001	.0016
3.6016	-.0069	.0104	.0915	-.0002	.0003	3.5970	-.0087	.0071	.0914	-.0002	.0002

RADIUS (INCHES) = 11.284	RADIUS (INCHES) = 11.984	RADIUS (INCHES) = 11.984
CHORD (INCHES) = 3.602	CHORD (INCHES) = 3.597	CHORD (INCHES) = 3.597
ZCSL (INCHES) = 1.9450	ZCSL (INCHES) = 1.9840	ZCSL (INCHES) = 1.9840
YCSL (INCHES) = .1565	YCSL (INCHES) = .1309	YCSL (INCHES) = .1309
LER (INCHES) = .0091	LER (INCHES) = .0089	LER (INCHES) = .0089
TER (INCHES) = .0092	TER (INCHES) = .0090	TER (INCHES) = .0090
X-AREA (SQ. IN.) = .4398	X-AREA (SQ. IN.) = .4509	X-AREA (SQ. IN.) = .4509
GAMMA-CHORD(DEG.) = 49.95	GAMMA-CHORD(DEG.) = 51.29	GAMMA-CHORD(DEG.) = 51.29
RADIUS (METERS) = 2.866	RADIUS (METERS) = 3.044	RADIUS (METERS) = 3.044
CHORD (METERS) = .0915	CHORD (METERS) = .0914	CHORD (METERS) = .0914
ZCSL (METERS) = .0494	ZCSL (METERS) = .0504	ZCSL (METERS) = .0504
YCSL (METERS) = .0040	YCSL (METERS) = .0033	YCSL (METERS) = .0033
LER (METERS) = .00231	LER (METERS) = .00226	LER (METERS) = .00226
TER (METERS) = .00234	TER (METERS) = .00229	TER (METERS) = .00229
X-AREA (SQ. METERS) = .00284	X-AREA (SQ. METERS) = .00291	X-AREA (SQ. METERS) = .00291
GAMMA-CHORD(RAD.) = .8717	GAMMA-CHORD(RAD.) = .8951	GAMMA-CHORD(RAD.) = .8951

TABLE IX

ROTOR MANUFACTURING COORDINATES
FOR SECTIONS NORMAL TO STACKING LINE

I				J			
INCHES		METERS		INCHES		METERS	
ZC	YP	YS	ZC	YP	YS	ZC	YP
-.0000	-.0082	.0083	-.0000	-.0081	.0081	.0000	-.0002
.1178	.0002	.0256	.1183	-.0015	.0232	.0030	-.0000
.2356	.0079	.0421	.2366	.0044	.0374	.0060	.0001
.3534	.0148	.0576	.3549	.0095	.0505	.0090	.0002
.4711	.0209	.0719	.4732	.0138	.0623	.0120	.0004
.5889	.0262	.0848	.5915	.0173	.0726	.0150	.0004
.7067	.0306	.0965	.7097	.0199	.0819	.0180	.0005
.8245	.0343	.1094	.8280	.0218	.0926	.0210	.0006
.9423	.0375	.1251	.9463	.0233	.1063	.0240	.0006
1.0601	.0402	.1416	1.0646	.0245	.1217	.0270	.0006
1.1778	.0427	.1578	1.1829	.0256	.1370	.0300	.0007
1.2956	.0449	.1735	1.3012	.0269	.1520	.0331	.0007
1.4134	.0471	.1887	1.4195	.0285	.1665	.0361	.0007
1.5312	.0494	.2035	1.5378	.0300	.1805	.0391	.0008
1.6490	.0517	.2177	1.6561	.0330	.1941	.0421	.0008
1.7668	.0539	.2315	1.7744	.0354	.2073	.0451	.0009
1.8846	.0557	.2443	1.8927	.0376	.2198	.0481	.0010
2.0023	.0568	.2548	2.0109	.0392	.2308	.0511	.0010
2.1201	.0570	.2608	2.1292	.0398	.2393	.0541	.0010
2.2379	.0557	.2609	2.2475	.0396	.2417	.0571	.0010
2.3557	.0537	.2513	2.3658	.0388	.2334	.0601	.0010
2.4735	.0510	.2367	2.4841	.0374	.2201	.0631	.0010
2.5913	.0477	.2199	2.6024	.0354	.2033	.0661	.0009
2.7091	.0437	.2013	2.7207	.0328	.1844	.0691	.0008
2.8268	.0390	.1813	2.8390	.0297	.1642	.0721	.0008
2.9446	.0337	.1602	2.9573	.0260	.1435	.0751	.0007
3.0624	.0278	.1384	3.0756	.0218	.1224	.0781	.0006
3.1802	.0213	.1160	3.1939	.0170	.1014	.0811	.0004
3.2980	.0141	.0925	3.3121	.0118	.0803	.0841	.0003
3.4158	.0064	.0671	3.4304	.0060	.0585	.0871	.0002
3.5336	-.0020	.0373	3.5487	-.0002	.0359	.0901	-.0000
3.6513	-.0109	.0073	3.6670	-.0069	.0028	.0931	-.0002
RADIUS (INCHES) = 12.694				RADIUS (INCHES) = 13.054			
CHORD (INCHES) = 3.651				CHORD (INCHES) = 3.667			
ZCSL (INCHES) = 1.9779				ZCSL (INCHES) = 1.9762			
YCSL (INCHES) = .1020				YCSL (INCHES) = .0857			
LER (INCHES) = .0085				LER (INCHES) = .0084			
TER (INCHES) = .0098				TER (INCHES) = .0053			
X-AREA (SQ. IN.) = .4244				X-AREA (SQ. IN.) = .4051			
GAMMA-CHORD(DEG.) = 53.66				GAMMA-CHORD(DEG.) = 55.19			
RADIUS (METERS) = .3224				RADIUS (METERS) = .3316			
CHORD (METERS) = .0927				CHORD (METERS) = .0931			
ZCSL (METERS) = .0502				ZCSL (METERS) = .0502			
YCSL (METERS) = .0026				YCSL (METERS) = .0022			
LER (METERS) = .000216				LER (METERS) = .000213			
TER (METERS) = .000249				TER (METERS) = .000135			
X-AREA (SQ. METERS) = .000274				X-AREA (SQ. METERS) = .000264			
GAMMA-CHORD(RAD.) = .9365				GAMMA-CHORD(RAD.) = .9632			

TABLE IX

ROTOR MANUFACTURING COORDINATES
FOR SECTIONS NORMAL TO STACKING LINE

INCHES			METERS			INCHES			L			METERS		
ZC	YP	YS	ZC	YP	YS	ZC	YP	YS	ZC	YP	YS	ZC	YP	YS
-.0000	-.0079	.0080	.0000	-.0002	.0002	-.0000	-.0079	.0080	.0000	-.0002	.0002	.0000	-.0002	.0002
.1196	-.0039	.0201	.0030	-.0001	.0005	.1193	-.0044	.0194	.0030	-.0001	.0005	.0030	-.0001	.0005
.2393	-.0007	.0312	.0061	-.0000	.0008	.2386	-.0016	.0298	.0061	-.0000	.0008	.0061	-.0000	.0008
.3589	.0017	.0411	.0091	.0000	.0010	.3580	.0003	.0391	.0091	.0000	.0010	.0091	.0000	.0010
.4786	.0032	.0497	.0122	.0001	.0013	.4773	.0013	.0471	.0121	.0000	.0012	.0121	.0000	.0012
.5982	.0038	.0568	.0152	.0001	.0014	.5966	.0014	.0538	.0152	.0000	.0014	.0152	.0000	.0014
.7179	.0036	.0627	.0182	.0001	.0016	.7160	.0006	.0587	.0182	.0000	.0015	.0182	.0000	.0015
.8375	.0026	.0699	.0213	.0001	.0018	.8353	-.0008	.0650	.0212	-.0000	.0016	.0212	-.0000	.0016
.9572	.0014	.0805	.0243	.0000	.0020	.9546	-.0025	.0742	.0242	-.0001	.0019	.0242	-.0001	.0019
1.0768	.0002	.0940	.0274	.0000	.0024	1.0739	-.0042	.0872	.0273	-.0001	.0022	.0273	-.0001	.0022
1.1965	-.0005	.1079	.0304	-.0000	.0027	1.1933	-.0053	.1008	.0303	-.0001	.0026	.0303	-.0001	.0026
1.3161	-.0004	.1218	.0334	-.0000	.0031	1.3126	-.0053	.1145	.0333	-.0001	.0029	.0333	-.0001	.0029
1.4358	.0008	.1352	.0365	.0000	.0034	1.4319	-.0042	.1278	.0364	-.0001	.0032	.0364	-.0001	.0032
1.5554	.0028	.1481	.0395	.0001	.0038	1.5512	-.0020	.1406	.0394	-.0001	.0036	.0394	-.0001	.0036
1.6751	.0056	.1606	.0425	.0001	.0041	1.6706	.0008	.1529	.0424	.0000	.0039	.0424	.0000	.0039
1.7947	.0086	.1727	.0456	.0002	.0044	1.7899	.0042	.1648	.0455	.0001	.0042	.0455	.0001	.0042
1.9144	.0116	.1842	.0486	.0003	.0047	1.9092	.0074	.1763	.0485	.0002	.0045	.0485	.0002	.0045
2.0340	.0139	.1941	.0517	.0004	.0049	2.0286	.0100	.1862	.0515	.0003	.0047	.0515	.0003	.0047
2.1537	.0155	.2021	.0547	.0004	.0051	2.1479	.0120	.1949	.0546	.0003	.0050	.0546	.0003	.0050
2.2733	.0165	.2071	.0577	.0004	.0053	2.2672	.0135	.2010	.0576	.0003	.0051	.0576	.0003	.0051
2.3930	.0170	.2066	.0608	.0004	.0052	2.3865	.0144	.2022	.0606	.0004	.0051	.0606	.0004	.0051
2.5126	.0170	.1961	.0638	.0004	.0050	2.5059	.0148	.1947	.0636	.0004	.0049	.0636	.0004	.0049
2.6323	.0165	.1780	.0669	.0004	.0045	2.6252	.0147	.1777	.0667	.0004	.0045	.0667	.0004	.0045
2.7519	.0154	.1577	.0699	.0004	.0040	2.7445	.0141	.1574	.0697	.0004	.0040	.0697	.0004	.0040
2.8716	.0139	.1367	.0729	.0004	.0035	2.8638	.0131	.1361	.0727	.0003	.0035	.0727	.0003	.0035
2.9912	.0119	.1156	.0760	.0003	.0029	2.9832	.0115	.1147	.0758	.0003	.0029	.0758	.0003	.0029
3.1109	.0095	.0954	.0790	.0002	.0024	3.1025	.0094	.0943	.0788	.0002	.0024	.0788	.0002	.0024
3.2305	.0066	.0765	.0821	.0002	.0019	3.2218	.0069	.0752	.0818	.0002	.0019	.0818	.0002	.0019
3.3502	.0032	.0588	.0851	.0001	.0015	3.3412	.0039	.0573	.0849	.0001	.0015	.0849	.0001	.0015
3.4698	-.0005	.0420	.0881	-.0000	.0011	3.4605	.0004	.0404	.0879	.0000	.0010	.0879	.0000	.0010
3.5895	-.0047	.0263	.0912	-.0001	.0007	3.5798	-.0036	.0236	.0909	-.0001	.0006	.0909	-.0001	.0006
3.7091	-.0094	.0080	.0942	-.0002	.0002	3.6992	-.0081	.0048	.0940	-.0002	.0001	.0940	-.0002	.0001
RADIUS (INCHES) = 13.614			RADIUS (METERS) = 34.58			RADIUS (INCHES) = 13.764			RADIUS (METERS) = 34.96			RADIUS (METERS) = 34.96		
CHORD (INCHES) = 3.709			CHORD (METERS) = .0942			CHORD (INCHES) = 3.699			CHORD (METERS) = .0940			CHORD (METERS) = .0940		
ZCSL (INCHES) = 1.9726			ZCSL (METERS) = .0501			ZCSL (INCHES) = 1.9652			ZCSL (METERS) = .0499			ZCSL (METERS) = .0499		
YCSL (INCHES) = .0603			YCSL (METERS) = .0015			YCSL (INCHES) = .0567			YCSL (METERS) = .0014			YCSL (METERS) = .0014		
LER (INCHES) = .0082			LER (METERS) = .000208			LER (INCHES) = .0082			LER (METERS) = .000208			LER (METERS) = .000208		
TER (INCHES) = .0092			TER (METERS) = .000234			TER (INCHES) = .0068			TER (METERS) = .000173			TER (METERS) = .000173		
X-AREA (SQ. IN.) = .3897			X-AREA (SQ. METERS) = .000251			X-AREA (SQ. IN.) = .3822			X-AREA (SQ. METERS) = .000247			X-AREA (SQ. METERS) = .000247		
GAMMA-CHORD (DEG.) = 57.54			GAMMA-CHORD (RAD.) = 1.0043			GAMMA-CHORD (DEG.) = 58.15			GAMMA-CHORD (RAD.) = 1.0149			GAMMA-CHORD (RAD.) = 1.0149		

TABLE IX
 ROTOR MANUFACTURING COORDINATES
 FOR SECTIONS NORMAL TO STACKING LINE

INCHES			METERS			INCHES			N			METERS		
ZC	YP	YS	ZC	YP	YS	ZC	YP	YS	ZC	YP	YS	ZC	YP	YS
-.0000	-.0080	.0080	.0000	-.0002	.0002	-.0000	-.0079	.0079	.0000	-.0002	.0002	.0000	-.0002	.0002
.1195	-.0047	.0189	.0030	-.0001	.0005	.1218	-.0052	.0177	.0031	-.0001	.0001	.0031	-.0001	.0001
.2390	-.0022	.0289	.0061	-.0001	.0007	.2437	-.0033	.0265	.0062	-.0001	.0001	.0062	-.0001	.0001
.3584	-.0005	.0377	.0091	-.0000	.0010	.3655	-.0023	.0341	.0093	-.0001	.0001	.0093	-.0001	.0001
.4779	.0002	.0452	.0121	.0000	.0011	.4873	-.0022	.0404	.0124	-.0001	.0001	.0124	-.0001	.0001
.5974	-.0001	.0515	.0152	-.0000	.0013	.6091	-.0031	.0453	.0155	-.0001	.0001	.0155	-.0001	.0001
.7169	-.0012	.0558	.0182	-.0000	.0014	.7310	-.0048	.0485	.0186	-.0001	.0001	.0186	-.0001	.0001
.8363	-.0030	.0613	.0212	-.0001	.0016	.8528	-.0073	.0516	.0217	-.0002	.0002	.0217	-.0002	.0002
.9558	-.0051	.0697	.0243	-.0001	.0018	.9746	-.0101	.0571	.0248	-.0003	.0003	.0248	-.0003	.0003
1.0753	-.0071	.0819	.0273	-.0002	.0021	1.0964	-.0124	.0667	.0278	-.0003	.0003	.0278	-.0003	.0003
1.1948	-.0083	.0956	.0303	-.0002	.0024	1.2183	-.0136	.0797	.0309	-.0003	.0003	.0309	-.0003	.0003
1.3143	-.0084	.1094	.0334	-.0002	.0028	1.3401	-.0135	.0937	.0340	-.0003	.0003	.0340	-.0003	.0003
1.4337	-.0071	.1227	.0364	-.0002	.0031	1.4619	-.0119	.1081	.0371	-.0003	.0003	.0371	-.0003	.0003
1.5532	-.0048	.1357	.0395	-.0001	.0034	1.5838	-.0092	.1219	.0402	-.0002	.0002	.0402	-.0002	.0002
1.6727	-.0017	.1481	.0425	-.0000	.0038	1.7056	-.0057	.1353	.0433	-.0001	.0001	.0433	-.0001	.0001
1.7922	-.0020	.1602	.0455	-.0001	.0041	1.8274	-.0017	.1482	.0464	-.0000	.0000	.0464	-.0000	.0000
1.9117	.0055	.1719	.0486	.0001	.0044	1.9492	.0018	.1607	.0495	.0000	.0000	.0495	.0000	.0000
2.0311	.0084	.1821	.0516	.0002	.0046	2.0711	.0048	.1721	.0526	.0001	.0001	.0526	.0001	.0001
2.1506	.0107	.1913	.0546	.0003	.0049	2.1929	.0071	.1824	.0557	.0002	.0002	.0557	.0002	.0002
2.2701	.0124	.1985	.0577	.0003	.0050	2.3147	.0089	.1919	.0588	.0002	.0002	.0588	.0002	.0002
2.3896	.0136	.2016	.0607	.0003	.0051	2.4366	.0102	.1989	.0619	.0003	.0003	.0619	.0003	.0003
2.5090	.0143	.1948	.0637	.0004	.0049	2.5584	.0109	.1969	.0650	.0003	.0003	.0650	.0003	.0003
2.6285	.0145	.1790	.0668	.0004	.0045	2.6802	.0111	.1852	.0681	.0003	.0003	.0681	.0003	.0003
2.7480	.0141	.1592	.0698	.0004	.0040	2.8020	.0108	.1651	.0712	.0003	.0003	.0712	.0003	.0003
2.8675	.0132	.1375	.0728	.0003	.0035	2.9239	.0100	.1421	.0743	.0003	.0003	.0743	.0003	.0003
2.9870	.0118	.1157	.0759	.0003	.0029	3.0457	.0088	.1189	.0774	.0002	.0002	.0774	.0002	.0002
3.1064	.0099	.0950	.0789	.0002	.0024	3.1675	.0072	.0967	.0805	.0002	.0002	.0805	.0002	.0002
3.2259	.0075	.0756	.0819	.0002	.0019	3.2894	.0052	.0760	.0835	.0001	.0001	.0835	.0001	.0001
3.3454	.0046	.0576	.0850	.0001	.0015	3.4112	.0030	.0572	.0866	.0001	.0001	.0866	.0001	.0001
3.4649	.0011	.0407	.0880	.0000	.0010	3.5330	-.0003	.0398	.0897	-.0000	.0000	.0897	-.0000	.0000
3.5844	-.0032	.0254	.0910	-.0001	.0006	3.6548	-.0041	.0222	.0928	-.0001	.0001	.0928	-.0001	.0001
3.7038	-.0080	.0052	.0941	-.0002	.0001	3.7767	-.0084	.0067	.0959	-.0002	.0002	.0959	-.0002	.0002
RADIUS (INCHES) = 13.914			RADIUS (METERS) = .3534			RADIUS (INCHES) = 14.474			RADIUS (METERS) = .3676			RADIUS (METERS) = .3676		
CHORD (INCHES) = 3.704			CHORD (METERS) = .0941			CHORD (INCHES) = 3.777			CHORD (METERS) = .0959			CHORD (METERS) = .0959		
ZCSL (INCHES) = 1.9742			ZCSL (METERS) = .0501			ZCSL (INCHES) = 2.0459			ZCSL (METERS) = .0520			ZCSL (METERS) = .0520		
YCSL (INCHES) = .0548			YCSL (METERS) = .0014			YCSL (INCHES) = .0498			YCSL (METERS) = .0013			YCSL (METERS) = .0013		
LER (INCHES) = .0082			LER (METERS) = .000208			LER (INCHES) = .0081			LER (METERS) = .000206			LER (METERS) = .000206		
TER (INCHES) = .0070			TER (METERS) = .000178			TER (INCHES) = .0079			TER (METERS) = .000201			TER (METERS) = .000201		
X-AREA (SQ. IN.) = .3797			X-AREA (SQ. METERS) = .000245			X-AREA (SQ. IN.) = .3787			X-AREA (SQ. METERS) = .000244			X-AREA (SQ. METERS) = .000244		
GAMMA-CHORD (DEG.) = 58.71			GAMMA-CHORD (RAD.) = 1.0246			GAMMA-CHORD (DEG.) = 60.95			GAMMA-CHORD (RAD.) = 1.0637			GAMMA-CHORD (RAD.) = 1.0637		

TABLE IX

ROTOR MANUFACTURING COORDINATES
FOR SECTIONS NORMAL TO STACKING LINE

O			P		
INCHES		METERS	INCHES		METERS
ZC	YP	YS	ZC	YP	YS
-.0000	-.0080	.0080	-.0000	-.0077	.0077
.1289	-.0100	.0130	.1379	-.0134	.0092
.2577	-.0128	.0065	.2759	-.0196	.0102
.3866	-.0155	.0098	.4138	-.0265	.0106
.5154	-.0212	.0218	.5518	-.0339	.0103
.6443	-.0267	.0225	.6897	-.0419	.0095
.7731	-.0330	.0220	.8277	-.0503	.0080
.9020	-.0402	.0201	.9656	-.0592	.0059
1.0309	-.0479	.0183	1.1036	-.0691	.0031
1.1597	-.0538	.0199	1.2415	-.0784	.0010
1.2886	-.0561	.0257	1.3795	-.0829	.0031
1.4174	-.0554	.0355	1.5174	-.0828	.0100
1.5463	-.0534	.0479	1.6554	-.0811	.0229
1.6751	-.0517	.0611	1.7933	-.0793	.0378
1.8040	-.0503	.0740	1.9312	-.0776	.0534
1.9329	-.0493	.0864	2.0692	-.0759	.0685
2.0617	-.0480	.0983	2.2071	-.0742	.0832
2.1906	-.0476	.1098	2.3451	-.0724	.0976
2.3194	-.0472	.1209	2.4830	-.0705	.1113
2.4483	-.0467	.1307	2.6210	-.0683	.1217
2.5772	-.0461	.1372	2.7589	-.0660	.1266
2.7060	-.0453	.1368	2.8969	-.0633	.1223
2.8349	-.0441	.1259	3.0348	-.0603	.1088
2.9637	-.0425	.1067	3.1728	-.0569	.0924
3.0926	-.0425	.0852	3.3107	-.0531	.0762
3.2214	-.0403	.0643	3.4487	-.0485	.0598
3.3503	-.0374	.0468	3.5866	-.0432	.0446
3.4792	-.0332	.0340	3.7246	-.0372	.0324
3.6080	-.0277	.0249	3.8625	-.0304	.0242
3.7369	-.0213	.0187	4.0004	-.0229	.0189
3.8657	-.0140	.0131	4.1384	-.0146	.0144
3.9946	-.0057	.0050	4.2763	-.0055	.0064
RADIUS (INCHES) = 15.324			RADIUS (INCHES) = 16.044		
CHORD (INCHES) = 3.995			CHORD (INCHES) = 4.276		
ZCSL (INCHES) = 2.1628			ZCSL (INCHES) = 2.3098		
YCSL (INCHES) = .0009			YCSL (INCHES) = -.0144		
LER (INCHES) = .0082			LER (INCHES) = .0079		
TER (INCHES) = .0057			TER (INCHES) = .0063		
X-AREA (SQ. IN.) = .3794			X-AREA (SQ. IN.) = .4232		
GAMMA-CHORD(DEG.) = 66.19			GAMMA-CHORD(DEG.) = 70.30		
RADIUS (METERS) = .3892			RADIUS (METERS) = .4075		
CHORD (METERS) = .1015			CHORD (METERS) = .1086		
ZCSL (METERS) = .0549			ZCSL (METERS) = .0587		
YCSL (METERS) = .0000			YCSL (METERS) = -.0004		
LER (METERS) = .000208			LER (METERS) = .00201		
TER (METERS) = .000145			TER (METERS) = .000160		
X-AREA (SQ. METERS) = .000245			X-AREA (SQ. METERS) = .000273		
GAMMA-CHORD(RAD.) = 1.1552			GAMMA-CHORD(RAD.) = 1.2269		

TABLE IX

**ROTOR MANUFACTURING COORDINATES
FOR SECTIONS NORMAL TO STACKING LINE**

Q				R			
INCHES		METERS		INCHES		METERS	
ZC	YP	YS	ZC	YP	YS	ZC	YP
-.0000	-.0076	.0076	-.0000	-.0077	.0077	.0000	-.0002
.1412	-.0148	.0077	.1480	-.0188	.0042	.0038	-.0001
.2823	-.0224	.0074	.2961	-.0297	.0008	.0075	-.0008
.4235	-.0303	.0068	.4441	-.0404	-.0025	.0113	-.0001
.5647	-.0387	.0057	.5921	-.0509	-.0057	.0150	-.0001
.7058	-.0473	.0042	.7401	-.0613	-.0089	.0188	-.0002
.8470	-.0563	.0023	.8882	-.0716	-.0120	.0226	-.0003
.9882	-.0654	.0000	1.0362	-.0814	.0150	.0263	-.0004
1.1293	-.0753	.0029	1.1842	-.0912	-.0183	.0301	-.0005
1.2705	-.0857	-.0052	1.3323	-.1036	.0338	-.0212	-.0005
1.4117	-.0921	-.0035	1.4803	-.1147	-.0209	.0376	-.0005
1.5528	-.0932	.0032	1.6283	-.1183	-.0153	.0414	-.0004
1.6940	-.0920	.0165	1.7764	-.1175	-.0027	.0451	-.0001
1.8352	-.0903	.0322	1.9244	-.1156	.0144	.0489	-.0004
1.9763	-.0887	.0486	2.0724	-.1135	.0320	.0526	-.0008
2.1175	-.0869	.0646	2.2205	-.1111	.0494	.0564	-.0013
2.2587	-.0850	.0801	2.3685	-.1085	.0662	.0602	-.0017
2.3998	-.0829	.0961	2.5165	-.1055	.0829	.0639	-.0021
2.5410	-.0806	.1097	2.6645	-.1021	.1012	.0677	-.0026
2.6822	-.0780	.1198	2.8126	-.0983	.1137	.0714	-.0029
2.8233	-.0750	.1236	2.9606	-.0940	.1191	.0752	-.0030
2.9645	-.0716	.1184	3.1086	-.0893	.1151	.0790	-.0029
3.1057	-.0677	.1058	3.2567	-.0840	.1015	.0827	-.0026
3.2468	-.0633	.0911	3.4047	-.0782	.0872	.0865	-.0022
3.3880	-.0584	.0764	3.5527	-.0719	.0751	.0902	-.0019
3.5292	-.0529	.0618	3.7008	-.0649	.0634	.0940	-.0016
3.6703	-.0467	.0476	3.8488	-.0573	.0519	.0978	-.0013
3.8115	-.0399	.0355	3.9968	-.0491	.0409	.1015	-.0012
3.9527	-.0324	.0270	4.1448	-.0402	.0319	.1053	-.0010
4.0938	-.0241	.0219	4.2929	-.0306	.0261	.1090	-.0008
4.2350	-.0151	.0185	4.4409	-.0202	.0233	.1128	-.0005
4.3762	-.0053	.0103	4.5889	-.0092	.0221	.1166	-.0002
RADIUS (INCHES) = 16.264				RADIUS (INCHES) = 16.734			
CHORD (INCHES) = 4.376				CHORD (INCHES) = 4.589			
ZCSL (INCHES) = 2.3799				ZCSL (INCHES) = 2.5333			
YCSL (INCHES) = -.0205				YCSL (INCHES) = -.0350			
LER (INCHES) = .0078				LER (INCHES) = .0079			
TER (INCHES) = .0083				TER (INCHES) = .0162			
X-AREA (SQ. IN.) = .4509				X-AREA (SQ. IN.) = .5088			
GAMMA-CHORD(DEG.) = 71.04				GAMMA-CHORD(DEG.) = 72.44			
RADIUS (METERS) = .4131				RADIUS (METERS) = .4250			
CHORD (METERS) = .1112				CHORD (METERS) = .1166			
ZCSL (METERS) = .0604				ZCSL (METERS) = .0643			
YCSL (METERS) = -.0005				YCSL (METERS) = -.0009			
LER (METERS) = .000198				LER (METERS) = .00201			
TER (METERS) = .000211				TER (METERS) = .00411			
X-AREA (SQ. METERS) = .000291				X-AREA (SQ. METERS) = .000328			
GAMMA-CHORD(RAD.) = 1.2398				GAMMA-CHORD(RAD.) = 1.2644			

STATOR MANUFACTURING COORDINATES FOR SECTIONS NORMAL TO STACKING LINE

89

TABLE X

**STATOR MANUFACTURING COORDINATES
FOR SECTIONS NORMAL TO STACKING LINE**

INCHES				METERS				INCHES				METERS			
ZC	YP	YS	ZC	YP	YS	ZC	YP	YS	ZC	YP	YS	ZC	YP	YS	
-.0000	-.0054	.0060	.0000	-.0001	.0002	-.0000	-.0056	.0063	.0000	-.0001	.0002	.0000	-.0001	.0002	
.0049	-.0035	.0087	.0001	-.0001	.0002	.0051	-.0035	.0092	.0001	-.0001	.0002	.0001	-.0001	.0002	
.0078	.0020	.0078	.0020	.0006	.0012	.0078	.0024	.0093	.0020	.0007	.0013	.0020	.0007	.0013	
.0156	.0050	.0078	.0040	.0014	.0022	.0157	.0026	.0093	.0040	.0014	.0024	.0040	.0014	.0024	
.0234	.0811	.1253	.0059	.0021	.0032	.0236	.0037	.1329	.0060	.0022	.0034	.0060	.0022	.0034	
.0312	.1065	.1608	.0079	.0027	.0041	.0317	.0107	.1497	.0080	.0023	.0043	.0080	.0023	.0043	
.0390	.1302	.1943	.0099	.0033	.0049	.0394	.0137	.1703	.0100	.0024	.0052	.0100	.0024	.0052	
.0468	.1524	.2261	.0119	.0039	.0057	.0471	.0157	.1955	.0120	.0024	.0060	.0120	.0024	.0060	
.0546	.1731	.2561	.0138	.0044	.0065	.0550	.0168	.2048	.0140	.0024	.0067	.0140	.0024	.0067	
.0624	.1926	.2843	.0158	.0049	.0072	.0625	.0190	.2119	.0160	.0025	.0074	.0160	.0025	.0074	
.0702	.2102	.3103	.0178	.0053	.0079	.0702	.0213	.2163	.0180	.0025	.0080	.0180	.0025	.0080	
.0780	.2259	.3330	.0198	.0057	.0085	.0780	.0235	.2255	.0200	.0027	.0086	.0200	.0027	.0086	
.0858	.2394	.3523	.0217	.0061	.0089	.0858	.0255	.2353	.0220	.0027	.0089	.0220	.0027	.0089	
.0936	.2507	.3684	.0237	.0064	.0094	.0942	.0272	.2448	.0240	.0028	.0094	.0240	.0028	.0094	
.1014	.2593	.3813	.0257	.0066	.0097	.1022	.0284	.2544	.0260	.0028	.0097	.0260	.0028	.0097	
.1089	.2668	.3910	.0277	.0068	.0101	.1101	.0286	.2603	.0280	.0028	.0101	.0280	.0028	.0101	
.1167	.2714	.3976	.0296	.0069	.0102	.1180	.0286	.2636	.0300	.0028	.0101	.0300	.0028	.0101	
.1244	.2738	.4011	.0316	.0070	.0102	.1237	.0289	.2639	.0320	.0028	.0101	.0320	.0028	.0101	
.1322	.2741	.4014	.0336	.0070	.0102	.1337	.0289	.2639	.0340	.0028	.0101	.0340	.0028	.0101	
.1400	.2717	.3986	.0356	.0069	.0101	.1416	.0289	.2639	.0360	.0028	.0100	.0360	.0028	.0100	
.1478	.2677	.3925	.0375	.0068	.0100	.1450	.0289	.2635	.0380	.0028	.0098	.0380	.0028	.0098	
.1556	.2613	.3836	.0395	.0066	.0097	.1537	.0280	.2555	.0400	.0028	.0095	.0400	.0028	.0095	
.1633	.2526	.3714	.0415	.0064	.0094	.1652	.0282	.2582	.0420	.0028	.0092	.0420	.0028	.0092	
.1711	.2416	.3558	.0435	.0061	.0090	.1731	.0261	.2450	.0440	.0027	.0088	.0440	.0027	.0088	
.1789	.2283	.3367	.0455	.0058	.0086	.1807	.0215	.2115	.0460	.0027	.0082	.0460	.0027	.0082	
.1867	.2115	.3138	.0474	.0054	.0080	.1884	.0194	.2007	.0480	.0027	.0076	.0480	.0027	.0076	
.1945	.1923	.2870	.0494	.0049	.0073	.1967	.0170	.2030	.0500	.0027	.0069	.0500	.0027	.0069	
.2022	.1699	.2557	.0514	.0043	.0065	.2045	.0159	.2132	.0520	.0027	.0061	.0520	.0027	.0061	
.2100	.1440	.2194	.0534	.0037	.0056	.2125	.0178	.2250	.0540	.0027	.0052	.0540	.0027	.0052	
.2178	.1142	.1774	.0553	.0029	.0045	.2203	.0196	.2369	.0560	.0025	.0042	.0560	.0025	.0042	
.2256	.0800	.1492	.0573	.0020	.0033	.2281	.0201	.2481	.0580	.0025	.0030	.0580	.0025	.0030	
.2334	.0406	.1228	.0593	.0010	.0018	.2365	.0232	.2651	.0600	.0025	.0017	.0600	.0025	.0017	
.2412	-.0028	.0998	.0612	-.0001	.0002	.2437	.0231	.2695	.0618	.0025	.0008	.0618	.0025	.0008	
.2490	-.0052	.0764	.0613	-.0001	.0002	.2439	.0232	.2695	.0620	.0025	.0002	.0620	.0025	.0002	
RADIUS (INCHES) = 11.075			RADIUS (METERS) = .2913			RADIUS (INCHES) = 11.500			RADIUS (METERS) = .2921			RADIUS (METERS) = .2921			
CHORD (INCHES) = 2.412			CHORD (METERS) = .0613			CHORD (INCHES) = 2.439			CHORD (METERS) = .0620			CHORD (METERS) = .0620			
ZCSL (INCHES) = 1.257			ZCSL (METERS) = .0319			ZCSL (INCHES) = 1.263			ZCSL (METERS) = .0321			ZCSL (METERS) = .0321			
YCSL (INCHES) = .2660			YCSL (METERS) = .0068			YCSL (INCHES) = .2603			YCSL (METERS) = .0066			YCSL (METERS) = .0066			
RLE (INCHES) = .0055			RLE (METERS) = .0014			RLE (INCHES) = .0057			RLE (METERS) = .00145			RLE (METERS) = .00145			
RTF (INCHES) = .0041			RTF (METERS) = .0013			RTF (INCHES) = .0053			RTF (METERS) = .00136			RTF (METERS) = .00136			
X-AREA (SQ. IN.) = .2152			X-AREA (SQ. METERS) = .00139			X-AREA (SQ. IN.) = .2152			X-AREA (SQ. METERS) = .00147			X-AREA (SQ. METERS) = .00147			
GAMMA-CHORD (DEG.) = 21.86			GAMMA-CHORD (RAD.) = .3815			GAMMA-CHORD (DEG.) = 21.06			GAMMA-CHORD (RAD.) = .3676			GAMMA-CHORD (RAD.) = .3676			

STATOR MANUFACTURING COORDINATES FOR SECTIONS NORMAL TO STACKING LINE

91

TABLE X

STATOR MANUFACTURING COORDINATES
FOR SECTIONS NORMAL TO STACKING LINE

G				H			
INCHES		METERS		INCHES		METERS	
ZC	YP	YS	ZC	YP	YS	ZC	YP
-.0000	-.0063	.0074	.0000	-.0002	.0002	.0000	-.0002
.0058	-.0039	.0111	.0001	-.0001	.0003	.0002	-.0001
.0817	.0264	.0586	.0021	.0007	.0015	.0021	.0007
.1634	.0570	.1065	.0041	.0014	.0027	.0042	.0015
.2451	.0853	.1499	.0062	.0022	.0038	.0063	.0014
.3268	.1113	.1896	.0083	.0028	.0048	.0083	.0021
.4084	.1352	.2255	.0104	.0034	.0057	.0105	.0022
.4901	.1569	.2581	.0124	.0040	.0066	.0125	.0023
.5718	.1764	.2872	.0145	.0045	.0073	.0146	.0034
.6535	.1938	.3132	.0166	.0049	.0080	.0167	.0044
.7352	.2093	.3361	.0187	.0053	.0085	.0188	.0044
.8169	.2227	.3559	.0207	.0057	.0090	.0209	.0052
.8986	.2340	.3728	.0228	.0059	.0095	.0230	.0056
.9803	.2433	.3866	.0249	.0064	.0098	.0251	.0054
1.0620	.2506	.3972	.0270	.0064	.0101	.0272	.0061
1.1437	.2556	.4047	.0290	.0065	.0103	.0293	.0064
1.2253	.2584	.4090	.0311	.0066	.0104	.0314	.0064
1.3070	.2590	.4101	.0332	.0066	.0104	.0334	.0064
1.3887	.2574	.4080	.0353	.0065	.0104	.0355	.0064
1.4704	.2536	.4027	.0373	.0064	.0102	.0376	.0063
1.5521	.2477	.3943	.0394	.0063	.0100	.0397	.0062
1.6338	.2395	.3826	.0415	.0061	.0097	.0418	.0060
1.7155	.2291	.3676	.0436	.0058	.0093	.0439	.0057
1.7972	.2165	.3492	.0456	.0055	.0089	.0460	.0054
1.8789	.2015	.3274	.0477	.0051	.0083	.0481	.0050
1.9606	.1842	.3019	.0498	.0047	.0077	.0502	.0046
2.0422	.1646	.2728	.0519	.0042	.0069	.0523	.0041
2.1239	.1426	.2397	.0539	.0036	.0061	.0543	.0035
2.2056	.1180	.2026	.0560	.0030	.0051	.0564	.0029
2.2873	.0910	.1611	.0581	.0023	.0041	.0585	.0023
2.3690	.0613	.1149	.0602	.0016	.0029	.0606	.0015
2.4507	.0269	.0637	.0622	.0007	.0016	.0627	.0007
2.5269	-.0037	.0110	.0642	-.0001	.0003	.0646	-.0001
2.5324	-.0060	.0072	.0643	-.0002	.0002	.0648	-.0002
RADIUS (INCHES) = 13.000				RADIUS (INCHES) = 13.500			
CHORD (INCHES) = 2.532				CHORD (INCHES) = 2.551			
ZCSL (INCHES) = 1.281				ZCSL (INCHES) = 1.285			
YCSL (INCHES) = .2616				YCSL (INCHES) = .2603			
RLE (INCHES) = .0066				RLE (INCHES) = .0070			
RTE (INCHES) = .0064				RTE (INCHES) = .0067			
X-AREA (SQ. IN.) = .2742				X-AREA (SQ. IN.) = .2886			
GAMMA-CHORD(DEG.) = 20.24				GAMMA-CHORD(DEG.) = 19.75			
RADIUS (METERS) = .3302				RADIUS (METERS) = .3429			
CHORD (METERS) = .0643				CHORD (METERS) = .0648			
ZCSL (METERS) = .0325				ZCSL (METERS) = .0326			
YCSL (METERS) = .0066				YCSL (METERS) = .0066			
RLE (METERS) = .000169				RLE (METERS) = .000178			
RTE (METERS) = .000162				RTE (METERS) = .000171			
X-AREA (SQ.METERS) = .000177				X-AREA (SQ.METERS) = .000186			
GAMMA-CHORD(RAD.) = .3533				GAMMA-CHORD(RAD.) = .3447			

STATOR MANUFACTURING COORDINATES FOR SECTIONS NORMAL TO STACKING LINE

93

TABLE X
STATOR MANUFACTURING COORDINATES
FOR SECTIONS NORMAL TO STACKING LINE

K			METERS			INCHES			L			METERS		
ZC	YP	YS	ZC	YP	YS	ZC	YP	YS	ZC	YP	YS	ZC	YP	YS
-.0000	-.0374	.0131	.0000	-.0002	.0003	-.0000	-.0083	.0103	.0000	-.0002	.0003	.0000	-.0002	.0003
.0071	-.0049	.0199	.0002	-.0001	.0005	.0074	-.0049	.0159	.0002	-.0001	.0004	.0002	-.0001	.0004
.0834	.0428	.0928	.0021	.0011	.0024	.0833	-.0029	.0729	.0021	.0004	.0019	.0021	.0004	.0019
.1663	.0917	.1671	.0042	.0023	.0072	.1665	.0651	.1306	.0042	.0017	.0033	.0042	.0017	.0033
.2502	.1357	.2315	.0064	.0034	.0059	.2498	.0972	.1809	.0063	.0025	.0046	.0063	.0025	.0046
.3336	.1758	.2882	.0085	.0045	.0073	.3331	.1265	.2268	.0085	.0032	.0058	.0085	.0032	.0058
.4170	.2116	.3385	.0106	.0054	.0086	.4163	.1532	.2679	.0106	.0039	.0068	.0106	.0039	.0068
.5005	.2441	.3827	.0127	.0067	.0097	.4996	.1775	.3048	.0127	.0045	.0077	.0127	.0045	.0077
.5839	.2731	.4218	.0148	.0069	.0107	.5829	.1993	.3374	.0148	.0051	.0086	.0148	.0051	.0086
.6673	.2987	.4559	.0169	.0076	.0116	.6661	.2186	.3662	.0169	.0056	.0093	.0169	.0056	.0093
.7507	.3213	.4853	.0191	.0082	.0123	.7494	.2356	.3911	.0190	.0060	.0099	.0190	.0060	.0099
.8341	.3407	.5105	.0212	.0087	.0130	.8327	.2502	.4123	.0211	.0064	.0105	.0211	.0064	.0105
.9175	.3571	.5314	.0233	.0091	.0135	.9159	.2625	.4300	.0233	.0067	.0109	.0233	.0067	.0109
1.0009	.3705	.5484	.0254	.0094	.0139	.9992	.2724	.4442	.0254	.0069	.0113	.0254	.0069	.0113
1.0843	.3808	.5614	.0275	.0097	.0143	1.0825	.2801	.4549	.0275	.0071	.0116	.0275	.0071	.0116
1.1677	.3882	.5705	.0297	.0099	.0145	1.1657	.2854	.4624	.0296	.0072	.0117	.0296	.0072	.0117
1.2512	.3927	.5759	.0318	.0100	.0146	1.2490	.2864	.4664	.0317	.0073	.0118	.0317	.0073	.0118
1.3346	.3945	.5776	.0339	.0100	.0147	1.3323	.2892	.4672	.0338	.0073	.0119	.0338	.0073	.0119
1.4180	.3936	.5758	.0360	.0100	.0146	1.4155	.2878	.4647	.0360	.0073	.0118	.0360	.0073	.0118
1.5014	.3901	.5704	.0381	.0099	.0145	1.4988	.2842	.4590	.0381	.0072	.0117	.0381	.0072	.0117
1.5848	.3836	.5612	.0403	.0097	.0143	1.5821	.2764	.4500	.0402	.0071	.0114	.0402	.0071	.0114
1.6682	.3740	.5482	.0424	.0095	.0139	1.6653	.2703	.4375	.0423	.0069	.0111	.0423	.0069	.0111
1.7516	.3614	.5309	.0445	.0092	.0135	1.7486	.2597	.4217	.0444	.0066	.0107	.0444	.0066	.0107
1.8350	.3456	.5092	.0466	.0088	.0129	1.8319	.2467	.4021	.0465	.0063	.0102	.0465	.0063	.0102
1.9184	.3264	.4832	.0487	.0083	.0123	1.9151	.2313	.3788	.0486	.0059	.0096	.0486	.0059	.0096
2.0018	.3028	.4521	.0508	.0077	.0115	2.0817	.1923	.3202	.0508	.0054	.0089	.0508	.0054	.0089
2.0853	.2755	.4153	.0530	.0070	.0105	2.1649	.1666	.2842	.0529	.0049	.0081	.0529	.0049	.0081
2.1687	.2436	.3723	.0551	.0062	.0095	2.2482	.1415	.2433	.0550	.0043	.0072	.0550	.0043	.0072
2.2521	.2065	.3221	.0572	.0052	.0082	2.3315	.1119	.1971	.0571	.0036	.0062	.0571	.0036	.0062
2.3355	.1640	.2633	.0593	.0042	.0067	2.4147	.0768	.1436	.0592	.0029	.0050	.0592	.0029	.0050
2.4189	.1144	.1946	.0614	.0029	.0049	2.4980	.0368	.0814	.0613	.0020	.0036	.0613	.0020	.0036
2.5023	.0570	.1128	.0636	.0014	.0029	2.5748	-.0043	.0156	.0634	.0009	.0021	.0634	.0009	.0021
2.5862	-.0043	.0195	.0655	-.0001	.0005	2.5813	-.0077	.0101	.0654	-.0001	.0004	.0654	-.0001	.0004
2.5857	-.0067	.0129	.0657	-.0002	.0003				.0656	-.0002	.0003			
RADIUS (INCHES) = 15.640			RADIUS (METERS) = .3973			RADIUS (INCHES) = 15.180			RADIUS (METERS) = .3854			RADIUS (METERS) = .3854		
CHORD (INCHES) = 2.586			CHORD (METERS) = .0657			CHORD (INCHES) = 2.581			CHORD (METERS) = .0656			CHORD (METERS) = .0656		
ZCSL (INCHES) = 1.2980			ZCSL (METERS) = .0330			ZCSL (INCHES) = 1.293			ZCSL (METERS) = .0328			ZCSL (METERS) = .0328		
YCSL (INCHES) = .3829			YCSL (METERS) = .0097			YCSL (INCHES) = .2878			YCSL (METERS) = .0074			YCSL (METERS) = .0074		
RLE (INCHES) = .0097			RLE (METERS) = .000246			RLE (INCHES) = .0088			RLE (METERS) = .000225			RLE (METERS) = .000225		
X-AREA (SQ. IN.) = .0084			X-AREA(SQ. METERS) = .000213			X-AREA (SQ. IN.) = .0081			X-AREA(SQ. METERS) = .000206			X-AREA(SQ. METERS) = .000206		
GAMMA-CHORD(DEG.) = 24.24			GAMMA-CHORD(RAD.) = .4231			GAMMA-CHORD(DEG.) = 14.66			GAMMA-CHORD(RAD.) = .3257			GAMMA-CHORD(RAD.) = .3257		

APPENDIX 6

NOMENCLATURE

<u>Symbol</u>	<u>Definition</u>
A	areas
A/A*	(area)/(sonic flow area)
a	= distance along chord line to maximum camber point from leading edge
b	rotor semi-chord at 75 percent of span from root
c	aerodynamic chord, i.e., along the flow surface
D	diffusion factor for rotor = $1 - \frac{V'_2}{V'_1} + \frac{r_2 V_{\theta 2} - r_1 V_{\theta 1}}{(r_1 + r_2) \sigma V'_1}$ for stator = $1 - \frac{V_4}{V_3} + \frac{r_3 V_{\theta 3} - r_4 V_{\theta 4}}{(r_3 + r_4) \sigma V_3}$
DCA	double-circular-arc
E	excitations per rotor revolution
H	stagnation enthalpy
i _m	incidence angle between inlet air direction and line tangent to blade mean camber line at leading edge, degrees
i _{ss}	incidence angle between inlet air direction and line tangent to blade suction surface at leading edge, degrees
\bar{K}	blockage factor, actual/effective flow area
K ₁₋₈	radial spring rates
K _t	stress concentration factor
LE	leading edge
M	Mach number
MCA	multiple-circular-arc blade

NOMENCLATURE (Continued)

<u>Symbol</u>	<u>Definition</u>
N	rotor speed, rpm
p	pressure
P/A	centrifugal pull stress
PC	precompression blade
r	radius
R	distance along conical surface from apex to blade (see Figure 50)
R_c	streamline radius of curvature
s	blade spacing
T	temperature
t	blade maximum thickness
TE	trailing edge
T_{1-4}	torsional spring rates
U	rotor tangential speed
V	air velocity
W	weight flow
WA	leading edge wedge angle
x conical	distance in unwrapped conical plane
Y_p	airfoil coordinate of pressure surface normal to chord line
Y_s	airfoil coordinate of suction surface normal to chord line
Y_{cgg}	vertical distance to airfoil center of gravity from chord line
y	length along calculation station
y conical	distance normal to x conical

NOMENCLATURE (Continued)

<u>Symbol</u>	<u>Definition</u>
Z	axial distance
Z^* ratio	shroud modulus/airfoil modulus
Z_c	airfoil coordinate parallel to chord line
Z_{ccg}	horizontal distance to airfoil center of gravity from leading edge along chord line
β	absolute air angle = $\text{COT}^{-1} (V_m/V_\theta)$
β'	relative air angle = $\text{COT}^{-1} \frac{(V_m)}{(V'_\theta)}$
β^*	metal angle, angle between tangent to mean camber line and meridional direction
γ	blade chord angle, angle between chord and axial direction
δ°	deviation angle - exit air angle minus metal angle at trailing edge
ϵ	angle between tangent to streamline projected on meridional plane and axial direction
$\bar{\epsilon}$	cone angle = $\text{TAN}^{-1} \frac{(r_{te} - r_{le})}{(Z_{te} - Z_{le})}$
η_{ad}	adiabatic efficiency
θ	circumferential direction
λ	angle of calculation station measured from axial direction
ρ	density
Σ	angle on conical surface of revolution - see Figure 50
σ	solidity or stress
ϕ	camber angle, difference between blade angles at leading and trailing edges on conical surface (Figure 50)
ϕ_Σ	camber angle, difference between blade angles at leading and trailing edges on the unwrapped conical surface (Figure 50)

NOMENCLATURE (Continued)

<u>Symbol</u>	<u>Definition</u>
$\phi_{f\Sigma}$	front camber angle, difference between blade angles at leading edge and MCA transition point on the unwrapped conical surface
ω	angular velocity
ω_t	torsional frequency
$\bar{\omega}$	total pressure loss coefficient, mass average defect in relative total pressure divided by difference between inlet stagnation and static pressures
	<u>Subscripts</u>
av	average
f	front
le	leading edge
m	meridional direction (r - z plane)
p	profile
r	radial direction
ss	suction surface
t	total or stagnation
te	trailing edge
z	axial direction
θ	circumferential
1	station into rotor along leading edge
2	station out of rotor along trailing edge
3	station into stator along leading edge
4	station out of stator along trailing edge

NOMENCLATURE (Continued)

superscripts

'	relative to rotor
*	designates blade metal angle
°	degrees of arc or temperature

REFERENCES

1. Sulam, D. H., Keenan, M. J., and Flynn, J. T., "*Single-Stage Evaluation of Highly-Loaded High-Mach-Number Compressor Stages - II. Data and Performance, Multiple-Circular-Arc Rotor*," NASA CR-72694, PWA-3772, 1970
2. Jahnsen, J. and Hartmann, M. J., "*Investigation of Supersonic Compressor Rotors Designed With External Compression*," NACA RM E54G27a, 1954
3. Carter, A. F. and Novak, R. A., "*Computed Aspect Ratio-Curvature Effects Upon the Performance of a High-Pressure-Ratio Single-Stage Compressor*," ASME Paper No. 65-WA/GTP-12
4. Reshotko, E. and Tucker, M., "*Approximate Calculation of Compressible Turbulent Boundary Layer With Heat Transfer and Arbitrary Pressure Gradient*," NACA Report 4154, 1957
5. Kantrowitz, A. and Donaldson, C. duP., "*Preliminary Investigation of Supersonic Diffusers*," NACA WR-713, 1945
6. Keenan, M. J. and Bartok, J. A., "*Experimental Evaluation of Transonic Stators*," NASA CR-72298, PWA-3470, 1969
7. Harley, K. G., and Burdsall, E. A., "*High-Loading Low-Speed Fan Study - II Data and Performance Unslotted Blades and Vanes*," NASA CR-72667, PWA-3653, 1970

DISTRIBUTION LIST

		Group 1 Data & Perf. Reports	Group 2 Anal. & Design Reports, Final Perf. & Analysis Reports
1.	NASA-Lewis Research Center 21000 Brookpark Road Cleveland, Ohio 44135 Attention:		
	Report Control Office	MS 5-5 1	1
	Technical Utilization Office	MS 3-19 1	1
	Library	MS 60-3 2	2
	Fluid System Components Div.	MS 5-3 1	1
	Compressor Branch	MS 5-9 5	5
	Dr. B. Lubarsky	MS 3-3 1	1
	R. S. Ruggeri	MS 5-9 1	1
	M. J. Hartmann	MS 5-9 1	1
	W. A. Benser	MS 5-9 1	1
	D. M. Sandercock	MS 5-9 1	1
	L. J. Herrig	MS 501-4 1	1
	T. F. Gelder	MS 5-9 1	1
	C. L. Ball	MS 5-9 1	1
	L. Reid	MS 5-9 1	1
	L. W. Schopen	MS 500-206 1	1
	S. Lieblein	MS 501-5 1	1
	C. L. Meyer	MS 60-4 1	1
	J. H. Povolny	MS 60-4 1	1
	C. H. Voit	MS 5-3 1	1
	E. E. Bailey	MS 5-9 1	1
	W. L. Beede	MS 5-3 1	1
2.	NASA Scientific and Technical Information Facility P. O. Box 33 College Park, Maryland 20740 Attention: NASA Representative	2	2
3.	NASA Headquarters Washington, D. C. 20546 Attention: N. F. Rekos (RLC)	1	1
4.	U. S. Army Aviation Material Laboratory Fort Eustis, Virginia 23604 Attention: John White	1	1
5.	Headquarters Wright-Patterson AFB, Ohio 45433 Attention: J. L. Wilkins, SESOS S. Kobelak, APTP R. P. Carmichael, SESSP	1 1 1	1 1 1

	Group 1 Data & Perf. Reports	Group 2 Anal. & Design Reports, Final Perf. & Analysis Reports
6. Department of the Navy Naval Air Systems Command Propulsion Division, AIR 536 Washington, D. C. 20360	1	1
7. Department of Navy Bureau of Ships Washington, D. C. 20360 Attention: G. L. Graves	1	1
8. NASA-Langley Research Center Technical Library Hampton, Virginia 23365 Attention: Mark R. Nichols John V. Becker	1 1	1 1
9. The Boeing Company Commercial Airplane Group P. O. Box 3707 Seattle, Washington 98124 Attention: G. J. Schott, G-8410, MS 73-24	1	1
10. Douglas Aircraft Company 3855 Lakewood Boulevard Long Beach, California 90801 Attention: J. E. Merriman Technical Information Ctr. CI-250	1	1
11. Pratt & Whitney Aircraft Florida Research & Development Center P. O. Box 2691 West Palm Beach, Florida 33402 Attention: J. Brent H. D. Stetson W. R. Alley R. E. Davis R. W. Rockenbach B. A. Jones J. A. Fligg	1 1 1 1 1 1 1	1 1 1 1 1 1 1

	Group 1 Data & Perf. Reports	Group 2 Anal. & Design Reports, Final Perf. & Analysis Reports
12. Pratt & Whitney Aircraft 400 Main Street East Hartford, Connecticut 06108 Attention: R. E. Palatine T. G. Slaiby H. V. Marman M. J. Keenan B. B. Smyth A. A. Mikolajczak Library (UARL) W. M. Foley (UARL)	 1 1 1 1 1 1	 1 1 1 1 1 1
13. Allison Division, GMC Department 8894, Plant 8 P. O. Box 894 Indianapolis, Indiana 46206 Attention: J. N. Barney G. E. Holbrook B. A. Hopkins R. J. Loughery Library J. L. Dillard P. Tramm	 1 1 1 1 1 1 1	 1 1 1 1 1 1 1
14. Northern Research and Engineering 219 Vassar Street Cambridge, Massachusetts 02139 Attention: K. Ginwala	 1	 1
15. General Electric Company Flight Propulsion Division Cincinnati, Ohio 45215 Attention: J. W. Blanton J-19 W. G. Cornell K-49 D. Prince H-79 E. E. Hood/J. C. Pirtle J-165 J. F. Klapproth H-42 J. W. McBride H-44 L. H. Smith H-50 S. N. Suci H-32 J. B. Taylor J-168 Technical Information Ctr. N-32 Marlen Miller H-50 C. C. Koch H-79	 1 1 1 1 1 1 1 1 1	 1 1 1 1 1 1 1 1 1 1 1

	Group 1 Data & Perf. Reports	Group 2 Anal. & Design Reports, Final Perf. & Analysis Reports
16. General Electric Company 1000 Western Avenue Lynn, Massachusetts 01910 Attention: D. P. Edkins - Bldg. 2-40 F. F. Ehrich - Bldg. 2-40 L. H. King - Bldg. 2-40 R. E. Neitzel - Bldg. 2-40 Dr. C. W. Smith - Library Bldg. 2-40M	 1 1	 1 1 1 1
17. Curtiss-Wright Corporation Wright Aeronautical Wood-Ridge, New Jersey 07075 Attention: S. Lombardo G. Provenzale	 1	 1 1
18. AiResearch Manufacturing Company 402 South 36th Street Phoenix, Arizona 85034 Attention: Robert O. Bullock John H. Deman Jack Erwin - Dept. 32-1-J Don Seylor - Dept. 32-1-J Jack Switzer - Dept. 32-1-M	 1 1 1 1 1	 1 1 1 1 1
19. AiResearch Manufacturing Company 2525 West 190th Street Torrance, California 90509 Attention: Linwood C. Wright Bob Carmody Library	 1 1 1	 1 1 1
20. Union Carbide Corporation Nuclear Division Oak Ridge Gaseous Diffusion Plant P. O. Box "P" Oak Ridge, Tennessee 37830 Attention: R. G. Jordan D. W. Burton, K-1001, K-25	 1 1	 1 1

		Group 1 Data & Perf. Reports	Group 2 Anal. & Design Reports, Final Perf. & Analysis Reports
21.	Avco Corporation Lycoming Division 550 South Main Street Stratford, Connecticut 06497 Attention: Clause W. Bolton	1	1
22.	Teledyne Cae 1330 Laskey Road Toledo, Ohio 43601 Attention: Eli H. Benstein Howard C. Walch	1	1 1
23.	Solar San Diego, California 92112 Attention: P. A. Pitt J. Watkins	1 1	1 1
24.	Goodyear Atomic Corporation Box 628 Piketon, Ohio 45661 Attention: C. O. Langebrake	1	2
25.	Iowa State University of Science & Tech. Ames, Iowa 50010 Attention: Professor George K. Serovy Dept. of Mechanical Engineering	1	1
26.	Hamilton Standard Division of United Aircraft Corp. Windsor Locks, Connecticut 06096 Attention: Mr. Carl Rohrbach Head of Aerodynamics and Hydrodynamics	1	1
27.	Westinghouse Electric Corporation Small Steam and Gas Turbine Engineering B-4 Lester Branch P. O. Box 9175 Philadelphia, Pennsylvania 19113 Attention: Mr. S. M. DeCorso	1	1
28.	Williams Research Corporation P. O. Box 95 Walled Lake, Michigan 48088 Attention: J. Richard Joy Supervisor, Analytical Section	1	1

	Group 1 Data & Perf. Reports	Group 2 Anal. & Design Reports, Final Perf. & Analysis Reports
29. Lockheed Missile and Space Company P. O. Box 879 Mountain View, California 94040 Attention: Technical Library	1	1
30. The Boeing Company 224 N. Wilkinson Dayton, Ohio 45402 Attention: James D. Raisbeck	1	1
31. Chrysler Corporation Research Office Dept. 9000 P. O. Box 1118 Detroit, Michigan 48231 Attention: James Furlong	1	1
32. Elliott Company Jeannette, Pennsylvania 15644 Attention: J. Rodger Schields Director-Engineering	1	1
33. Dresser Industries Inc. Clark Gas Turbine Division 16530 Peninsula Boulevard P. O. Box 9989 Houston, Texas 77015 Attention: R. V. Reddy	1	1
34. California Institute of Technology Pasadena, California 91109 Attention; Prof. Duncan Rannie	1	1
35. Massachusetts Institute of Technology Cambridge, Massachusetts 02139 Attention: Dr. J. L. Kerrebrock	1	1
36. Caterpillar Tractor Company Peoria, Illinois 61601 Attention: J. Wiggins	1	1

		Group 1 Data & Perf. Reports	Group 2 Anal. & Design Reports, Final Perf. & Analysis Reports
37.	Penn State University Department of Aerospace Engineering 233 Hammond Building University Park, Pennsylvania 16802 Attention: Prof. B. Lakshminarayana	1	1
38.	Texas A&M University Department of Mechanical Engineering College Station, Texas 77843 Attention: Dr. Meherwan P. Boyce P.E.	1	1
39.	National Technical Information Service Springfield, Virginia 22151	13	13